DISS. ETH NO. 15898

MODELING THE EFFECTS OF SHORT AND LONG-TERM SOLAR VARIABILITY ON OZONE AND CLIMATE

A dissertation submitted to the

SWISS FEDERAL INSTITUTE OF TECHNOLOGY ZURICH

for the degree of

Doctor of Natural Sciences

presented by

TATIANA EGOROVA

Dipl. Meteorologist, The Russian State Hydrometeorological Institute

born 09.03.1968

citizen of Russia

accepted on the recommendation of

Prof. Dr. Thomas Peter, examiner
Prof. Dr. Atsumu Ohmura, co-examiner
Prof. Dr. Joanna Haigh, co-examiner

2005

Contents

Abstract

The Sun is the primary source of energy for Earth's atmosphere. One possible natural cause of climatic change is a variation in the Sun's luminosity. The Sun emits its radiative energy in a broad spectral range. One major and well-known mechanism of the Sun's influence on climate is the variability at short wavelengths that affect upper atmospheric ozone. The task on hand is to understand how the Earth's climate system responds to variations of the Sun. The research undertaken within the present dissertation is centered on the influence of the solar radiation on the middle atmosphere and on the downward propagation of the resulting signal. Therefore, this work investigates the effect of variations of the solar irradiance, in particular of the *spectral* variability with emphasis on the UV radiation, on ozone and other trace gases, and evaluates their influence on the temperature and dynamics of the entire atmosphere, from the mesopause to the Earth's surface.

To fulfill this goal a new Chemistry Climate Model (CCM) with interactive photochemistry on the basis of MA-ECHAM4 has been developed. The middle-atmosphere general circulation model (GCM) MA-ECHAM4 is made available through collaboration with the Max-Planck Institute for Meteorology in Hamburg. MA-ECHAM4 has been coupled to the photochemistry-transport model MEZON. The resulting CCM has been called SOCOL (modeling tool for studies of SOlar Climate Ozone Links, Russian "Falcon").

To validate how well SOCOL reproduces a present-day climatology, a 40-year long control run for present day conditions has been carried out and compared with observational and reanalysis data. The model performance is shown to be very satisfactory applying an overall inspection of the simulated physical and chemical fields as well as using a rigorous statistical analysis. At the same time a number of weaknesses have been identified in the model that need to be addressed for future model improvement. In particular, the analysis of the simulated zonal wind and temperature deviations shows that for an improvement it will be necessary to pay special attention to the tropopause region in the tropics and at high latitudes as well as to the description of the processes in the upper stratosphere and mesosphere, where statistically significant cold biases have been found in the model during boreal summer. Despite of these model deficiencies, the overall performance of the CCM SOCOL as a modeling tool is reasonable and many features of the real atmosphere are simulated rather well.

The CCM SOCOL has been ported on regular PCs and was shown to attain good wall-clock performance. Thus many research groups can use it for studies of chemistry-climate problems even without access to large super-computer facilities.

With the CCM SOCOL several 20-year-long steady-state model simulations have been performed with detailed, realistic spectral energy distributions at maximum and minimum of the solar irradiance to determine their potential effects on the entire atmosphere and Earth's climate. The original MA-ECHAM4 radiation code has not been designed for solar variability studies: it has only one interval in the UV and visible parts of the solar spectrum and does not account at all for the solar flux at wavelengths shorter than 250 nm. Therefore, heating rates due to absorption in the UV by ozone and oxygen have been parameterized in the Lyman-α line, Schumann-Runge band and Hartley band, which are important in the stratosphere and mesosphere.

First, the annual mean zonal mean solar signal in ozone, temperature, zonal wind and surface air temperature has been analyzed. Annual mean zonal mean values of ozone, temperature and zonal wind have been compared with various results of observation analysis. An analysis for annual mean solar-induced changes for several species has been performed.

Second, the annual mean analysis has been extended to seasonal and geographical patterns. The simulated response of ozone to the imposed changes in solar ultraviolet flux shows a positive correlation in the tropical stratosphere and a negative correlation in the tropical mesosphere, in agreement with theoretical expectation. The model suggests an acceleration of the polar night jets in both hemispheres and a dipole structure in the temperature changes at high latitudes. The model results also show an alteration of the tropospheric circulation and of the surface air temperature resulting in a statistically significant warming of 1 K in the annual mean over North America and Siberia. This supports the idea of a solar-climate connection, which propagates downward into the low levels of the troposphere.

The influence of variations of UV and visible radiation on the atmosphere has been investigated separately because the atmosphere absorbs very differently. Two additional 20-year long runs have been carried out, one only with perturbations in UV radiation and another one only with changes in visible radiation. The results show that UV radiation variations may quite substantially alter stratospheric jet in contrast to visible radiation. The analysis shows that the changes in UV radiation do play a significant role in determining the surface air temperature distribution, similar to changes in visible, but due to a lag in the response with different strengths during different seasons.

The study of the 27-day solar rotation cycle is also suitable for the model validation, because the observational data cover more then 100 such cycles, while only two 11-year cycles occurred during the satellite era. Nine 1-year long runs have been performed applying daily spectral solar irradiance. The correlation of zonal mean hydroxyl radical, ozone and temperature averaged over the tropics with solar irradiance time series have been analyzed. The correlation of the hydroxyl with the solar irradiance changes is positive in the upper stratosphere and mesosphere and is in a good agreement with previous estimations, which confirms the model's treatment of chemical processes in the middle atmosphere. The response of the ozone to the increase of the solar irradiance is negative in the mesosphere for zero phase lags, reflecting the enhancement of the hydroxyl radical destroying the ozone. The simulated ozone sensitivity is in a reasonable agreement with observations. The temperature correlations with solar irradiance are not robust, because its variability strongly depends on non-linear dynamics and transport in the atmosphere.

Finally, the possible ways of model improvement and future activity aimed to study solar-climate links are discussed. Further investigation of the identified solar-climate link is required, including overcoming the steady-state assumption made here, i.e. implying perpetual solar maximum or/and solar minimum conditions.

The work has been supported by the Poly-Project "Variability of the Sun and Global Climate" of ETHZ and partly by PMOD/WRC, Davos.

Zusammenfassung

Die Sonne ist die primäre Energiequelle der Erdatmosphäre. Ein möglicher natürlicher Grund für eine Klimaänderung sind Variationen in der Luminosität der Sonne. Die Sonne emittiert ihre Strahlungsenergie in einem breiten Spektralbereich. Ein wesentlicher, gut bekannter Mechanismus des Einflusses der Sonne auf das Klima ist die Variabilität bei kurzen Wellenlängen, welche das Ozon in der höheren Atmosphäre beeinflusst. Die vorliegende Aufgabe besteht darin zu verstehen, wie das Klimasystem der Erde auf Variationen der Sonne reagiert. Die mit der vorliegenden Dissertation unternommene Forschung konzentriert sich aus den Einfluss solarer Strahlung auf die mittlere Atmosphäre und auf die abwärtsgerichtete Ausbreitung des resultierenden Signals. Daher untersucht diese Arbeit den Einfluss von Variationen der solaren Strahlungsintensität, insbesondere der *spektralen* Variabilität mit Schwerpunkt auf UV-Strahlung, Ozon anderen Spurengasen. Sie wertet denen Einfluss auf die Temperatur und Dynamik der gesamten Atmosphäre aus, von der Mesopause bis zur Erdoberfläche.

Zum Erreichen dieses Ziels wurde ein neues Chemie-Klima-Modell (CCM) mit interaktiver Photochemie auf der Basis von MA-ECHAM4 entwickelt. Im Rahmen einer Zusammenarbeit wurde das allgemeine Zirkulationsmodell (GCM) der mittleren Atmosphäre MA-ECHAM4 durch das Max-Planck-Institut für Meteorologie in Hamburg zur Verfügung gestellt. MA-ECHAM4 wurde an das Photochemie-Transportmodell MEZON gekoppelt. Das so entstandene CCM heisst SOCOL (Modell für die Studien der solaren Klima-Ozon-Kopplung, russ. „Falke").

Zur Erfassung, wie gut SOCOL die aktuelle Klimatologie reproduziert, wurde ein 40-jähriger Kontrolllauf für heutige Verhältnisse durchgeführt und mit Beobachtungen und Re-analysedaten verglichen. Die Leistungsmerkmale des Modells sind sehr zufriedenstellend aufgrund einer allgemeinen Beurteilung der simulierten physikalischen und chemischen Felder sowie aufgrund einer rigorosen statistischen Analyse. Gleichzeitig wurde eine Anzahl von Schwächen identifiziert, die für zukünftige Modellverbesserungen aufgegriffen werden müssen. Besonders die Analyse die Abweichungen der simulierten zonalen Winde und Temperaturen zeigt, dass für eine Verbesserung der tropischen und polaren Tropopausenregion besondere Aufmerksamkeit geschenkt werden muss, sowie einer verbesserten Beschreibung der Prozesse in der oberen Stratosphäre and Mesosphäre, wo statistisch signifikante systematische Abweichungen mit zu niedrigen Temperaturen während des nordhemisphärischen Sommers bestehen. Trotz dieser Schwächen sind die Funktionen des CCM SOCOL als Modellwerkzeug angemessen, und viele Eigenschaften der realen Atmosphäre werden gut beschrieben.

Das CCM SOCOL wurde auf reguläre PCs portiert, worauf gute CPU-Laufzeiten erreicht werden. Daher kann das Modell für Studien des Chemie-Klima-Problems durch viele Forschungsgruppen sogar ohne Zugang zu grossen Supercomputern eingesetzt werden.

Mit dem CCM SOCOL wurden mehrere stationäre Modellsimulationen über je 20 Jahre durchgeführt mit detaillierten, realistischen spektralen Energieverteilungen der solaren Strahlungsintensität bei Bedingungen des solaren Maximums and Minimums, um die potentiellen Effekte auf die gesamte Atmosphäre und das Erdklima zu bestimmen. Das Original des Strahlungscodes von MA-ECHAM4 ist für Untersuchungen der Sonnenvariabilität: es gibt nur ein Intervall im UV und in den sichtbaren Teilen des Sonnenspektrums und nimmt keine Rücksicht auf den Strahlungsfluss bei Wellenlängen kürzer als 250 nm. Daher mussten die Heizraten aufgrund der UV-Absorption durch Ozon und Sauerstoff im Bereich der solaren Lyman-α-Line, der Schumann-Runge-Bande und der Hartley-Bande parametrisiert werden, welche in der Stratosphäre und Mesosphäre wichtig

sind.

Für die Modellvalidierung wurden zunächst Jahresmittelwerte der zonalen Mittel des solaren Signals in Ozon, der Temperatur, des zonalen Windes und der Bodenlufttemperatur analysiert. Jahresmittelwerte von Ozon, Temperatur und zonalem Wind wurden mit verschiedenen aus Beobachtungen abgeleiteten Analysen verglichen. Weiterhin wurde eine Analyse der Jahresmittelwerte sonneninduzierter Änderungen verschiedener Spezies durchgeführt. Zweitens wurde die Analyse der Jahresmittelwerte auf saisonale und geographische Muster ausgedehnt. Der modellierte Response des Ozons auf den solaren Antrieb zeigt eine positive Korrelation in der tropischen Stratosphäre und negative Korrelation in der tropischen Mesosphäre, in Übereinstimmung mit der theoretischen Erwartung. Das Modell legt eine Beschleunigung der polaren Strahlströme und eine Dipolstruktur der Temperaturveränderungen in hohen Breiten nahe. Das Modell zeigt auch eine Veränderung der troposphärischen Zirkulation und der Oberflächentemperatur, die zu einer statistisch signifikanten Erwärmung von 1 K im Jahresdurchschnitt über Nordamerika und Sibirien führen. Dies stützt die Idee einer Sonnen-Klima-Verbindung, welche sich abwärts bis in die unteren Schichten der Troposphäre ausbreitet.

Der atmosphärische Einfluss der Variationen im UV- und sichtbaren Spektralbereich wurde getrennt untersucht, weil die Atmosphäre in beiden Bereichen sehr unterschiedlich absorbiert. Zwei zusätzliche 20 jahre lange Läufe wurden durchgeführt, einer nur mit den Veränderungen im UV, der andere nur mit Änderungen in der sichtbaren Bestrahlung. Die Resultate zeigen, dass die Änderungen im UV – im Gegensatz zu den Veränderungen im Sichtbaren – substanziell den Strahlstrom beeinflussen können. Die Analyse zeigt, dass Änderungen in der UV-Strahlung eine signifikante Rolle bei der Einstellung der Oberflächentemperatur spielen, ähnlich wie die Änderungen im sichtbaren Spektralbereich, aber aufgrund einer zeitlichen Verzögerung zu unterschiedlichen Jahreszeiten.

Das Studium des 27-Tageszyklus der Sonnenrotation bietet eine weitere Möglichkeit zur Modellvalidierung, weil die Beobachtungen mehr als 100 solcher Zyklen erfassen, wohingegen nur zwei 11-Jahres-Zyklen in die Satellitenära fallen. Neun einjährige Läufe wurden durchgeführt und dabei tägliche, spektral aufgelöste Leistungsdichten angewendet. Die Korrelation zwischen der zonal gemittelten Konzentration des Hydroxylradikals, des Ozons und der Temperatur über den Tropen wurden bestimmt. Die Korrelation zwischen OH und der solaren Leistungsdichte ist positiv in der oberen Strarosphäre und Mesosphäre und ist in guter Übereinstimmung mit früheren Abschätzungen, was die Behandlung der chemischen Prozesse in der mittleren Atmosphäre in SOCOL bestätigt. Die Korrelation des Ozons ist negativ in der Mesosphäre, bedingt durch die Ozonzerstörung durch das zusätzliche OH und in Übereinstimmung mit Beobachtungen. Die Temperatur-Korrelation ist nicht robust, weil ihre Variabilität stark von nichtlinearer Dynamik und Transport abhängt.

Die möglichen Wege zur Modellverbesserung und zukünftige Aktivitäten in Bezug auf die Sonne-Erde-Verbindung diskutiert. Zusätzliche Untersuchungen sind nötig, inklusive der Überwindung der hier gemachten Stationaritätsannahme, welche fortwährendes solares Maximum oder Minimum annimmt.

Die Arbeit wurde ermöglicht durch das Poly-Projekt "Variability of the Sun and Global Climate" der ETHZ und teilweise durch PMOD/WRC, Davos.

1. Introduction

Diverse aspects of Sun-Earth climate relationship have been received researchers' interest for at least two hundred years. Recently, various groups have started to examine the relationship between solar variability and the terrestrial weather/climate system by comparing results from numerical models to statistical analyses of observational data. Very recently, investigations of the solar variability contribution to the climate change gained a new impetus, because it is of great societal importance to know what part of the warming observed during the last decades might be due to the solar variation (e.g., IPCC, 2001). Evidence for the existence of such a relation is given in extensive reviews by McCormac and Seliga (1978) and Pittock (1978, 1983), together with discussions of its robustness. It is also known that there is a correlation between the variation of the solar luminosity and the mean temperature on Earth (e.g., Reid, 2000; Muscheler et al., 2004). It has been claimed (e.g., Reid, 2000) that the terrestrial climate may react with variations of the order of up to 0.5 K to changes in luminosity in the course of the 20th century. Although such a strong response on a relatively short time-scale is highly questionable, this claim underlines the potential influence of the Sun on climate. From indirect proxies, such as solar spots, radio nuclides, it is deduced that the average solar luminosity increased over the past 100 years, and there have been a number of articles in newspapers and science journals discussing the role of the Sun for global warming in this context (e.g., Bond et al., 2001). It is commonly believed that the very recent rapid temperature increase over the past 20 years is not due to the Sun but most probably caused by man-made changes in the greenhouse effect. However, it is suspected that the Sun has contributed from 1/3 to 1/2 of the long-term change in pre-industrial climate (Crowley, 2000; Rind, 2002). Moreover, there have been periods with a climate remarkably different from the present one, such as during the Little Ice Age in the 17th century, and the most plausible explanation for the climate variation is based on a reduced solar luminosity during that time period.

However, the physicochemical mechanisms behind the above-mentioned correlations have not been clearly identified and the uncertainty of the solar forcing is still estimated by the experts as rather high (IPCC, 2001). The first process to be considered is the variation of the total solar irradiance (TSI), which depends on the activity of the Sun. With precise measurements of the total solar irradiance over the past 20 years it has been shown that the

1

total irradiance of the Sun varies by about 0.1 % (~2 W/m^2) over the duration of one 11-year solar activity cycle (Fröhlich, 2004). However, climate models showed that this forcing appears to be too small (North et al., 2004) to explain the response of the climate established from the statistical analysis of the observation records. From energy balance considerations the solar forcing of ~ 2 W/m^2 can change the surface temperature by about 0.2 K, if one assumes a mean value of climate sensitivity (IPCC, 2001). Therefore, if we believe in the results of the data analysis we have to consider some other mechanisms, which are able to amplify the response of the climate to the solar variability. Several ideas have been suggested for further investigation of the Sun's influence on Earth's climate. Reid (2000) formulated a short list of the most promising candidates comprising of the variability of

- solar particles outflow (solar wind) resulting in variable energetic particles input to the terrestrial atmosphere, and

- spectral solar irradiance, which in the ultraviolet is by orders of magnitude higher than in the visible.

However, from an entirely energy-balance-related point of view neither of these mechanisms can substantially change the global mean temperature, which is constrained by the total energy input; but they can redistribute the energy and modify the climate patterns, possibly causing significant local climate changes.

This work is devoted to the study of the latter mechanism, i.e. to the influence of the *spectral* solar irradiation variability on the chemistry and global climate. Satellite monitoring revealed that UV radiation is much more variable than the total radiation: the UV irradiance variability increases in general toward shortwave part of the spectrum and its magnitude during 11-year solar cycle can reach almost 100 % for Lyman-α line (Rottman et al., 2004). The visible radiation carries substantial energy (~ 43 % of the Total Solar Irradiance, TSI, or ~ 590 W/m^2), but its relative contribution to the TSI variability from the solar maximum to the solar minimum case is only of about 0.14 % (~ 0.8 W/m^2). Because the atmosphere is almost transparent for the visible radiation, most of this energy will be deposited at the surface or in the lower part of the troposphere, where a fraction of it can be absorbed by water vapour and aerosol. Despite the total energy carried by the UV radiation is much smaller (~ 8 % of TSI or ~ 110 W/m^2), the relative contribution of the UV variability to the total TSI variability is as high as 67 % (~ 1.6 W/m^2). In contrast to the visible radiation a substantial part of this energy is deposited in the middle atmosphere due to intensive absorption by the atmospheric ozone, oxygen and some other species (Brasseur and Solomon, 1984; Haigh, 2004). An enhancement of the UV irradiance results in an enhanced oxygen photolysis,

2

which in turn, results in an intensification of the ozone production, and a subsequent increase of the ozone mixing ratios in the middle stratosphere. The direct heating of the stratosphere due to absorption of an enhanced solar UV radiation and the indirect heating via elevated ozone levels provides an additional source of energy for the solar maximum case and heats the stratosphere mostly in the tropics and in the summer hemisphere, leading to the enhancement of the temperature gradient between winter hemisphere high-latitudes and tropical area. In general, this is expected to result in an intensification of the Polar Night Jet (PNJ) and changes in wave absorption. It further weakens the Brewer-Dobson circulation with subsequent ozone enhancement and warming in the tropical lower stratosphere. The lower stratosphere warming can be considered as a key element of this mechanism and can be used for its validation. The change of the planetary wave pattern in the troposphere (breaking Rossby and gravity waves at a given level) alters the Hadley-cell position and strength and redistribution of the surface air temperature similar to the positive phase of the Arctic oscillation (Thompson and Wallace, 1998; Rozanov *et al.*, 2004). This mechanism of downward propagation of direct solar UV-induced effects put forward by several groups (Hines, 1974; Haigh, 1996, 1999; Kodera, 1996; Hood *et al.*, 1993; Shindell *et al.*, 1999; Kodera and Kuroda, 2002) on the basis of theoretical investigations and model simulations. Thus, the primary effects of the solar irradiance changes from solar maximum to solar minimum should be clearly seen in the composition, temperature and dynamics of the middle atmosphere. Moreover, the above-mentioned mechanism of dynamical coupling can facilitate downward propagation of this purely radiative perturbation to the troposphere. The tropospheric effects are expected to be the most pronounced during the cold season, when the PNJ exists in the stratosphere. The validation of this mechanism focused on the analysis of the solar signal in the atmosphere during 1978-2003, because this period of time is covered by several satellite data sets and reanalysis products of global coverage (SPARC, 2000) based on the available observations. On the other hand many attempts to simulate the response of the atmosphere to the solar variability have been performed with different models. An extensive review of obtained results published by Hood (2004). However, the proposed mechanism could not be qualified as established, because the solar signal in ozone, temperature and zonal wind simulated by virtually all models does not agree well with the solar signal extracted from the observational data by means of various statistical analyses (e.g., Hood, 2004; and references therein). For example, all hitherto known models fail to reproduce the acceleration of the PNJ and the lower tropical stratosphere warming for the solar maximum case in comparison to the solar minimum case. Several potential reasons for the disagreement

3

between the simulated and the observed solar signal must be considered. First, the data analysis could be misleading because the available data sets reliably cover only two solar cycles, which from a statistical point of view is barely sufficient for a reliable retrieval of the solar signal. The coincidence of the solar maxima with large sulphur-rich volcanic eruptions (El Chichón 1982 and Mt. Pinatubo 1991) further complicates the proper extraction of the solar signal. As a consequence the analysis of different temperature data sets yields contradictory results. The analysis of the satellite data (e.g., Hood, 2004) does not reveal a significant annual mean temperature increase in the lower tropical stratosphere and therefore does not support the proposed mechanism. In contrast, the evaluations of the reanalysis data published by Hood (2004) and also by Labitzke (2001), Labitzke *et al.* (2002) and Rozanov *et al.* (2004) reveal a warming in the lower tropical stratosphere for the solar maximum as compared to the solar minimum. A better basis for the validation of the simulated ozone and temperature response in the middle atmosphere can be provided by the analysis of atmospheric response to the variability of the solar irradiance during the Sun's rotational cycle (see Hood, 2004; and references therein). However, given the very different time scale of this process such a comparison will not answer all questions, and is likely to help in understanding only the direct forcing of the middle atmospheric chemistry and thermodynamics due to the solar irradiance variability.

Setting aside the accuracy of the solar signal obtained from the observations, one must conclude that the models applied to study solar-climate issues are imperfect. The model suitable for this kind of studies should contain state-of-the-art description of the atmospheric dynamics in the troposphere, stratosphere and mesosphere and its sensitivity to radiative changes. The inclusion of the mesosphere appears to be essential because according to Kodera and Kuroda (2002) the downward propagation starts from the alteration of the subtropical night jet near the stratopause, which is controlled by the thermal state of the upper stratosphere and lower mesosphere. Also the perturbation of ozone plays an important role as became clear from the findings of Haigh (1996, 1999). Accordingly the model should have a full representation of the chemistry in the stratosphere and mesosphere. The radiation processes, as main drivers of solar-induced changes in the middle atmosphere, should be given specific attention. Furthermore, a reasonably good representation of the troposphere (dynamics, radiation, clouds, evaporation and precipitation, convection, turbulent mixing and so on) and surface (radiation, energy balance, heat capacity, evaporation and so on) is necessary to evaluate the climate change due to introduced perturbation of the solar spectral irradiation. Thus, a model suitable for studies of the solar-climate connection must be a

chemistry-climate model (CCM) with sufficient resolution of the necessary process in the middle and higher atmosphere. Of course, such a model should also have a good performance in simulating the present day climatology. For example, the observed connections between the strength of the polar vortex and other simulated quantities should be properly taken into account. The latter is very important because the proposed coupling mechanism is based on the response of the polar vortices and subsequent alteration of other quantities.

Several attempts to simulate the solar signal using state-of-the-art CCMs have been performed by Shindell *et al.* (1999), Rozanov *et al.* (2000, 2004), Labitzke *et al.* (2002), Tourpali *et al.* (2003). However, none of these models meets all of the above-mentioned criteria. The GISS model (Shindell *et al.*, 1999) has rather low horizontal resolution and the chemistry is highly parameterised. The UIUC CCM (Rozanov *et al.*, 2000, 2004) extends vertically only up to 1 hPa, which presumably hampers its ability to simulate atmospheric dynamics and temperature in the upper stratosphere. Two CCMs presented by Labitzke *et al.* (2002) do not properly account for mesospheric processes such as radiative heating and photolysis at the Lyman-α line, which has the highest variability during solar cycle. Tourpali *et al.*'s (2003) model has only two spectral intervals (250-680 nm and 680-4000 nm), which is not sufficient to represent the solar heating in the stratosphere and mesosphere. Therefore, three years ago, at the start of the present work, it appeared to be of utmost interest to develop a new CCM, which can better address all relevant processes, simulate the global chemistry and climate response to the solar irradiance variability at different time scales, and compare the results with observations and other models.

Thus, the main goals of this study were:

- to develop a state-of-the-art CCM spanning the atmosphere from the ground to the mesopause, which includes extensive representation of the physical and chemical processes relevant to the troposphere, stratosphere and mesosphere and suitable for the study of different aspects of Sun-Earth relationship with steady-state and transient modes;

- to validate the model performance by simulating the present day climatology and the sensitivity of the model quantities to the strength of the polar vortices;

- to perform a number of time-slice simulations with prescribed monthly sea-surface temperature and sea ice (SST/SI) distributions in order to simulate the response of the atmospheric chemistry and dynamics to the spectral solar irradiance variability during

5

the 11-year solar activity cycle and the 27-day Sun rotation cycle, and to estimate their statistical significance;

- to separate the effects of the ultraviolet and visible radiation changes on the atmospheric chemistry and dynamics;

- to compare the simulated results with the solar signal obtained from statistical analyses of various observational data;

- to analyze the chain of chemical and dynamical processes responsible for the atmospheric response to the solar irradiance variability;

- to offer the basis for extensive transient runs spanning several decades in comparison with observations;

- to propose ways forward for further model development and advanced studies of the solar-climate connection.

The results obtained during the study have been presented in five papers, which form Chapters 2-5 of the thesis. The CCM SOCOL developed in the framework of this thesis will be described in the Chapter 2 together with its detailed validation against available observation data (work published in the *Atmospheric Chemistry and Physics Discussion*). In Chapter 3 the simulated response of the atmospheric chemistry and climate to the decadal scale spectral solar irradiance variability is presented (one paper published in *Geophysical Research Letters*, a second paper is in press to *Advances in Space Research*, a third paper is in preparation for *Journal of Geophysical Research*). Chapter 4 is devoted to the analysis of the atmospheric response to the short-term variability of the solar irradiance during the Sun's rotational cycle (work prepared for submission to *Journal of Atmospheric and Solar-Terrestrial Physics*). The possible ways of model improvement and future activity aimed to study solar-climate links in a frame of ETHZ Poly-Project "Variability of the Sun and Global Climate" are discussed in the Chapter 5.

Specifically, my (T.E.) contributions to the various papers contained in this thesis are as follows:

Chapter 2:

- modification of chemistry-transport model: include mesospheric chemistry; update of photolysis rate coefficients according to the latest relevant publications; implementation of new PSC parameterisation;

- model validation against available observation data;

- writing the paper.

Chapter 3:

- implementation of additional heating due to oxygen and ozone absorption parameterisation on the basis of Strobel approach;
- performing the experiments;
- analysis of the results;
- comparison with analysis of observations;
- writing the paper

Chapter 4:

- performing the experiments;
- analysis of the results;
- comparison with observations.

References:

Bond G., Kromer B., Beer J., Muscheler R., Evans, Showers W., Hoffmann Sh., Lotti-Bond R., Hajdas I., Bonani G. (2001). Persistent solar influence on North Atlantic climate during the Holocene, *Science,* 294, 2130-2136.

Brasseur, G. and S. Solomon (1986). Aeronomy of the Middle Atmosphere, D. Reidel Publish. Comp., Dordrecht, 452 pp.

Crowley, T.J. (2000). Causes of climate change over the past 1000 years, *Science,* 289, 270-277.

Fröhlich, C. (2004). Solar irradiance variability, in Geophysical Monograph **141**: Solar Variability and its Effects on Climate, *AGU,* 97-110.

Intergovernmental Panel of Climate Change (IPCC) (2001). *Climate Change 2001: The Scientific Basis,* 881pp., Cambridge Univ. Press, New York.

Haigh, J.D. (1996). The impact of solar variability on climate, *Science,* **272**, 981-984, 1996.

Haigh, J. (1999). A GCM study of climate change in response to the 11-year solar cycle, *Quart. J. Roy. Meteorol. Soc.,* **125**, 871-892.

Haigh, J. (2004). Fundamentals of the Earth's atmosphere and climate, in Geophysical Monograph **141**: Solar Variability and its Effects on Climate, *AGU,* 65-82.

Hines, C. O. (1974). A possible mechanism for the production of Sun-weather correlations, *J. Atmos. Sci,* **31**, 589-591.

Hood, L.L., J. Jirikovich & J. P. McCormack (1993). Quasi-decadal variability of the stratosphere: Influence of long-term solar ultraviolet variations, *J. Atmos. Sci.*, **50**, 3941-3958.

Hood, L. L. (2004). Effects of solar UV variability on the stratosphere, in Geophysical Monograph **141**: Solar Variability and its Effects on Climate, *AGU*, 283-303.

Kodera, K. (1996). On the origin and nature of the interannual variability of the winter stratospheric circulation in the northern hemisphere, *J. Geophys. Res.*, **100**, 14077-14087.

Kodera, K. and Y. Kuroda (2002). Dynamical response to the solar cycle, *J. Geophys. Res.*, *107*,4749,doi:10.1029/2002JD002224.

Labitzke, K. (2001). The global signal of the 11-year sunspot cycle in the stratosphere: Differences between solar maxima and minima, *Meteorol. Zs.*, **10**, 83-90.

Labitzke, K., J. Austin, N. Butchart, J. Knight, M. Takahashi, M. Nakamoto, T. Nagashima, J. Haigh, V. Williams (2002). The global signal of the 11-year solar cycle in the stratosphere: observations and models, *J. Atm. Sol. Terr. Phys.*, **64**, 203-210.

McCormac, B. M., and T. A. Seliga (eds.) (1978). Solar-Terrestrial influences on weather and climate, D. Reidel Publ. Company, 346 pp.

Muscheler, R., J. Beer, and P. Kubik (2004). Long-term solar variability and climate change based on radionuclide data from ice cores, in Geophysical Monograph **141**: Solar Variability and its Effects on Climate, *AGU*, 221-236.

North, G., Q. Wu, and M. Stevens (2004). Detecting the 11-year solar cycle in the surface temperature field, in Geophysical Monograph **141**: Solar Variability and its Effects on Climate, *AGU*, 251-260.

Pittock, A. B. (1978). A critical look at long-term sun-weather relationships, *Rev. of Geophys. and Space Physics*, **16**, 400-420.

Pittock, A. B. (1983). Solar variability, weather and climate: an update, *Quart. J .Roy. Meteorol. Soc.*, **109**, 23-55.

Reid, G. (2000). Solar variability and Earth's climate: introduction and overview, in "Solar variability and climate", E. Frils-Christiansen, C. Fröhlich, J. Haigh, M. Schüssler, and R. von Steiger (Eds.), *Space Sciences Series of ISSI*, **11**, Kluwer Academic Publisher, 1-14.

Rind, D. (2002). The sun's role in climate variability, *Science*, 296, 673-677.

Rottman, G., L. Floyd, and R. Viereck (2004). Measurement of the Solar Ultraviolet Irradiance, in Geophysical Monograph **141**: Solar Variability and its Effects on Climate, *AGU*, 111-125.

Rozanov, E., M. E. Schlesinger, F. Yang, S. Malyshev, N. Andronova, V. Zubov, and T. Egorova (2000). Sensitivity of the UIUC Stratosphere/Troposphere GCM with Interactive Photochemistry to the Observed Increase of Solar UV Radiation, *Proceedings of the Second SPARC General Assembly.*

Rozanov, E.V., Schlesinger M.E., Egorova T.A., Li B., Andronova N., Zubov V.A. (2004). Atmospheric response to the observed increase of solar UV radiation from solar minimum to solar maximum simulated by the UIUC climate-chemistry model. *J. Geophys. Res.* **109**, D01110, doi:10.1029/2003JD003796.

Shindell, D., D. Rind, N. Balachandran, J. Lean, and P. Lonergran (1999). Solar cycle variability, ozone, and climate, *Science*, **284**, 305-308.

SPARC (2002): SPARC Intercomparison of Middle Atmosphere Climatologies. *SPARC Rep.* 3, 96 pp.

Thompson, D., and J. Wallace (1998). The arctic oscillation signature in the wintertime geopotential height and temperature fields, *Geophys. Res. Lett.*, **25**, 1297-1300.

Tourpali, K., Schuurmans, C., van Dorland, R., Steil, B., Brühl, C. (2003). Stratospheric and tropospheric response to enhanced solar UV radiation: A model study. *Geophys. Res. Lett.*, **30**, 1231, doi: 10.1029/2002GL016650.

Seite Leer /
Blank leaf

2. Modeling tool

Chemistry-Climate Model SOCOL:
A Validation of the Present-Day Climatology

T. Egorova[1,2], E. Rozanov[1,2], V. Zubov[3], E. Manzini[4], W. Schmutz[1], and T. Peter[2]

Abstract. In this paper we document "SOCOL", a new chemistry-climate model, which has been ported for regular PCs and shows good wall-clock performance. An extensive validation of the model results against present-day climate obtained from observations and assimilation data sets shows that the model describes the climatological state of the atmosphere for the late 1990s with reasonable accuracy. The model has a significant temperature bias only in the upper stratosphere and near the tropopause in the tropics and high latitudes. The latter is the result of the rather low vertical resolution of the model near the tropopause. The former can be attributed to a crude representation of the radiation heating in the middle atmosphere. A comparison of the simulated and observed link between the tropical stratospheric structure and the strength of the polar vortex shows that in general, both observations and simulations reveal a higher temperature and ozone mixing ratio in the lower tropical stratosphere for the case with stronger Polar night jet (PNJ) as predicted by theoretical studies.

2.1 Introduction

Forecasting future ozone and climate changes is among the most pressing and challenging problems in contemporary environmental science. The Earth's climate is determined by a variety of physical and chemical processes within a complex system reacting to various external forcings, as well as by short-term and long-term internal variability (IPCC, 2001). Therefore, projections of the atmospheric state can be made only by means of sophisticated modeling tools, which are able to represent all known atmospheric physical and chemical processes and their interactions. During the previous decade the development of such tools was substantially advanced reflecting the need for reliable climate and ozone layer forecasting on the one hand and the tremendous growth of computational capabilities on the other hand. Part of these advances lead to the development of atmosphere and chemistry coupled models, the so-called

---

[1] Institute for Atmospheric and Climate Science ETH, Zürich, Switzerland
[2] Physical-Meteorological Observatory/World Radiation Center, Davos, Switzerland
[3] Main Geophysical Observatory, St.-Petersburg, Russia
[4] National Institute for Geophysics and Volcanology, Bologna, Italy

Chemistry-Climate Models (CCMs) (see Austin et al. (2003), and references therein). Each of these models comprises a General Circulation Model (GCM) of the atmosphere plus a representation of the atmospheric gas phase and heterogeneous chemistry in an interactive way and is able to simulate most of the physical and chemical processes in 3-dimensional space and their evolution in time. However, when applied to the simulation of future climate changes and ozone recovery in the 21th century these models may produce rather different results. For example, the GISS CCM (Shindell et al., 1998) predicted a delay of ozone recovery over the Arctic due to the influence of greenhouse gases (GHG), while the DLR CCM (Schnadt et al., 2002) predicted acceleration and the CCSR/NIES CCM (Nagashima et al., 2002) did not show any changes in ozone recovery under changing climate conditions. This controversy undermines the credibility of models and their reliability in producing climate forecasts useful for society and policymakers.

To increase model credibility more attention needs to be paid to extensive model validation. First, the climatology simulated by ensemble runs (using a single model) should be compared with available data sets to make sure that the model has no substantial biases caused by erroneous representations of important processes. Second, the simulated time evolution of the atmospheric state in response to all known forcing mechanisms should be validated against observed trends to examine the model's ability of simulating atmospheric responses. Third, the model should be evaluated with respect to the reproduction of the internal variability of the atmosphere. This process-oriented model validation has been discussed by Eyring et al. (2004), who assembled many useful processes in tabular form for consideration by the modeling community. Each of these three steps in model validation is not straightforward and has their own caveats, mostly because our knowledge of atmospheric climatology and processes is incomplete. In this paper we only discuss model validation with regard to the first and third points.

At the moment we have a great deal of information about the global present-day atmosphere from the last 25 years of intensive satellite measurements, but only limited knowledge about potential variability in global atmospheric parameters before this period. On the other hand, there is evidence from historical studies (e.g., Brönnimann et al., 2004) that atmospheric variability could have been much larger in the past than in the present day atmosphere. Therefore, the present day climatology obtained mainly from satellite observations should be considered as only one particular realization of a general sequence. Deviations of a simulated climatology from the particular observed climatology, or even from a particular reality (namely the one assumed by planet Earth), should be interpreted with caution. The statis-

tical significance of deviations must be estimated to determine where the deviations between model and reality are significant, i.e. where the discrepancies are not compatible with the null hypothesis that the deviation could be explained in terms of a system anomaly. The particular locations, time periods, physical quantities or relationships, where significant deviations occur, might be called "hotspots". In practical terms a determination of "hotspots" may be rather difficult simply because we often do not know the statistical properties of the real atmosphere for certain conditions. For the validation of a model climatology one usually applies assimilated data products (e.g. Butchart and Austin, 1998; Pawson et al., 2000). These data sets are the results of simulations with a comprehensive model running in assimilation mode, e.g. a numerical weather prediction model with a variety of available observations integrated into the model to enable better representation of the mean state of the atmosphere and its variability. The various assimilation schemes and applied models differ substantially and provide alternative atmospheric states, which can be considered as different realizations of the contemporary climate. This variability together with interannual variability of the observed and simulated meteorological fields provides a basis to estimate the statistical significance of the model errors and define model "hotspots", i.e. regions in space and time where the model deficiency is the most pronounced and statistically significant.

Recently, process-oriented validation of CCMs has gained a lot of attention because this approach opens new opportunities to validate models. This kind of validation was designed to reinforce the standard comparisons of simulated results with an observed climatology. Model abilities to reproduce atmospheric processes can be directly compared with observations (Eyring et al., 2004). The first attempt of process-oriented validation of CCMs has been performed by Austin et al. (2003). In 2003 a workshop on process-oriented validation of coupled chemistry-climate models was organized in Garmisch-Partenkirchen/Grainau, Germany, where a list of processes, diagnostics, and data sets of key importance for model validation was compiled. Presently (2004/05) the list is open for discussion at URL::://www.pa.op.dlr.de/workshops/ccm2003/. Here we present an example of process-oriented validation that we believe can be used to validate CCMs in general, namely the comparison of the simulated and observed response of stratospheric ozone and temperature to the strength of the northern polar vortex during boreal winter. It is well known (e.g., Baldwin, 2000) that during the winter season, a strong polar vortex coincides with the positive phase of the Arctic Oscillation (AO).

In this paper we present the description and validation of the present day climatology of the new CCM SOCOL (modeling tool for studies of SOlar Climate Ozone Links) that has

13

been developed at PMOD/WRC, Davos in collaboration with ETH Zürich and MPI Hamburg. The meteorological fields generated by the model are compared with the data obtained from different assimilation products and model "hotspots" are defined. For the validation of chemical species we resort again to the standard approach (i.e., the comparison of the simulated and observed climatologies without statistical significance analysis), because only one reference data set (URAP: Upper Atmosphere Research Satellite Reference Atmosphere Project) is available at the moment.

The layout of this paper is as follows: In Section 2.2 we describe the CCM SOCOL and the design of the runs performed with it, in Section 2.3 we describe data that we use for model validation, and in Section 2.4 we present the results of the model validation. In particular, we show the deviation of the simulated meteorological fields from the observations and their statistical significance. We also present a comparison of the simulated total ozone and other gases with satellite measurements and illustrate the sensitivity of the ozone and temperature to the strength of the northern polar vortex during boreal winter. The last section presents our conclusions.

2.2 Description of Chemistry-Climate Model SOCOL

The chemistry-climate model SOCOL has been developed as a combination of a modified version of the MA-ECHAM4 GCM (Middle Atmosphere version of the "European Center/Hamburg Model 4" General Circulation Model) (Manzini et al., 1997; Charron and Manzini, 2002) and a modified version of the UIUC (University of Illinois at Urbana-Champaign) atmospheric chemistry-transport model MEZON described in detail by Rozanov et al. (1999, 2001) and Egorova et al. (2001, 2003).

2.2.1   GCM Module

The MA-ECHAM4 model is the middle atmosphere version of ECHAM4 (Roeckner et al., 1996a,b), which has been developed at the Max Planck Institute for Meteorology in Hamburg. It is a spectral model with T30 horizontal truncation resulting in a grid spacing of about 3.75°; in the vertical direction the model has 39 levels in a hybrid sigma-pressure coordinate system spanning the model atmosphere from the surface to 0.01 hPa; a semi-implicit time stepping scheme with weak filter is used with a time step of 15 min for dynamical processes and physical process parameterizations; full radiative transfer calculations are performed every 2

14

hours, but heating and cooling rates are calculated every 15 min. The radiation scheme is based on the ECMWF radiation code (Fouquart and Bonnel, 1980; Morcrette, 1991). The orographic gravity wave parameterization is based on the formulation of McFarlane (1987). The parameterization of momentum flux deposition due to a continuous spectrum of vertically propagating gravity waves follows Hines (1997a,b), and the implementation of the Doppler spread parameterization is according to Manzini et al. (1997). A more detailed description of MA-ECHAM4 can be found in Manzini and McFarlane (1998), and references therein. With respect to the standard MA-ECHAM4, the gravity wave source spectrum of the Doppler spread parameterization has been modified. Namely, the current model version uses a spatially and temporally constant gravity wave parameter for the specification of the source spectrum, as in case UNI2 of Charron and Manzini (2002). Therefore, an isotropic spectrum with a gravity wave wind speed of 1 m/s and an effective wave number $K^*=2\pi(126 \text{ km})^{-1}$ is launched from the lower troposphere, at about 600 hPa.

2.2.2 CTM Module

The chemical-transport part MEZON (Model for the Evaluation of oZONe trends) simulates 41 chemical species (O_3, $O(^1D)$, $O(^3P)$, N, NO, NO_2, NO_3, N_2O_5, HNO_3, HNO_4, N_2O, H, OH, HO_2, H_2O_2, H_2O, H_2, Cl, ClO, HCl, HOCl, $ClNO_3$, Cl_2, Cl_2O_2, CF_2Cl_2, $CFCl_3$, Br, BrO, $BrNO_3$, HOBr, HBr, BrCl, $CBrF_3$, CO, CH_4, CH_3, CH_3O_2, CH_3OOH, CH_3O,CH_2O, and CHO) from the oxygen, hydrogen, nitrogen, carbon, chlorine and bromine groups, which are determined by 118 gas-phase reactions, 33 photolysis reactions and 16 heterogeneous reactions on/in sulfate aerosol (binary and ternary solutions) and polar stratospheric cloud (PSC) particles (Carslaw et al., 1995). The diagnostic thermodynamic scheme for the calculation of the condensed phase content of PSCs also makes use of the vapor pressure of nitric acid trihydrate (NAT) following Hanson and Mauersberger (1988). The PSC scheme uses predescribed cloud particle number densities and assumes the cloud particles to be in thermodynamic equilibrium with their gaseous environment. It allows the description of the condensation and evaporation of the PSC without detailed microphysical calculations. Sedimentation of NAT and ice (type I and II) PSC particles is described according to the approach proposed by Butchart and Austin (1996). The chemical solver is based on the implicit iterative Newton-Raphson scheme. The basic routine of the solver has been accelerated to improve its computational performance. A special acceleration technique for solving a sparse system of linear algebraic equations was developed and used. This technique utilizes the following main ideas: (1) the algorithm of the LU-decomposition/back-substitution of the Jacobian matrix is modi-

fied to include only nonzero operations (LU denotes the lower/upper triangular matrix decomposition regularly used in numerical analysis to solve a system of linear equations); (2) the Jacobian matrix is rearranged according to the number of nonzero elements in the row: this rearranging allows minimization of the number of the nonzero calculations during the LU decomposition/back-substitution process; and (3) the sequence of rows of the Jacobian matrix depends only on the photochemical reaction table used in the model and is the same for all grid cells of the model domain (Sherman and Hindmarsh, 1980; Jacobson and Turco, 1994). The reaction coefficients are taken from DeMore et al. (1997) and Sander et al. (2000). The photolysis rates are calculated at every step using a look-up-table approach (Rozanov et al., 1999). The transport of all considered species is calculated using the hybrid numerical advection scheme of Zubov et al. (1999). The transport scheme is a combination of the Prather scheme (Prather, 1986), which is used in the vertical direction, and a semi-Lagrangian (SL) scheme, which is used for horizontal advection on a sphere (Williamson and Rasch, 1989). The use of the Prather scheme ensures good representation of concentration gradients in the vertical direction. The SL scheme for the horizontal transport allows a significantly larger time step even near the poles where the sizes of the grid cells are smaller. Furthermore, use of the Prather scheme for transport in only one dimension (instead of three) reduces the number of moments that define the distribution of species in each model grid box from 10 to 3. Thus, the combination of the SL scheme with the Prather scheme yields a significant gain in economy in the transport calculations compared with using the Prather scheme alone, while attaining accuracy higher than that of the SL scheme alone. A detailed description of the design and performance of the hybrid transport scheme based on simple analytical tests is given by Zubov et al. (1999). MEZON has been extensively validated against observations in off-line mode, driven by UKMO meteorological fields (Rozanov et al, 1999; Egorova et al., 2003) and in on-line mode as a part of UIUC CCM (Rozanov et al., 2001). It has been coupled to different GCMs to study Pinatubo aerosol effects (Rozanov et al., 2002a) and influence of 11-year solar variability influence on global climate and photochemistry (Rozanov et al., 2004; Egorova et al., 2004).

2.2.3 GCM-CTM Interface

For the coupling with MA-ECHAM4, MEZON has been improved to take into account the latest revisions of the chemical reaction constants. Several photolytic and gas-phase reactions that are potentially important for mesospheric chemistry have been added to the model. They are manly photolysis of water vapor and methane and reactions of hydrogen with oxygen and

16

ozone. The new scheme for photolysis rate calculations spans the spectral region 120-750 nm divided into 73 spectral intervals and now specifically includes the Lyman-α line and the Schumann–Runge continuum. We have tested its performance using a 1-D chemistry-climate model (Rozanov et al., 2002b). The GCM and CTM modules of SOCOL are fully coupled via the three-dimensional fields of wind, temperature, ozone and water vapor. The GCM provides the horizontal and vertical winds, temperature and tropospheric humidity for the CTM, which returns 3-D fields of the ozone and stratospheric water vapor mixing ratios back to the GCM in order to calculate radiation fluxes and heating rates.

2.2.4 Community Model

To make SOCOL available for a wide scientific community we ported the entire CCM on desktop personal computers (PCs). A 10-year long simulation takes about 40 days of wall-clock time on a PC with a processor running at 2.5 GHz, which allows the performance of multiyear integrations. The simultaneous use of several PCs allows the performance of ensemble calculations with ease. Reasonable model performance and availability of personal desktop computers makes SOCOL available for application by scientific groups around the world without access to large super-computer facilities, opening wide perspectives for model exploitation and improvement. The technical information is given at the end of the paper.

As a first step toward the validation of SOCOL we have carried out a 40-year long control run for present day conditions (for our steady-state experiment, the 40-year control run is equivalent to a one year ensemble run with 40 ensemble members). For this run we used sea surface temperature and sea ice (SST/SI) distributions prescribed from AMIP II monthly mean distributions, which are averages from 1979 to 1996 (Gleckler, 1996). The lower boundary conditions for the source gases have been prescribed following Rozanov et al. (1999) and are representative for conditions of 1995. The mixing ratio of CO_2 is set to 356 ppmv everywhere. The initial distributions of the meteorological quantities and gas mixing ratios have been adopted from MA-ECHAM4 and from an 8-year long Stratospheric CTM run (Rozanov et al., 1999). As a source for the chemical species we use prescribed mixing ratios of the source gases in the planetary boundary layer, prescribed NO_y sources from airplanes, anthropogenic activity and lightning, similar to Rozanov et al. (1999). Later on in this paper we will analyze the 40-year mean of the simulated quantities (model climatology) and their standard deviations, which reflect the interannual variability of the model.

17

2.3 Description of the data used for validation

To validate the large-scale atmospheric behavior of the SOCOL model and to specify the significance of the model errors we use data sets for the middle atmosphere which are the results of the efforts of different meteorological institutions around the world: the European Center for Medium Range Weather Forecast (ECMWF), United Kingdom Meteorological Office (UKMO), National Center of Environmental Predictions (NCEP) and Climate Prediction Center (CPC) reanalysis projects. All data sets have been downloaded from the SPARC Data Center (http://www.sparc.sunysb.edu). Detailed descriptions of data sets used have been presented in the SPARC inter-comparison project of the middle atmosphere (SPARC, 2002). Some characteristic parameters of applied data sets are summarized in Table 1. According to the SPARC comparison report (SPARC, 2002) UKMO, CPC and NCEP are warm biased in the tropical tropopause area by 2-3 K, while ERA-15 and UKMO are warm biased in the upper stratosphere up to 5 K. To estimate the significance of the deviation of the simulated climatology from the observed climatology we have combined all data sets listed in Table 2.1 (except URAP data) in one data set. In doing this we obtained 64 years of observational data in a row for the validation (only 28 years of these include data are above 10 hPa). From this extended data set we have calculated a monthly mean climatology of the zonal wind and temperature as the mean of this 64-year long ensemble as well as the standard deviation of these quantities, which includes the interannual variability as well as variability due to differences between data sets. To validate the model winds in the mesosphere we used Upper Atmosphere Research Satellite (UARS) Reference Atmosphere Project (URAP) (http://code916.gsfc.nasa.gov) zonal mean zonal wind, which is a combination of UKMO winds in the stratosphere and the High Resolution Doppler Imager (HRDI) winds in the mesosphere (Swinbank and Ortland, 2003).

Table 2.1: Climatological data sets used for model validation.

Data source	Time period used	Upper level
UKMO	1992-1999 (8 years)	0.3 hPa
CPC	1979-1998 (20 years)	1 hPa
NCEP	1979-1999 (21 years)	10 hPa
ERA-15	1979-1999 (15 years)	10 hPa
URAP	1992-1999 (8 years)	0.01 hPa

18

Total ozone data have been taken from Nimbus 7, Meteor 3, ADEOS, Earth Probe TIROS Operational Vertical Sounder (TOVS), and Global Ozone Monitoring Experiment measurements and averaged over 10 years (1993-2002). For the comparison of ozone (O_3), water vapor (H_2O), and methane (CH_4) in the stratosphere we used the URAP data set (http://code916.gsfc.nasa.gov) that provides a comprehensive description of the reference stratosphere from the data recorded by several instruments onboard of UARS.
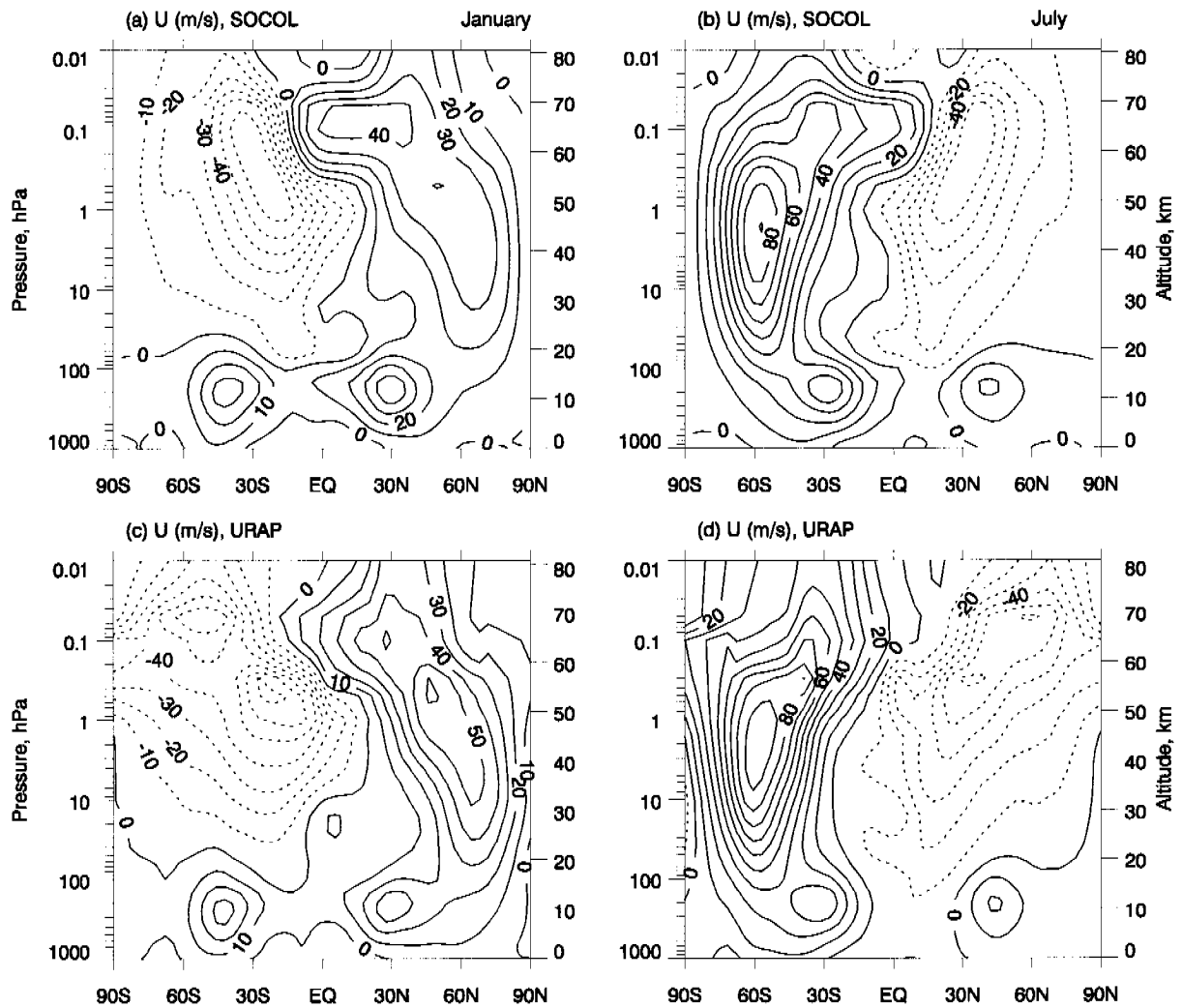

Figure 2.1: *Meridional cross-section of the zonal mean zonal wind (ms^{-1}) for January (left panel) and July (right panel): (a, b) simulated, (c, d) observed. Observed values are from URAP database.*

2.4 Results

2.4.1 Annual mean zonal mean zonal wind and temperature

2.4.1.1 Temperature and wind fields

Monthly means of zonally averaged zonal winds for January and July are presented in Figure 2.1 in comparison with the 8-year means of the same quantities acquired from the URAP data sets. The model reproduces all main climatological features of the observed zonal wind distribution qualitatively, and with a few exceptions even quantitatively. The separation of the stratospheric and tropospheric westerly jets is well simulated by SOCOL. The tropospheric subtropical jets, their shape and location are in good agreement as is the polar night jet (PNJ) core, in the middle and upper stratosphere. However, for January in the Northern Hemisphere
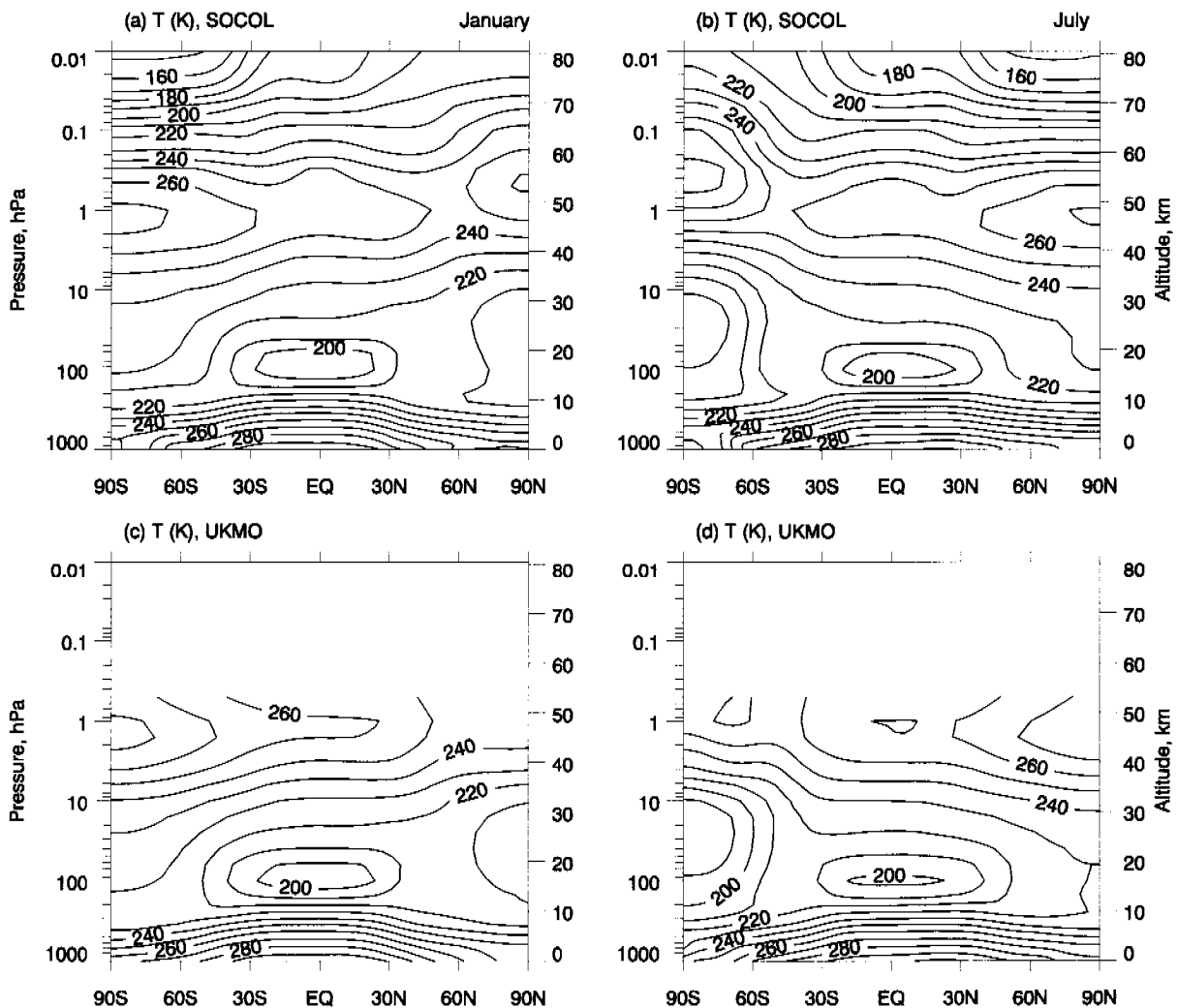

Figure 2.2: *Same as Figure 2.1 but for the zonal mean temperature (K). Observed values are from UKMO reanalysis.*

20

the intensity of the tropospheric subtropical jet is overestimated by about 10 ms^{-1}. The PNJ's intensity is underestimated by the same amount, and its maximum is located at higher altitudes than in the URAP data. SOCOL captures the observed equatorward tilt of the stratospheric westerly core. The most noticeable disagreement occurs in the lower mesosphere, where the simulated easterly winds do not penetrate to the high-latitude area over the summer hemisphere.

Figure 2.2 presents a comparison of latitude-pressure cross-sections of simulated and UKMO zonal mean temperatures for January and July. The evaluation of the temperature distribution reveals that in the lower stratosphere the general agreement of the location and magnitude of the simulated extremes is rather good. SOCOL reproduces the main observed features of zonal mean temperature distribution well: warm troposphere, cold tropical tropopause without apparent bias, cold winter middle stratosphere, warm summer stratopause, and the polar temperature minimum associated with the formation of the polar vortices.
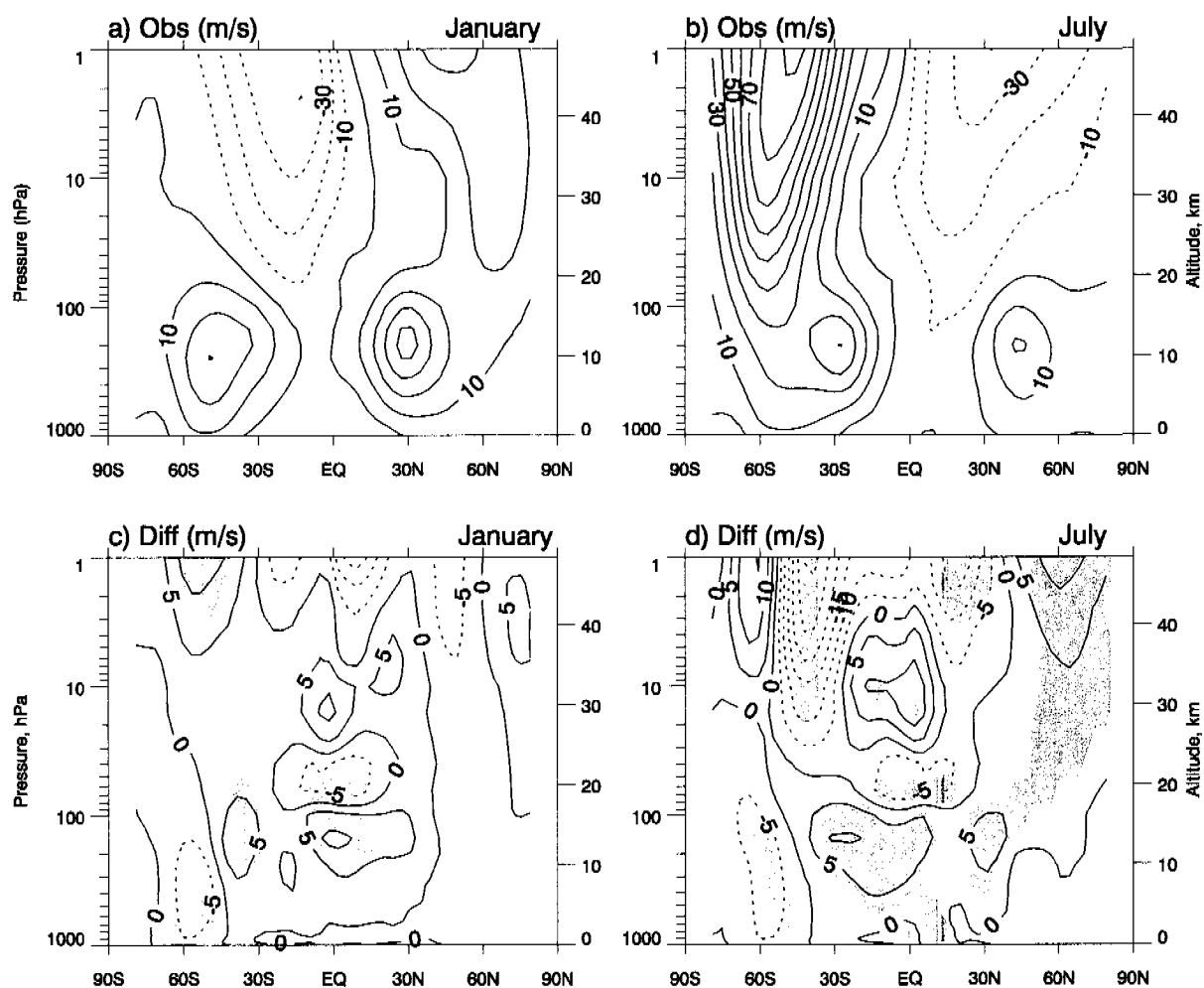

Figure 2.3: *Zonal mean zonal wind difference (ms^{-1}) between simulated and observed data, shaded hotspots areas means that the deviation is 95% statistically significant.*

2.4.1.2 Model/observation difference fields

A simple visual comparison of temperature and zonal wind fields has often been used to validate CCMs (e.g., Takigawa et al., 1999; Hein et al., 2001). From this kind of comparison one can only conclude how well a model reproduces the main observed features of the zonal mean temperature and zonal mean zonal wind structures in general. However, differences between simulated and observed fields do exist and it is very helpful to use a more quantitative analysis of model deviations from observations as it has been presented by Rozanov et al. (2001) and Jonsson et al. (2002). Due to noticeable discrepancies among the available reanalysis data (e.g., SPARC, 2002) it is difficult to judge the model performance precisely and to give recommendations on how a model could be improved. To estimate the significance of the model deficiencies we use a monthly mean observed climatology of the zonal wind (see Figure 2.3 a, b) and temperature (see Figure 2.4 a, b) and the standard deviation of these quantities described in Section 3. From the results of the 40-year long SOCOL integration we have also
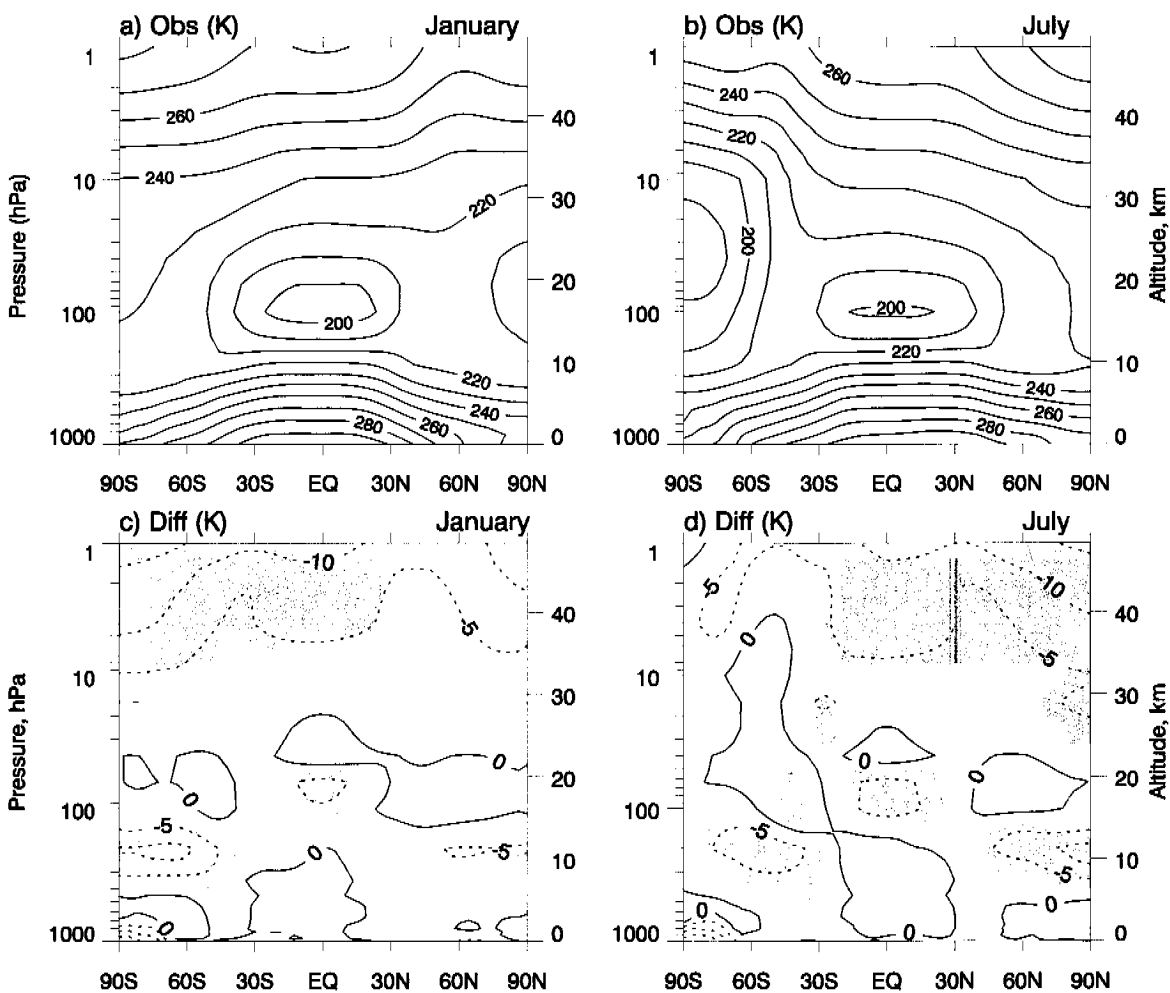

Figure 2.4: *Same as for Figure 2.3, but for temperature (K).*

22

calculated the climatology of the zonal wind (see Figure 2.1 a, b) and temperature (see Figure 2.2 a, b) and their standard deviations. Using these data sets we have calculated the difference between simulated and observed climatology and estimated the statistical significance of these deviations using the Student t-test.

Figure 2.3 (c, d) and 2.4 (c, d) show ensemble mean monthly mean deviations of the model from the observational data in January and July for zonal means of zonal wind and temperature accordingly. The gray spots mark the area where the model deviations from the observational data are statistically significant at the 95 % confidence level. In the zonal wind field these spots appear in the region of the extra tropical jets implying that SOCOL has a tendency to reproduce stronger (up to 5-10 m/s) jets in the troposphere. In July the model produces weaker (up to 10 m/s) easterlies in the upper stratosphere. Also significant deviations of simulated zonal mean zonal wind of up to 25 m/s can be seen over 30°S-60°S in July, suggesting that the meridional gradient of temperature in the model is too weak. All other deviations appear not to be statistically significant. In the temperature field (Figure 2.4 c, d) the model substantially deviates from the observational data near the tropopause and in the upper stratosphere of the summer hemisphere in high and middle latitudes. At the tropical tropopause and winter high latitude tropopause the discrepancies between simulated and observed data reach about -6 K and in the summer hemisphere tropopause the deviation is up to -10 K. There are also statistically significant deviations in the upper stratosphere over the summer hemisphere high latitudes of up to 10 K. All deviations are negative, showing that the model is cold biased relative to the data. The analysis of the simulated zonal mean zonal wind (U) and zonal mean temperature (T) deviations reveals the "hot spots" for SOCOL: for the further improvements of SOCOL it is necessary to pay special attention to the tropopause region in the tropics and at high latitudes as well as to the processes in the upper stratosphere and mesosphere where large cold bias has been found during summer time.

Figure 2.5 shows the seasonal variation of the simulated temperature (left panel) and zonal wind (right panel) deviations from observations at 1, 10 and 100 hPa (70 hPa for zonal wind). The shaded areas mark the "hotspots", i.e. statistically significant discrepancies between simulated and observed data. At 10 hPa the simulated temperature deviations from the observations are statistically insignificant. The simulated zonal wind at 10 hPa deviates in the middle latitudes of the Southern Hemisphere (SH) during summer, however the deviations do not exceed 5 m s^{-1}. At 1 hPa a statistically significant cold bias of about 9 K has been found in January and February over southern high latitudes, in May, June and November at the equator, and of about 6 K over the high latitudes in the Northern Hemisphere (NH) in June and

July. The positive deviations over the high latitudes in both hemispheres are not significant. At 100 hPa the model has a cold bias at the equator of up to 6 K and warm bias of up to 3 K in the extra tropical area during the boreal summer. The zonal wind deviation at 70 hPa is about ± 5ms^{-1} in the tropical and southern middle latitudes.

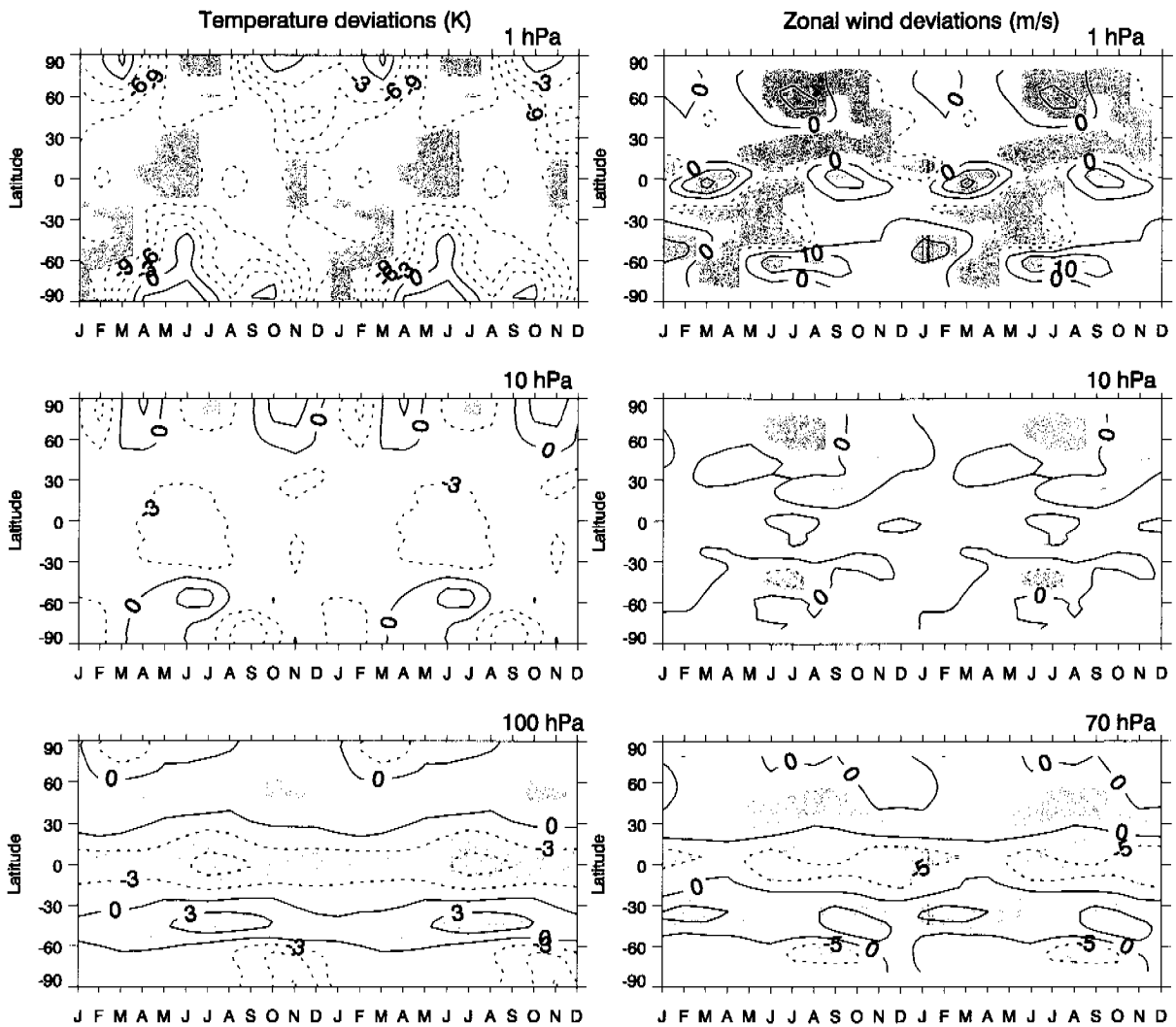**Figure 2.5:** *Deviations of the simulated temperature and zonal wind seasonal variation from the data for 1, 10 and 100 (70 for zonal wind) hPa.*

2.4.1.3 Summary

From the zonal mean and seasonal variation analysis of zonal wind and temperature we conclude that during boreal summer our model does not have enough heating at high latitudes and at the equator. This might be connected to the problem in radiation code of MA-ECHAM4, which describes the absorption of solar UV radiation by ozone and oxygen with a rather simplified scheme. We will return to this problem in Section 2.5. There are pronounced

temperature differences near the tropopause in the tropics and high latitudes. These model deficiencies can be explained by the rough vertical model resolution in the upper troposphere-lower stratosphere (E. Roeckner, presentation on COSMOS workshop, Hamburg, May, 2003).

2.4.2 Chemical aspects of the validation
2.4.2.1 Methane

Altitude dependence. Methane is the most abundant hydrocarbon in the atmosphere and useful as a tracer of atmospheric circulation because of its long photochemical lifetime. Hence, the methane distribution is determined mainly by features of the circulation. Figure 2.6 shows the meridional cross section of the CH_4 mixing ratio climatology simulated by SOCOL and observed by UARS together with their difference. The overall zonal mean distribution (CH_4 decreases with height and latitude) is similar to the observed one and the agreement is within ~ 10-20 % in the stratosphere. As a result of the transport by Brewer-Dobson circulation the tropical maxima of CH_4 concentration is shifted to the North during boreal summer and to the South during boreal winter. The subtropical transport barrier is also well simulated. The model reproduces downward motion over the poles but slightly too intensively and, therefore, at 10 hPa a 20 % (~ 0.1 ppmv) underestimation of the average CH_4 mixing ratio occurs.

Seasonal cycle. Latitude-time variations in the observed and simulated zonal average mixing ratio of CH_4 at 25 hPa are shown in Figure 2.7 (this is where CH_4 shows largest latitudinal gradients). The model reproduces the seasonal variation, which is similar to the HALOE data with a relative minimum over the high latitudes during December-February for the NH and September-November for the SH, while in the tropical area there is no apparent seasonal cycle. At 25 hPa the difference between simulated and observed data in the tropics and northern high latitudes is about 5 % and in the southern high latitudes the difference reaches about 15 % because of a half month shift of the minimum methane mixing ratio due to an unidentified reason.

2.4.2.2 Water vapor

Altitude dependence. Water vapor is an important tracer in the upper troposphere and lower stratosphere. In both regions H_2O is a source of HO_x radicals, which are involved in photosmog reactions producing ozone in the upper troposphere and in catalytic ozone destruction cycles in the stratosphere. Figure 2.8 presents meridional cross-sections of water vapor mixing ratios. The zonal-mean distribution of H_2O is well reproduced by SOCOL. However,

the model overestimates mixing ratio of H_2O compared to URAP data in the stratosphere by 0.5-1.0 ppmv (or 10-20 %), which is within the range of accuracy of HALOE measurements
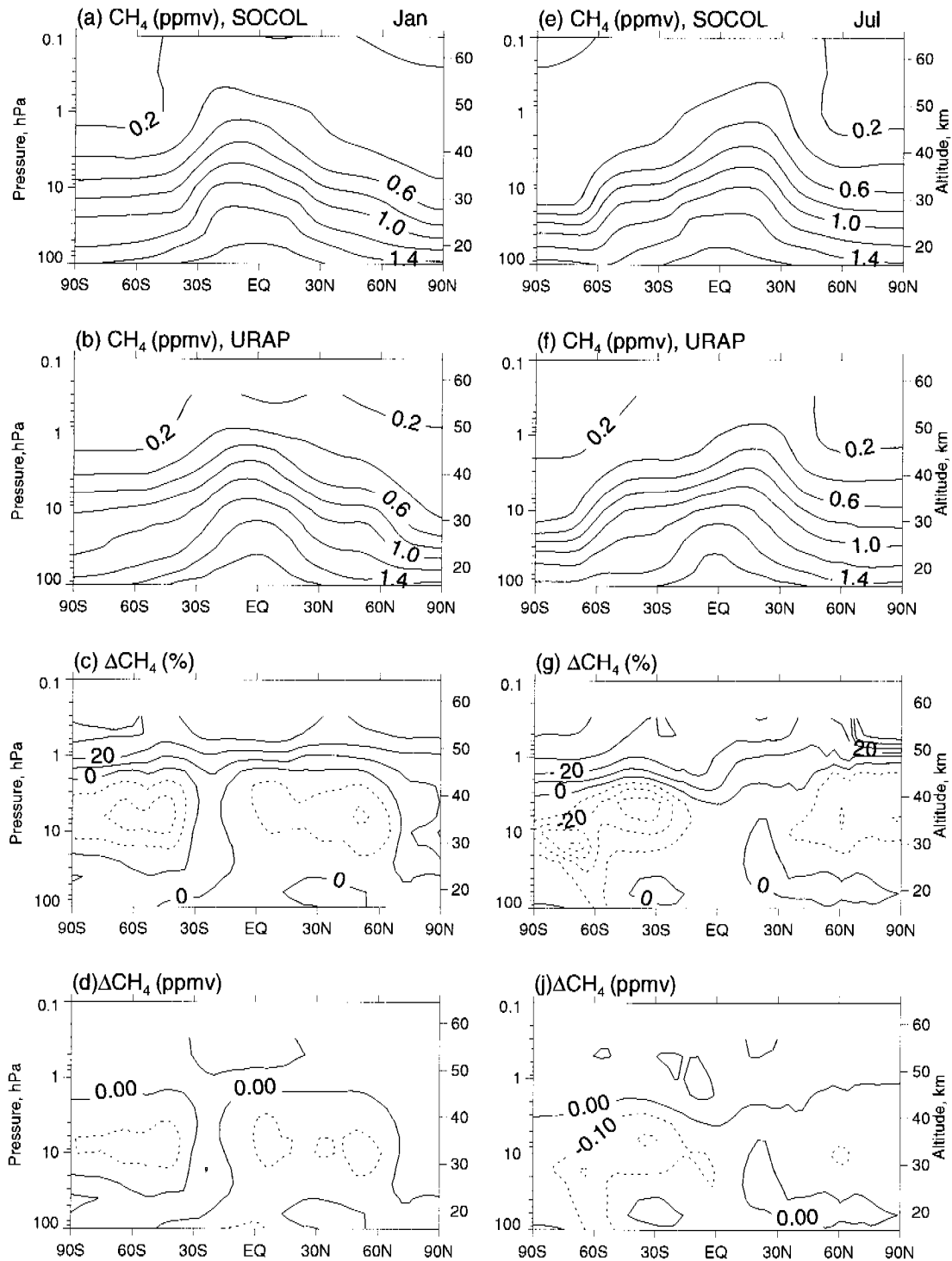

Figure 2.6: *Latitude-pressure cross-section of the CH₄ (ppmv) for January (left panel) and July (right panel): simulated (a, e), observed (b, f), and their differences in steps of ± 10 % (c, g) and in ±0.1 ppmv (d, j). Observed values are from URAP data set.*

26

(Harries et al., 1996). There are two sources of H_2O in the stratosphere: CH_4 oxidation in the stratosphere and upward H_2O transport from the troposphere. The latter depends in turn on the intensity of the upward branch of the Brewer-Dobson circulation, which determines vertical transport and the H_2O mixing ratio at the entry level. Figure 2.6 shows a small underestimation of CH_4 mixing ratios in the middle stratosphere, which implies that the vertical transport in our model is just slightly underestimated, therefore the overestimation of stratospheric H_2O is more likely connected to the overestimated H_2O mixing ratio at the entry level of the model.
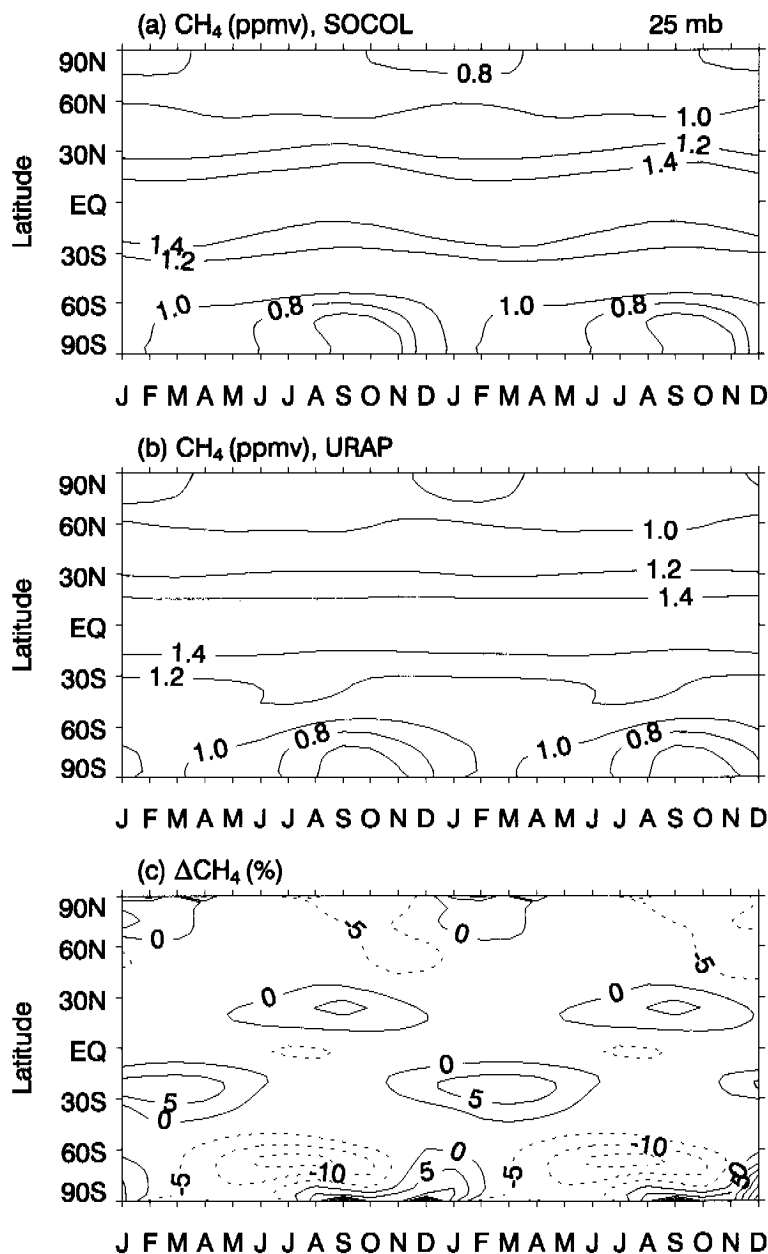
Figure 2.7: *Seasonal variation of methane at 25 hPa: (a) simulated, (b) observed, and (c) their difference in percents. Observed values are from the URAP data set.*
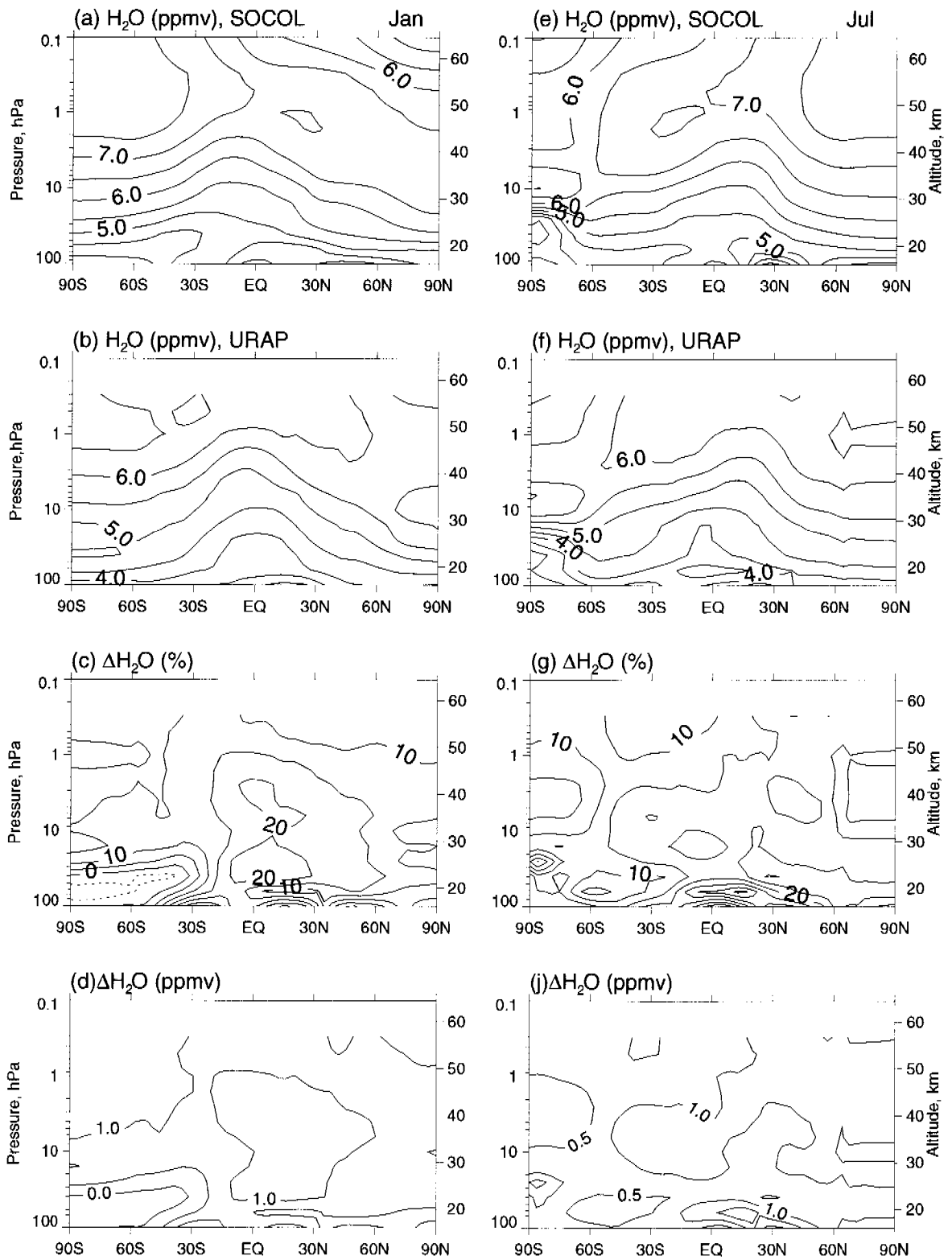
Figure 2.8: *Same as for Figure 2.6, but for water vapor (ppmv).*

Seasonal cycle. The seasonal variation of simulated H_2O mixing ratios at 10 hPa is compared with URAP data in Figure 2.9. The model and URAP data do not show a sufficiently strong annual cycle in the tropical middle stratosphere. Over the high latitudes both model and observations reveal elevated H_2O mixing ratios during wintertime, associated with aged air with low CH_4 descending into the polar vortices.
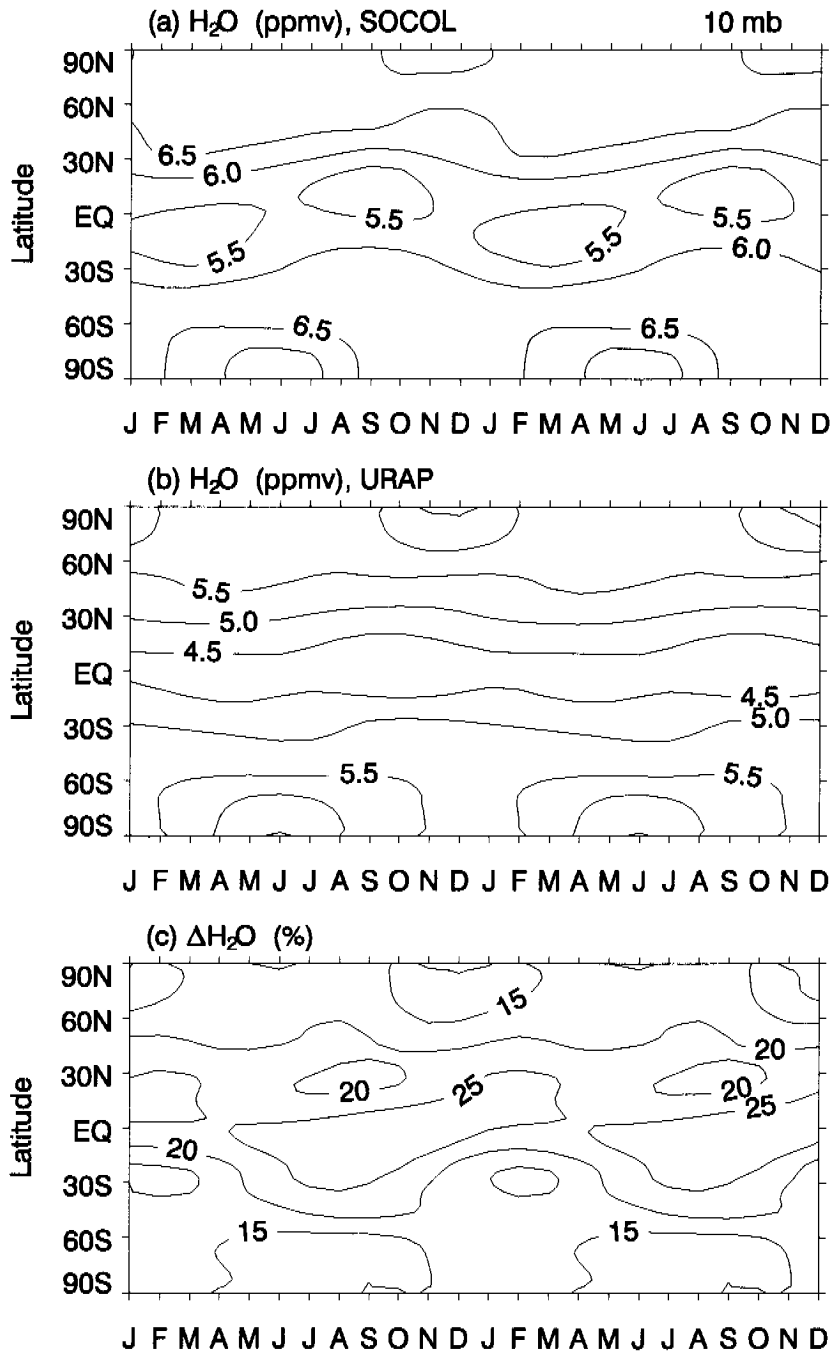
Figure 2.9: *Same as for Figure 2.7 but for water vapor at 10 hPa.*

Figure 2.10: *Altitude-time evolution of water vapor mixing ratio anomaly over the equator, derived from (a) SOCOL simulation and (b) HALOE observation. The data are shown as two consecutive seasonal cycles.*
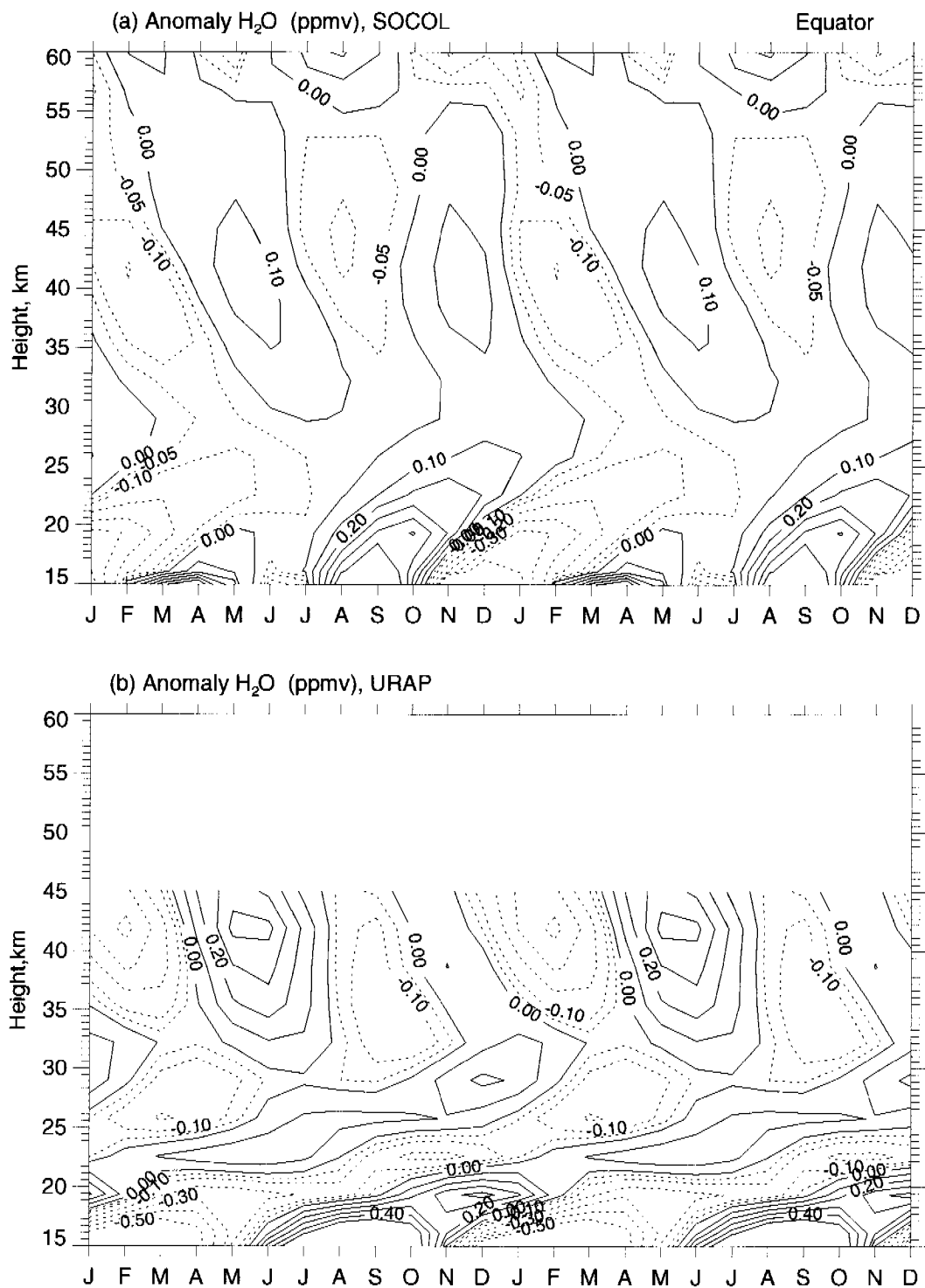
Figure 2.10 presents a comparison of the simulated and URAP-derived data set of the altitude-time anomaly in the H$_2$O mixing ratio (deviation from annual mean) over the equator.

The model reproduces the vertical propagation of the dry (negative) and wet (positive) anomalies induced by the water vapor changes in the lower stratosphere, i.e. water vapor "tape recorder" described by Mote et al. (1998). However, the model upward transport is up to twice as fast as observed. In order to quantitatively estimate the intensity of the upward water vapor transport we have calculated lagged correlations between deseasonalized H_2O mixing ratio anomalies at 16 km altitude and at different altitudes in the equatorial stratosphere. The correlation coefficients are plotted in Figure 2.11 for the 19.4, 22.7, 25.9, 29.1 and 32.3 km levels. The time when the maximum correlation is reached and the distance between levels allow the estimation of the vertical velocities in the equatorial lower stratosphere. For the plotted data the mean vertical velocity between 16 and 32.3 km is equal to ~0.6 mm/s, which exceeds the value obtained from the observed H_2O distribution by about 50-90%. The vertical velocity is larger in the lower stratosphere (around 1 mm/s), while between 29.1 and 32.3 km its magnitude is about 0.25 mm/s. Similar distributions of the vertical velocities have been reported by Steil et al. (2003). It is still not clear which part of the model is responsible for these discrepancies between the simulated and observed "tape recorder" features. In the upper stratosphere the model quantitatively matches the observed semi-annual oscillation with positive anomalies. (Figure 2.10).

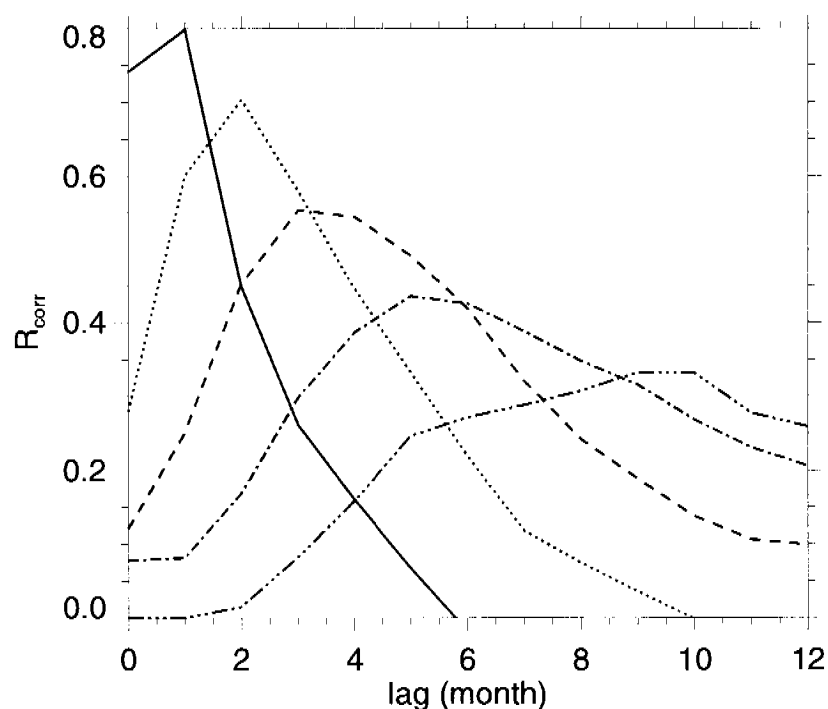**Figure 2.11:** *Lagged correlation coefficients of deseasonalised H_2O mixing ratio anomalies in the equatorial stratosphere at 16 km with the same quantity at 19.4 (solid line), 22.7 (dotted line), 25.9 (dashed line), 29.1 (dot-dashed line) and 32.3 (dot-dot-dashed line) km levels.*
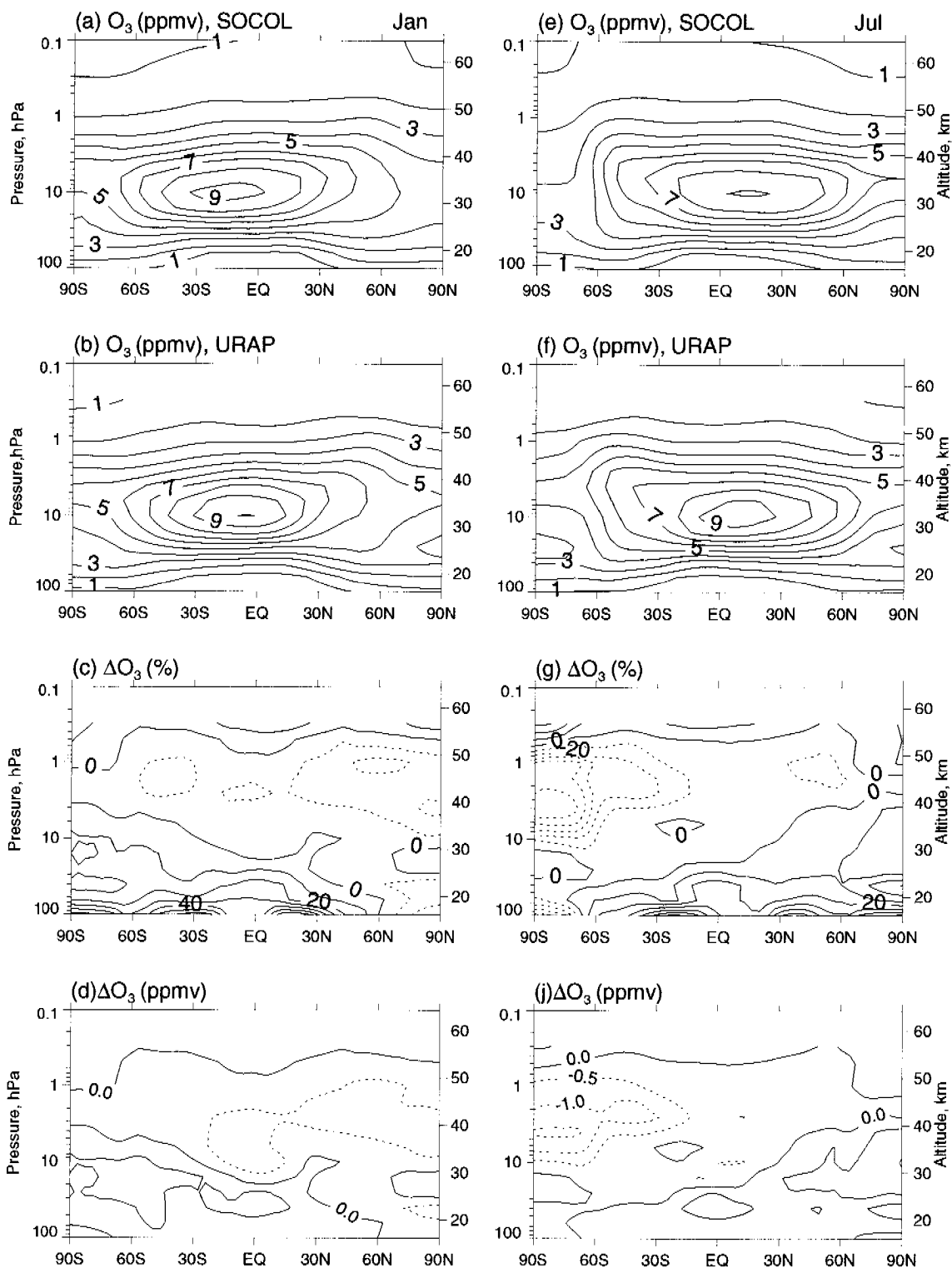
Figure 2.12: *Same as for Figure 2.6 but for O₃ (contour lines in steps of 1 ppmv). The difference in (c) is shown in steps of ± 10 %.*

2.4.2.3 Ozone

Altitude dependence. Figure 2.12 presents meridional cross sections of zonal mean monthly mean O_3 mixing ratios, simulated by SOCOL and observed by UARS together with their difference. The distribution of the simulated ozone is in good agreement with the observations throughout the stratosphere where the model errors remain basically within ± 10 %. The simulated maximum of the zonal mean (~ 9 ppmv) appears at the equator, at around 10 hPa, which is consistent with the observations. The so-called "banana" shape of the ozone distribution is also well captured by the model with high ozone regions extending to the upper polar stratosphere. The model substantially underestimates ozone over the southern high latitudes in the upper stratosphere during the austral winter season. The cause of the ozone underestimation could be related to (or identical to) the causes as for the underestimation of methane and the overestimation of water vapor in the same region: this could stem from a too strong isolation of the southern polar vortex and a too strong downward transport in the simulation. The fact that methane is longer-lived than ozone in these regions could be the reason for the methane discrepancy appearing only at lower altitudes.

Seasonal cycle. The comparison of the seasonal variation of the simulated total ozone column (TOC) with the observations is presented in Figure 2.13. There are no gaps during polar nights in the observations because the observed total ozone fields are the composite of the available satellite data for 1993-2002, which includes the infrared-based TOVS data. SOCOL reproduces a seasonal maximum in the NH and a maximum and minimum in the SH with reasonable accuracy. The overall agreement between the model and the observation data composite is within ± 5 % in the tropics, ± 10 % in the northern middle and high latitudes, and within ± 10-20 % in the southern middle and high latitudes. Figure 2.14 illustrates the comparison of the total ozone simulated by SOCOL in March over the NH and in October over the SH with corresponding satellite observations. The position and magnitude of the ozone 'hole' is very well reproduced by SOCOL, implying that the amount of PSCs during the spring season and chemical ozone destruction are reasonably well captured by the chemical routine of the model. The position of the total ozone maximum in the Australian sector is also well captured by SOCOL, however the magnitude of the maximum is slightly underestimated (by about 8 DU or ~ 2 %). Some CCMs (see Austin et al., 2003, their figure 2) substantially overestimate the magnitude of the total ozone maxima over the middle latitudes in the Australian sector. This could imply that the relevant wave forcing and subsequently meridional transport in these models are too strong, but SOCOL seems not to suffer from this problem.

33

We have compared the pattern correlation and absolute deviation (not shown) of total ozone simulated by SOCOL and simulated by CCMs that participated in the model intercomparison presented by (Austin et al., 2003). The comparison shows that among the other models SOCOL has the smallest absolute deviation from the observations in the SH, which is ~ 2 % and very high pattern correlation (more than 0.95) over both hemispheres. In March SOCOL underestimates the total northern hemispheric ozone maximum by about 75 DU, but nevertheless has one of the smallest mean deviations (~ 5 %) of total ozone from the observational data among the models compared by Austin et al. (2003) when averaging over the entire northern hemisphere.
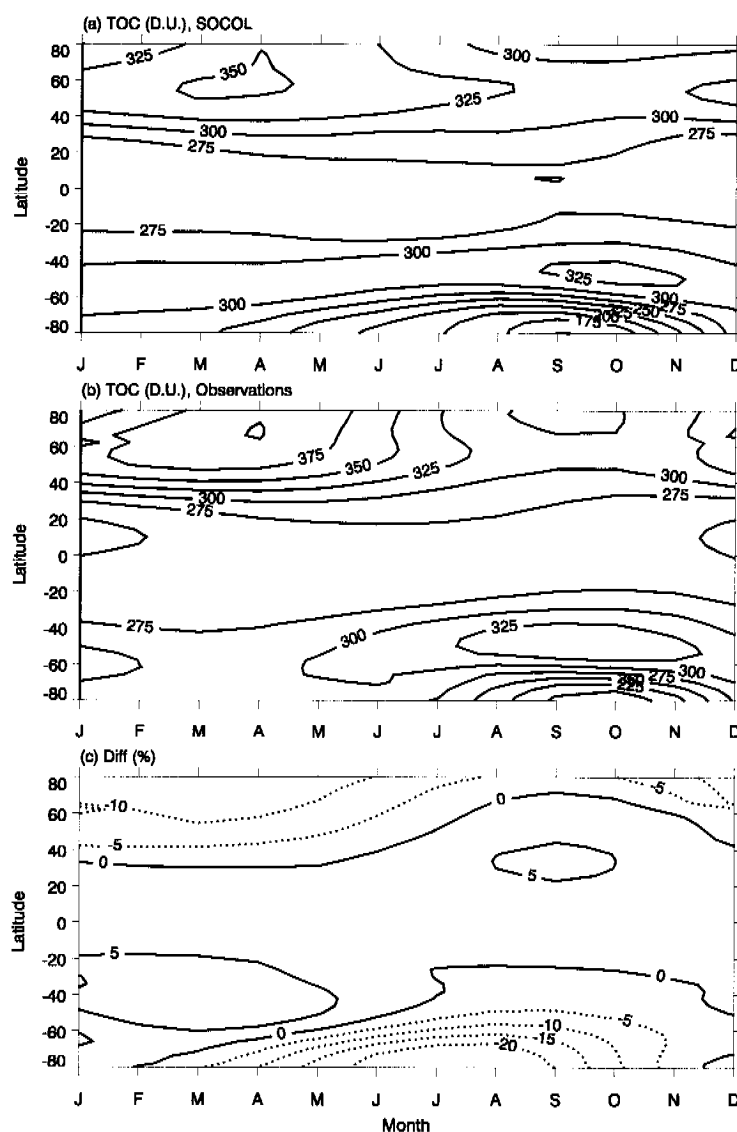
Figure 2.13: *Seasonal variation of the total ozone: (a) simulated, (b) observed, and (c) their difference in percents. The observed values are the composite of different satellite instruments.*
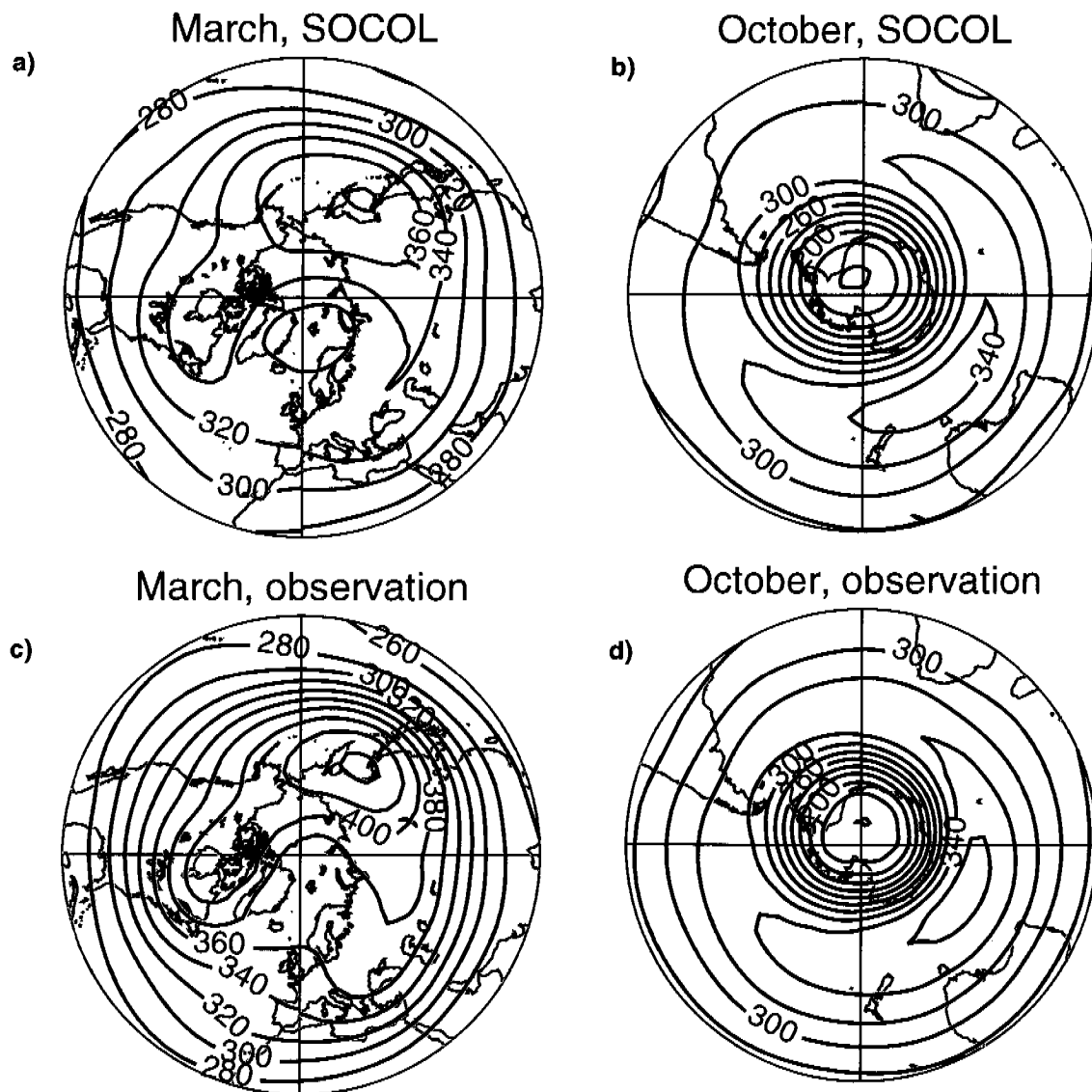
Figure 2.14: *Geographical distribution of the simulated (a, b) and observed (c, d) total ozone for March over the Northern Hemisphere and October over the Southern Hemisphere in Dobson Units (DU).*

2.4.3 Sensitivity of ozone and temperature to the strength of the Arctic winter vortex

The aim of this particular exercise is to validate the ability of SOCOL to simulate the imprint of the Arctic Oscillation (AO) in stratospheric ozone and temperature during the boreal winter. It is well known that the positive phase of the AO is characterized by a deeper vortex and a more intensive Polar Night Jet (e.g., *Thompson and Wallace*, 1998). Therefore, it is theoretically expected (e.g., *Kodera and Kuroda*, 2002) that the positive AO phase results in a weaker meridional circulation and consequently leads to warmer temperatures and elevated ozone in the tropical lower stratosphere. Here we attempt to find these features in the observational

data and model simulations and compare them.

To analyze this process a 25-year long simulation of the present day atmosphere with the CCM SOCOL has been used. We divided the simulated data into two groups according to the intensity of the polar vortex during the boreal winter season defined by the anomaly of North Pole geopotential height at 100 hPa and contrasted the difference between these two groups against observational data processed in an identical way. The observations we used are NMC data (for 1978-1998) and SAGE I/II ozone density (for 1979-2001) compiled by W. Randel et al. (www.acd.ucar.edu/~randel).

Figure 2.15: *Observed and simulated differences between positive and negative AO phase in the zonal mean geopotential heights (m), contours: -500, -300, -200, -100, -50, -20, -10, 0, 10, 20, 50 m.*

Figures 2.15-2.18 illustrate the differences between the two groups mentioned above, in zonal mean geopotential height, zonal wind, temperature and ozone mixing ratio averaged over the boreal winter season (December-January-February). Figure 2.15 shows that the simulated and observed differences in geopotential heights are broadly similar in the NH and tropi-

36

cal stratosphere. The deepening of the polar vortex and formation of the ridges over mid-latitudes is clearly visible for the positive AO phase in both data sets. The zonal wind difference in the composite (Figure 2.16) consists of an acceleration of the PNJ by 10-15 m s^{-1} in the simulated and observed data. The changes of zonal wind in the rest of the atmosphere are rather small.
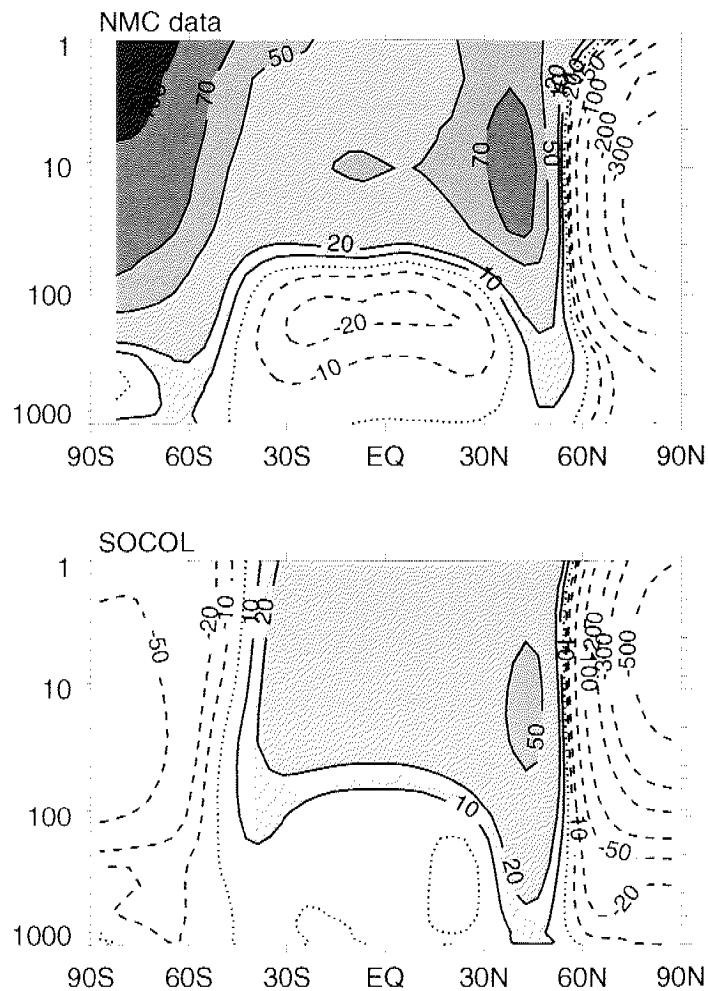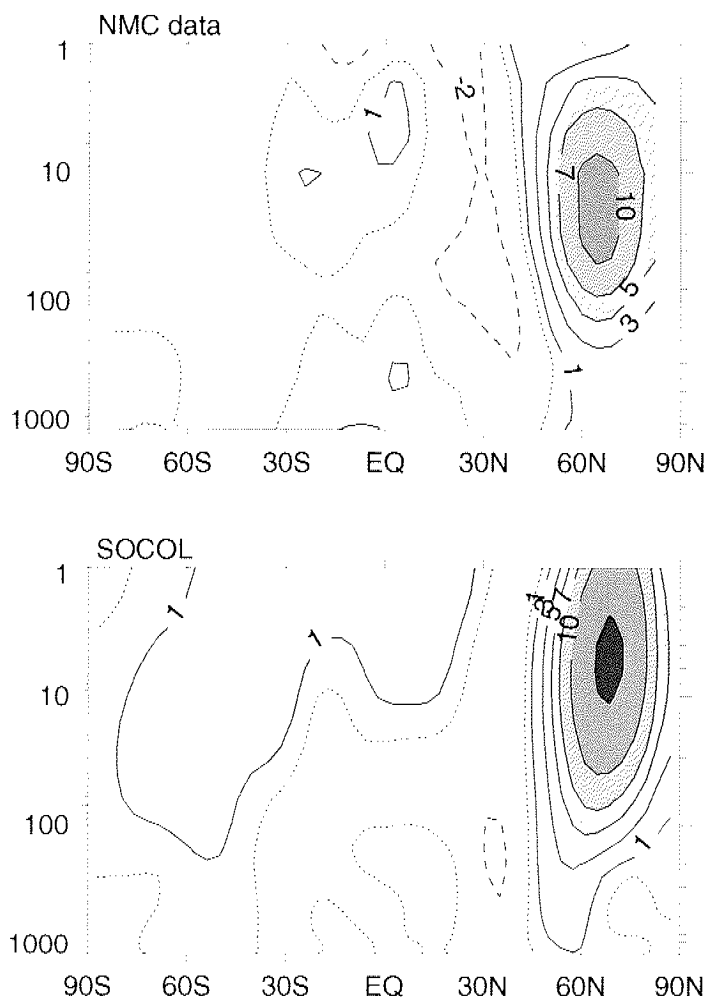

Figure 2.16: *Observed and simulated differences between positive and negative AO phase in the zonal mean zonal wind (ms^{-1}), contour: -2, 0, 1, 3, 5, 7, 10, 15 ms^{-1}. Plots are for DJF.*

Figure 2.17 demonstrates the pattern of the temperature response. The simulated and observed temperature responses over the NH are similar and consist of a pronounced dipole-like structure with cooling (warming) in the middle-lower (upper) stratosphere. In the tropics, the model matches the warming in the lower stratosphere, although the magnitude of the simulated warming is about 2 times smaller. The model is unable to capture warming in the upper tropical stratosphere. The simulated dipole-like temperature changes are at a higher alti-

37

tude than the observed temperature changes. The ozone response is shown in Figure 2.18. The simulated and observed changes are in qualitative agreement only in the lower tropical stratosphere, where the model is able to simulate the elevated ozone mixing ratio. The model cannot reproduce the observed substantial (more than 2 %) ozone increase in the upper stratosphere over mid-latitudes. The simulated ozone difference over the northern high-latitudes reflects a deceleration of the meridional ozone transport and is consistent with temperature and zonal wind changes. However, it is not so clearly visible in the observational data analysis.

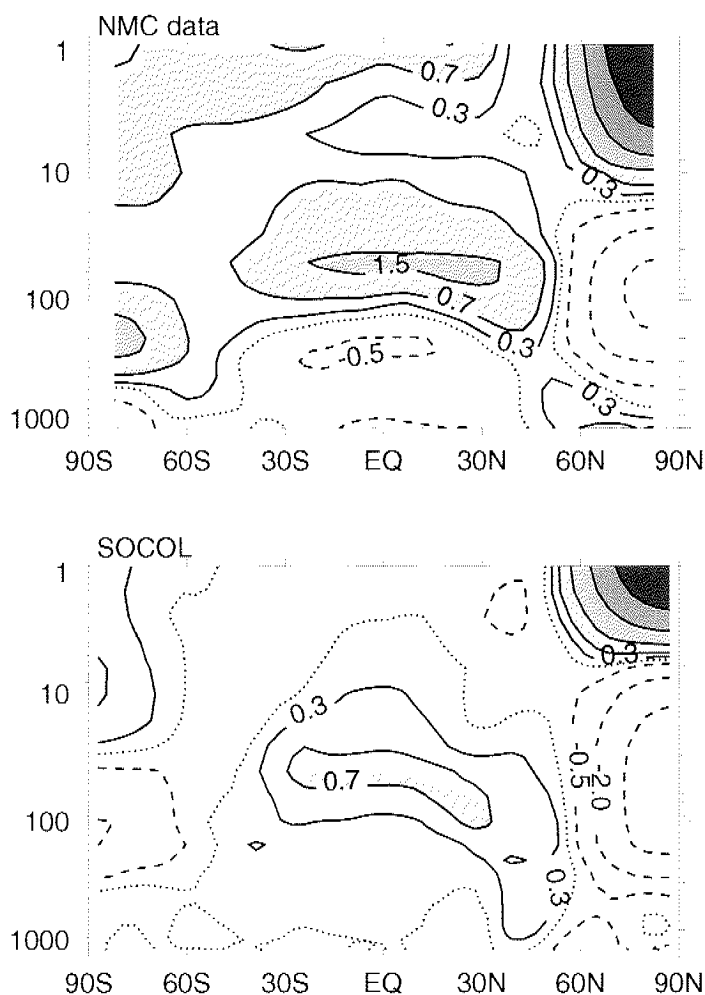**Figure 2.17:** *Observed and simulated differences between positive and negative AO phase in the zonal mean temperature (K).*

2.5 Conclusions

In this paper we presented a description of a new modeling tool, the CCM SOCOL, together with the validation of the simulated present-day climatology against a variety of observational data. We also present an example of processes-oriented validation. While the model perform-

38

ance is quite satisfactory based on an overall inspection of simulated fields and on a proper statistical analysis, we have identified a number of weaknesses in the model that need to be addressed for the future improvement of the model. In particular, the analysis of the simulated zonal wind and temperature deviations shows that for an improvement it will be necessary to pay special attention to the tropopause region in the tropics and at high latitudes as well as to the description of the processes in the upper stratosphere and mesosphere, where significant cold biases have been found in the model during boreal summer.
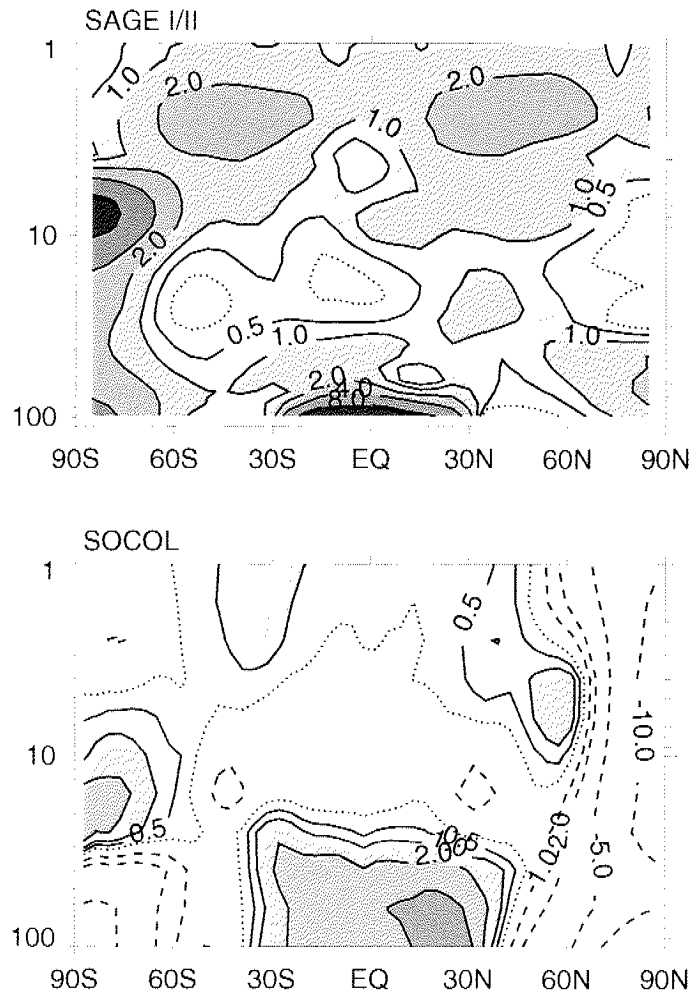
Figure 2.18: *Observed and simulated differences between positive and negative AO phase in the zonal mean ozone mixing ratio (%).*

The model's too cold upper stratosphere is most likely related to the radiation code of MA-ECHAM4 (see Section 2.4), which does not take into account the absorption of the solar irradiance for the wavelengths shorter than 250 nm. To illustrate the importance of this spectral region we have applied a 1-D radiative convective model (RCM) described by Rozanov et al. (2002b) and calculated the temperature profiles with and without absorption of the solar

irradiance in the spectral region 120-250 nm. Temperature differences due to absorption of the solar irradiance in the 120-250 nm spectral interval have been calculated with the 1-D RCM for three cases: (1) a tropical atmosphere model, with Solar Zenith Angle (SZA) = 45°, duration of the day (DoD) = 12 hours; (2) a middle latitude summer atmosphere model, with SZA = 60°, DoD = 14.4 hours; (3) a subarctic summer atmosphere model, with SZA = 70°, DoD = 24 hours. The results are depicted in Figure 2.19, suggesting that near the stratopause the contribution of the 120-250 nm spectral region could reach up to 9 K. Therefore we hypothesize that the missing source of the heat would substantially improve temperature and zonal wind distributions in the summer extra-tropical upper stratosphere and mesosphere also in the 3-D model.

The simulated descent of the air is too strong in the polar stratosphere, leading to a significant underestimation of CH_4 and O_3 mixing ratios in this area. The tropopause region is cold biased by 5-10 K, which might be related to an insufficient vertical resolution. An analysis of the water vapor zonal mean and seasonal distributions reveals an overestimation of stratospheric H_2O, which is probably related to the transport of H_2O from the troposphere.
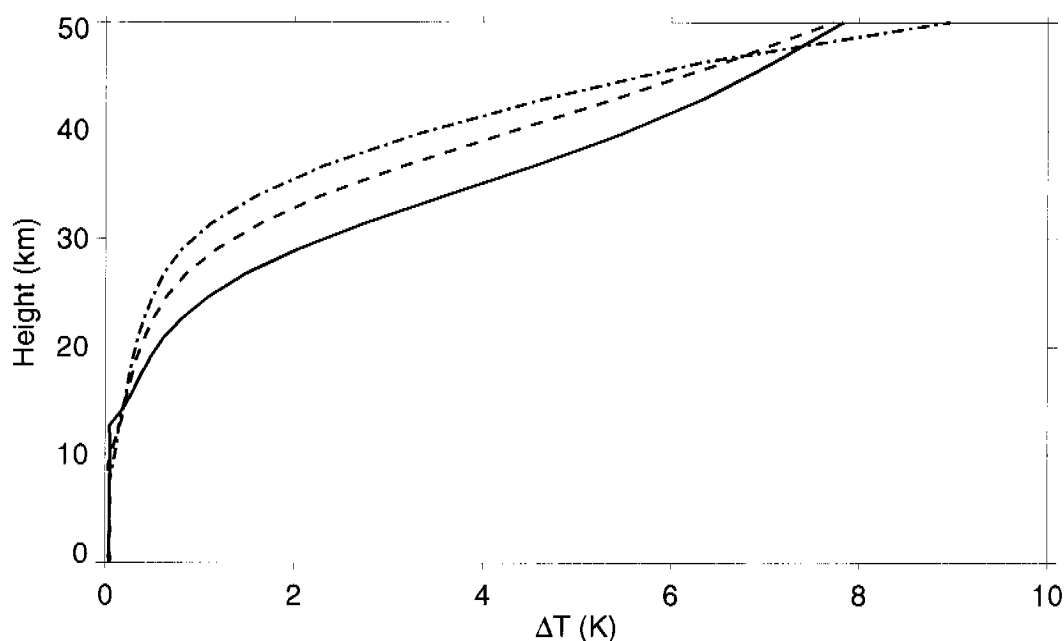
Figure 2.19: *Temperature difference due to absorption of the solar irradiance in the 120 – 250 nm spectral interval calculated with 1-D RCM for three cases: Tropical atmosphere model, SZA = 45°, duration of the day = 12 hours (solid line); Middle latitude summer atmosphere model, SZA = 60°, duration of the day = 14.4 hours (dashed line); Subarctic summer atmosphere model, SZA = 70°, duration of the day = 24 hours (dash-dotted line).*

As a process-oriented part of the validation we analyzed how SOCOL reproduces the imprint of the AO onto the temperature and ozone fields. During the boreal winter (DJF) a signature of the positive AO phase or strong northern polar vortex is clearly visible in the observed and simulated data. Therefore the applied approach can be used for the validation of CCMs. SOCOL reasonably well reproduces AO-like patterns of the inter-annual variability, which consist of a deepening of the polar vortex and an acceleration of the PNJ during positive AO phases. The model also captures the concomitant deceleration of the meridional circulation, the subsequent warming, and the ozone increase in the lower tropical stratosphere. The model also matches the pronounced dipole-like temperature response over the northern high-latitudes. However, the simulated warming in the tropical lower stratosphere is underestimated by a factor of 2. In the upper stratosphere the model almost completely fails to reproduce the observed warming. The observed ozone response in the tropical lower stratosphere is confined mostly to the lowermost stratosphere while the simulated ozone response extends to the middle stratosphere. Moreover, the ozone response over the northern high-latitudes disagrees with observed ozone changes. Additional observation and simulation data should be analyzed in order to elucidate the causes of the noticeable disagreement between simulated and observed atmospheric imprints of the AO phase.

Despite these model deficiencies, the overall performance of the modeling tool CCM SOCOL is reasonable and many features of the real atmosphere are simulated rather well. The CCM SOCOL has been ported for regular PCs and shows good wall-clock performance. Thus, many research groups can use it for studies of chemistry-climate problems even without access to large super-computer facilities.

Software availability

Name of the software: Modeling tool for studies Solar Climate Ozone links (SOCOL)

Contact address: PMOD/WRC, Dorfstrasse, 33, CH-7260, Davos Dorf, Switzerland

Telephone and fax: tel. +41 081 4175138, fax. +41 081 4175100

E-mail: t.egorova@pmodwrc.ch

Hardware required: Intel Pentium based PC, 512 MB memory at least

Software required: LINUX, Fujitsu/Lahey FORTRAN

Availability and cost: signed Max Planck Institute for Meteorology Software License Agreement(http://www.mpimet.mpg.de/en/extra/models/distribution/mpi-m_sla_200403.pdf), appropriate citation required, collaboration preferable, free of charge.

2.6 Acknowledgments.

2.7 References

Austin, J., Shindell, D., Beagley, S. R., et al.: Uncertainties and assessments of chemistry-climate models of the stratosphere, Atmos.Chem.Phys., 3,1-27, 2003, SRef-ID: 1680-7324/acp/2003-3-1.

Baldwin, M. (2000). The Arctic Occillation and its role in stratosphere-troposphere coupling, SPARC newsletter n°14, 10-14.

Brönnimann, S, J. Luterbacher, J. Staehelin and T. Svendby (2004). An extreme anomaly in stratospheric ozone over Europe in 1940-1942, *Geophys. Res. Lett.*, **31**, L08101, doi: 10.1029/2004GL019611.

Butchart, N. and Austin, J. (1996). On the relationship between the quasi-biennial oscillation, total chlorine and the severity of the Antarctic ozone hole, *Q. J. R. Meteorol. Soc.*, **122**, 183-217.

Butchart, N. and Austin J. (1998). Middle Atmosphere Climatologies from *the Troposphere-Stratosphere Configuration of the UKMO's Unified Model*, J. Atmos.Sci., **.35**, 2782-2809.

Carslaw, K. S., B. P. Luo, and Th. Peter (1995). An analytic expression for the composition of aqueous HNO_3-H_2SO_4 stratospheric aerosols including gas phase removal of HNO_3, *Geophys. Res. Lett.*, **22**, 1877-1880.

Charron M. and Manzini, E. (2002). Gravity waves from fronts: Parameterization and middle atmosphere response in a general circulation model, *J. Atmos. Sci.*, 59, 923-941.

DeMore, W.B., Sander, S.P., Golden, D.M., Hampson, R.F., Kurylo, M.J., Howard, C.J., Ravishankara, A.R., Kolb, C.E., and Molina, M.J. (1997). Chemical Kinetics and Photochemical Data for Use in Stratospheric Modeling, Evaluation 12, JPL Publication, no. 97-4.

Egorova, T. A., E. V. Rozanov, M. E. Schlesinger, N. G. Andronova, S. L. Malyshev, V. A. Zubov, and I. L. Karol (2001). Assessment of the effect of the Montreal Protocol on atmospheric ozone, *Geoph. Res. Lett.*, **28**, 2389-2392.

Egorova, T. A., E. V. Rozanov, V. A. Zubov, and I. L. Karol (2003). Model for Investigating Ozone Trends (MEZON). *Izvestiya, Atmospheric and Oceanic Physics*, **39**, 277-292.

Egorova, T., E. Rozanov, E. Manzini, M. Haberreiter, W. Schmutz, V. Zubov, and T. Peter, (2004). Chemical and dynamical response to the 11-year variability of the solar irradiance simulated with a chemistry-climate model, *Geophys.Res.Lett.*,**31**, L06119,doi:10.1029/2003GL019294.

Eyring, V., Harris N., Rex M., et al. (2004). Comprehensive Summary on the Workshop on "Process-Oriented Validation of Coupled Chemistry-Climate Models", SPARC, Newsletter N23, 5-11.

Fouquart, Y. and B. Bonnel (1980). Computations of solar heating of the Earth's atmosphere: A new parameterization. *Beitr. Phys. Atmos.*, **53**, 35-62.

Gleckler, P. E. (1996). AMIP Newsletter: AMIP-II guidelines, *Lawrence Livermore Natl. Lab,* Livermore, Calif.

Hanson, D. and Maursberger, K. (1988). Laboratory studies of the nitric acid trihydrate: Implications for the south polar stratosphere, *Geophys. Res. Lett.,***15**, 855-858.

Harries, J.E, Russell, J. M., III, Tuck, A. F., et al (1996). Validation of measurements of water vapor from the halogen occultation experiment (HALOE), *J. Geophys. Res.*, **101** (D6), 10205-10216.

Hein, R., Dameris, M., Schnadt, C., et al. (2001). Results of an interactively coupled atmospheric chemistry - general circulation model: Comparison with observations, *Ann. Geophys.*, **19**, 435-457.

Hines, C. O. (1997a). Doppler spread parameterization of gravity wave momentum deposition in the middle atmosphere, 1, Basic formulation, *J. Atmos. Solar Terr. Phys.*, **59**, 371-386.

Hines, C. O. (1997b). Doppler spread parameterization of gravity wave momentum deposition in the middle atmosphere, 2, Broad and quasi monochromatic spectra and implementation, *J. Atmos. Solar Terr. Phys.*, **59**, 387-400.

Intergovernmental Panel of Climate Change (2001). *Climate Change 2001: The Scientific Basis*, 881pp., Cambridge Univ. Press, New York.

Jacobson, M.Z., and R.P. Turco (1994). SMVGEAR: A sparse-matrix, vectorized code for atmospheric models, *Atmos. Environ.*, **28**, 273-284.

Jonsson, A., de Grandpre J., and J.C. McConnell (2002). A comparison of mesospheric temperatures from the Canadian Middle Atmospheric Model and HALOE observations: Zonal

mean and signature of the solar diurnal tide, *Geophys. Res. Lett.*, **29**, doi: 10.1029/2001GL014476.

Kodera, K. and Y. Kuroda (2002). Dynamical response to the solar cycle, *J. Geophys. Res.*, **107** (D24),4749,doi:10.1029/2002JD002224.

Manzini, E., N. A. McFarlane, and C. McLandress (1997). Impact of the Doppler Spread Parameterization on the simulation of the middle atmosphere circulation using the MA/ECHAM4 general circulation model, *J. Geophys. Res.*, **102**, 25751-25762.

Manzini, E. and McFarlane N.A. (1998). The effect of varying the source spectrum of a gravity wave parameterization in the middle atmosphere general circulation model, *J. Geophys. Res.*, *103*, 31523-31539.

McFarlane, N.A. (1987). The effect of orographically exited gravity wave drag on the general circulation of the lower stratosphere and troposphere, *J. Atmos. Sci.*, **44**, 1775-1800.

Morcrette, J.J. (1991). Radiation and cloud radiative properties in the European Center for Medium-Range Weather Forecasts forecasting system, *J.Geophys.Res.*, **96**, 9121-9132.

Mote, P. W., T.J. Dunkerton, M.E. McIntyre, E.A. Ray, P.H. Haynes, and J.M. Russell (1998). Vertical velocity, vertical diffusion, and dilution by midlatitude air in the tropical lower stratosphere, *J.Geophys.Res.*, **103**, 8651-8666.

Nagashima, T., M. Takahashi, M. Takigawa, and H. Akiyoshi (2002). Future development of the ozone layer calculated by a general circulation model with fully interactive chemistry. *Geoph. Res. Lett.*, **29**, doi:10.1029/2001GL014026.

Pawson, S., Kodera, K., Hamilton, K., et al. The GCM-reality intercomparison project for SPARC (GRIPS): Scientific issues and initial results, *Bull.Amer.Meteor.Soc.*, **81**,781-796.

Prather, M.J. (1986). Numerical Advection by Conservation of Second-Order Moments, *J. Geophys. Res.*, **91**, 6671--6681.

Roeckner, E., K. Arpe, L. Bengtsson, M. Christoph, M. Claussen, L. Dümenil, M. Esch, M. Giorgetta, U. Schlese, and U. Schulzweida (1996a). The atmospheric general circulation model ECHAM4: Model description and simulation of the present day climate, *Tech.Rep.* *218*, Max Planck Ins. for Meteorol., Hamburg, Germany.

Roeckner, E., J. M. Oberuber, A. Bacher, M. Christoph, and I. Kirchner (1996b). ENSO variability and atmospheric response in a global coupled atmosphere-ocean GCM, *Clim.Dyn.*, **12**, 734-754.

Rozanov, E. V., M. E. Schlesinger, V. A. Zubov, F. Yang, and N. G. Andronova (1999). The UIUC three-dimensional stratospheric chemical transport model: Description and evaluation of the simulated source gases and ozone, *J. Geophys. Res.*, **104**, 11755-11781.

Rozanov, E. V., M. E. Schlesinger, and V. A. Zubov (2001). The University of Illinois, Urbana-Champaign three-dimensional stratosphere-troposphere general circulation model with interactive ozone photochemistry: Fifteen-year control run climatology, *J. Geophys. Res.*, **106**, 27233-27254.

Rozanov, E. V., M. E. Schlesinger, N. G. Andronova, F. Yang, S. L. Malyshev, V. A. Zubov, T.A.Egorova, and B. Li (2002a). Climate/chemistry effects of the Pinatubo volcanic eruption simulated by the UIUC stratosphere/troposphere GCM with interactive photochemistry, *J. Geophys. Res.*, **107**(D21), 4594, doi:10.1029/2001JD000974.

Rozanov, E., T. Egorova, C. Fröhlich, M. Haberreiter, T. Peter, and W. Schmutz (2002b). Estimation of the ozone and temperature sensitivity to the variation of spectral solar flux, In: "From Solar Min to Max: Half a Solar Cycle with SOHO", *ESA* SP-508, 181-184.

Rozanov, E.V., Schlesinger, M.E., Egorova T.A., et al. (2004). Atmospheric Response to the Observed Increase of Solar UV Radiation from Solar Minimum to Solar Maximum Simulated by the UIUC Climate-Chemistry Model, *J. Geophys. Res.*, **109**, D01110, doi:10.1029/2003JD003796.

Sander, S.P., Friedl, R.R., DeMore, W.B., Golden, D.M., Hampson, R.F., Kurylo, M.J., Huie, R.E., Moortgat, G.K., Ravishankara, A.R., Kolb, C.E., and Molina, M.J. (2000). Chemical Kinetics and Photochemical Data for Use in Stratospheric Modeling: Supplement to Evaluation 12: Update of Key Reactions, Evaluation 13, JPL Publication..

Sherman, A.H., and A.C. Hindmarsh (1980). GEARS: A package for the solution of sparse stiff, ordinary differential equations, *Lawrence Livermore Lab. Rep. UCID-30114*.

Shindell, D.T., D. Rind, and P.Lonergan (1998). Increased polar stratospheric ozone losses and delayed eventual recovery owing to increasing greenhouse-gas concentrations, *Nature*, **392**, 589-592.

Schnadt, C., M. Dameris, M. Ponater, R. Hein, V. Grewe, and B. Steil (2002). Interaction of atmospheric chemistry and climate and its impact on startospheric ozone, *Clim. Dyn.*, **18**, 507-517.

SPARC, 2002: SPARC Intercomparison of Middle Atmosphere Climatologies. SPARC Rep. 3, 96 pp.

Steil, B., Bruhl, C., Manzini E., et al (2003). A new interactive chemistry-climate model: 1. Present-day climatology and interannual variability of the middle atmosphere using the model and 9 years of HALOE/UARS data, *J. Geophys. Res.*, **108**(D9), 4290, doi:10.1029/2002JD002971.

Swinbank, R. and Ortland, D.A. (2003). Compilation of wind data for the UARS Reference Atmosphere Project, *J. Geophys. Res.*, **108**(D19), 4615, doi:10.1029/2002JD003135.

Takigawa, M., M. Takahashi, and H. Akiyoshi (1999). Simulation of ozone and other chemical species using a Center for Climate System Research/National Institute for Enviromental Studies atmospheric GCM with coupled stratospheric chemistry, *J. Geophys. Res.*, **104**, 14003-14018.

Thompson, D., and J. Wallace (1998). The arctic oscillation signature in the wintertime geopotential height and temperature fields, *Geophys. Res. Lett.*, **25**, 1297, 1998.

Zubov, V., E. Rozanov, and M. Schlesinger (1999). Hybrid scheme for tree-dimensional advective transport, *Mon. Wea. Rev.*, **127**, 1335-1346.

Williamson, D.L. and Rasch, P.J. (1989). Two-dimensional semi-lagrangian transport with shape-preserving interpolation, *Mon. Weather Rev.*, 117, 102-129.

3. Study of the long-term solar variability effects

3.1 Additional heating rate parameterization

Four 20-year long steady state simulations have been performed using prescribed present day distributions of sea surface temperature and sea ice (SST/SI), and prescribed surface concentrations of greenhouse gases (GHG) and ozone depleting substances (ODS). The observed spectral solar fluxes have been applied for:

(1) solar minimum, with a solar irradiance corresponding to solar minimum conditions;

(2) solar maximum, with a solar irradiance corresponding in the UV *and* visible parts of the spectrum to solar maximum conditions;

(3) solar maximum, with a solar irradiance corresponding only in the UV part of the spectrum to solar maximum conditions, else to solar minimum conditions;

(4) solar maximum, with a solar irradiance corresponding only in the visible part of the spectrum to solar maximum conditions (~ 0.15 % increase), else to solar minimum conditions.

For the investigation of the solar-climate connection it is very important to take into account the heating rates in the spectral area below 250 nm because this part of the solar spectrum includes Lyman-α line, Schumann-Runge band, Herzberg continuum and part of the ozone Hartley band, which are important for the thermal and chemical state of the mesosphere and upper stratosphere. Absorption of the solar irradiance by oxygen in Schumann-Runge band (175-205 nm) and Lyman-α line substantially contribute to atmospheric heating at 60-100 km. Ozone absorption in the Hartley band (200-300 nm) is the dominant heat source in the upper stratosphere. The radiation code of the MA-ECHAM4 was designed mostly for the tropospheric applications and therefore does not describe these processes properly. This radiation code has only two spectral intervals: 250-680 nm and 680-4000 nm. Therefore the oxy-

gen absorption is completely absent. Part of the ozone absorption in Hartley band is accounted for in the first spectral interval, but the code cannot take the solar variability of the spectrum into account. In the entire spectral interval of the code the solar irradiance varies by only about ± 0.15 %, whereas the substantial increase of the solar variability toward short wavelengths cannot be taken into account. Therefore, the study of the solar-climate issue requires a proper parameterization of the solar heating rates changes between solar maximum and solar minimum.

To establish the parameterization a set of equations proposed by Strobel (1978) has been used. All coefficients for these equations for Lyman-α and Schumann-Runge bands have been recalculated by means of the detailed 1-D radiation code of Rozanov et al. (2002) to match the difference in heating rates between solar maximum and minimum. An absorption by ozone is partially represented in the MA-ECHAM4 radiation code, therefore the procedure for the parameterization of the heating rates due to ozone absorption is more complicated. First, using the detailed radiation code of Rozanov et al. (2002) the heating rates have been calculated between solar maximum and minimum using the coarse MA-ECHAM4 spectral representation. (For this case the difference in the solar irradiance between solar maximum and solar minimum cases integrated over the MA-ECHAM4 spectral interval has been calculated.) Effective absorption cross section for the first spectral interval of MA-ECHAM4 has also been calculated. These quantities allow the calculation of the heating rate difference between solar maximum and solar minimum, which emulates MA-ECHAM4 radiation code. Then the same heating rates have been calculated using the above mentioned reference 1-D radiation code. The difference of radiation heating rates between solar maximum and solar minimum calculated by the reference and the MA-ECHAM4-like code was parameterized using equations from Strobel (1978). The following expressions have been used for calculations:

(a)   for heating rates at the Lyman-α line and within the Schumann-Runge band due to oxygen absorption

$$Q_{Ly-\alpha} = [O_2] \times P_{Ly-\alpha} \times \sigma_{Ly-\alpha} \times \exp(-\sigma_{Ly-\alpha} \cdot S_{O_2})$$

$$Q_{SRB} = \frac{[O_2] \times P_{SRB}}{a \cdot S_{O_2} + b \cdot S_{O_2}^{0.5}}$$

48

where S_{O_2} is slant column abundances of oxygen (mol cm^{-2}); $[O_2]$ is oxygen number density (mol cm^{-3}); $\sigma_{Ly-\alpha}$ is the oxygen absorption cross-section at the Lyman-α line (cm^2); $a = 0.143$, $b = 9.64 \times 10^8$ cgs units; $P_{Ly-\alpha}$ and P_{SRB} are coefficients of the parameterization, which depend on the difference in solar irradiance between the solar maximum and solar minimum.

(b)   for heating rates due to ozone absorption

$$Q_{Ha} = [O_3] \times P_{Ha} \times \sigma_{Ha} \times \exp(-\sigma_{Ha} \cdot S_{O_3})$$

where S_{O_3} is slant column abundances of ozone (mol cm^{-2}); $[O_3]$ is ozone number density (mol cm^{-3}); σ_{Ha} is the ozone absorption cross-section in the Hartley band (cm^2); P_{Ha} is the coefficients of the parameterization, which depends on the difference in solar irradiance between the solar maximum and solar minimum.

The unchanged MA-ECHAM4 radiation code with the original heating rates was applied to calculate the solar minimum case. Next, to calculate the solar maximum case the parameterization for solar radiative heating has been introduced into the model (as the difference [solar max – solar min] obtained from Strobel's equations). Clearly, this is an approximation. An alternative way would be a substantial modification of the original MA-ECHAM4 radiation code itself with subsequent retuning of many other model parameterizations in the model, which could not be completed in a reasonable time frame and also is not necessary to obtain the leading contribution from solar variability. The simulated stratospheric temperature response using the presented parameterization is much improved (see Egorova *et al.*, 2004, here section 3.2) and similar to results obtained with a GCM with prescribed ozone (Matthes et al., 2003) and with a CCM with a more detailed radiation code but reaching only 1 hPa (Rozanov et al., 2004). This further justifies the parameterization.

3.2 Annual mean effects

Chemical and Dynamical Response to the 11-year Variability of the Solar Irradiance Simulated with a Chemistry-Climate Model

T. Egorova[1,2], E. Rozanov[1,2], E. Manzini[3], M. Haberreiter[1,4],
W. Schmutz[1], V. Zubov[5], and Th. Peter[2]

Abstract. Atmospheric effects of the solar irradiance variations during 11-year solar cycle are investigated using a chemistry-climate model. The model is enhanced by a more detailed parameterization of the oxygen and ozone UV heating rates. The simulated ozone response to the imposed solar forcing shows a positive correlation in the tropical stratosphere and a negative correlation in the tropical mesosphere, in agreement with theoretical expectation. The model suggests an acceleration of the polar night jets in both hemispheres and a dipole structure in the temperature changes at high latitudes. The model results also show an alteration of the tropospheric circulation with the surface air temperature influence resulting in a statistically significant warming of 1 K in the annual mean surface air temperature over North America and Siberia. This supports the idea of a solar-climate connection.

3.2.1 Introduction

There are at least three properties of the sun which may contribute to climate change on Earth (Reid, 2000): (1) total solar irradiance changes, (2) variations in the ultra-violet (UV) part of the solar spectrum, and (3) varying energetic electron and proton precipitation. This paper discusses the effect of the spectral solar irradiance variation with emphasis on changes in UV radiation during the 11-year solar cycle.

Some of the previous attempts to simulate the effects of solar variability on the Earth's climate used 2D models (e.g., Huang and Brasseur, 1993). In the meantime it has become clear that 2D models are not adequate to study solar-climate interactions, as they do not properly represent [1]three-dimensional planetary scale waves. According to Haigh (1996) and Kodera and Kuroda (2002) this could play an important role in the propagation of the solar signal from the middle atmosphere to the troposphere. Other studies used Global Circulation Models

---

[1] Institute for Atmospheric and Climate Science ETH, Zürich, Switzerland
[2] Physical-Meteorological Observatory/World Radiation Center, Davos, Switzerland
[3] National Institute for Geophysics and Volcanology, Bologna, Italy
[4] Institute for Astrophysics ETH, Zürich, Switzerland
[5] Main Geophysical Observatory, St.-Petersburg, Russia

(e.g., Matthes *et al.*, 2003), but with prescribed ozone or simplified chemistry. Fully interactive Chemistry-Climate Model (CCM) calculations have been performed using the UKMO and University of Tokyo models, analyzing the response of total ozone, global mean values of the ozone mixing ratio and temperature (Labitzke *et al.*, 2002). The MAECHAM4/CHEM and UIUC CCMs have been used concentrating on an analysis of seasonal and monthly means of ozone, temperature and zonal wind (Tourpali *et al.*, 2003, Rozanov *et al.*, 2004). However, the UIUC CCM does not include the mesosphere and, the treatment of solar heating in MAECHAM4/CHEM is too simplified to simulate a direct solar influence on the middle atmosphere. Here we evaluate the effects of the spectral solar flux variability on chemistry and dynamics from the mesopause to the Earth's surface using a newly developed CCM with more detailed parameterization of the heating rates. The main goals of this paper are to show how sensitive the solar signal is to the introduced model improvements and to evaluate the solar signal in the surface air temperature.

3.2.2 Model description and experimental set-up

To study Sun-climate connections we have developed SOCOL, which couples the MAECHAM4 spectral GCM (Manzini and McFarlane, 1998; Manzini *et al.*, 1997) with a chemistry-transport model MEZON (Egorova *et al.*, 2003).

MAECHAM4 is a spectral model with T30 horizontal truncation. In vertical direction the model extends from the surface to 0.01 hPa and has 39 levels. The time step for dynamics and physics is 15 min, and for radiation processes is 2 hours. The model applies the parameterization of gravity waves from Manzini and McFarlane (1998), which leads to realistic stratospheric temperature distributions.

The chemical-transport part of the model simulates the atmospheric concentrations of the 41 chemical species, which are determined by 118 gas-phase, 33 photolysis and 16 heterogeneous reactions on/in sulfate aerosol (binary and ternary solutions) and polar stratospheric cloud particles. The chemical solver is based on the implicit iterative Newton-Raphson scheme. The transport of all considered species is calculated using the Hybrid numerical advection scheme. The photolysis rates are calculated 2-hourly with a look-up-table approach taking into account the radiation in the spectral range between 120 and 700 nm. The MAECHAM4 radiation code has not been designed for solar variability studies: it has only one interval in the UV and visible parts of the solar spectrum and does not account at all for the spectral solar flux below 250 nm. Therefore we have parameterized heating rates, dT/dt (O_2,O_3), due to absorption in the UV by ozone and oxygen, $\sigma^{abs}(O_2,O_3)$, in the Lyman-α line,

51

Schumann-Runge band, Herzberg continuum and Hartley band, which are important in the stratosphere and mesosphere. This parameterization has been developed on the basis of the *Strobel* (1978) formalism with new coefficients calculated using the detailed radiation code of Rozanov *et al.* (2002).

Using SOCOL we performed two 20-year long steady-state simulations for the present day distributions of sea surface temperature, sea ice, greenhouse gases and ozone destroying substances: one simulation for solar maximum and the other for solar minimum conditions, applying two solar UV spectral irradiance distributions obtained from satellite measurements (Haberreiter *et al.*, 2002). Visible solar irradiance for the solar maximum case was increased by 0.16%. These solar fluxes have been used in SOCOL to calculate the radiation fluxes, and heating and photolysis rates. The statistical significance of the simulated solar signal is calculated using known T-Student test.

3.2.3 Ozone response

Figure 3.1 illustrates the simulated and observed annual mean changes in ozone mixing ratio between the solar maximum and solar minimum conditions. In the mesosphere ozone decreases due to intensified H_2O photolysis in the Lyman-α line and subsequent increase of HO_x. The simulated ozone signal by SOCOL is closer to the theoretical expectations (e.g., Huang and Brasseur, 1993) than MAECHAM/CHEM, which does not produce an ozone decrease in the mesosphere.

Enhanced solar irradiance also yields a statistically significant ozone increase in the stratosphere, mainly because of an intensification of the oxygen photolysis in the Herzberg continuum. The obtained stratospheric ozone response is similar to other models (e.g., Huang and Brasseur, 1993, Tourpali *et al.*, 2003) and consists of an almost homogenous increase over middle and low latitudes, which maximizes around 35 km. Two maxima also appear in the lower stratosphere around 30°N and 30°S reflecting an alternation of the circulation.

In the stratosphere our results still disagree with the ozone response obtained from the analysis of satellite data (Hood, 2003; SPARC, 1998). Figure 3.1b illustrates substantial disagreement in the tropical middle and mid-latitude upper stratosphere. It has been argued by Lee and Smith (2003) that the former is the result of problems with the isolation of the solar signal from the short observational records and this minimum would disappear if the QBO and volcanic effects are accounted for. We conclude that our results may therefore agree reasonably well with the observations below 38 km. However, more observational studies are needed to resolve this issue.
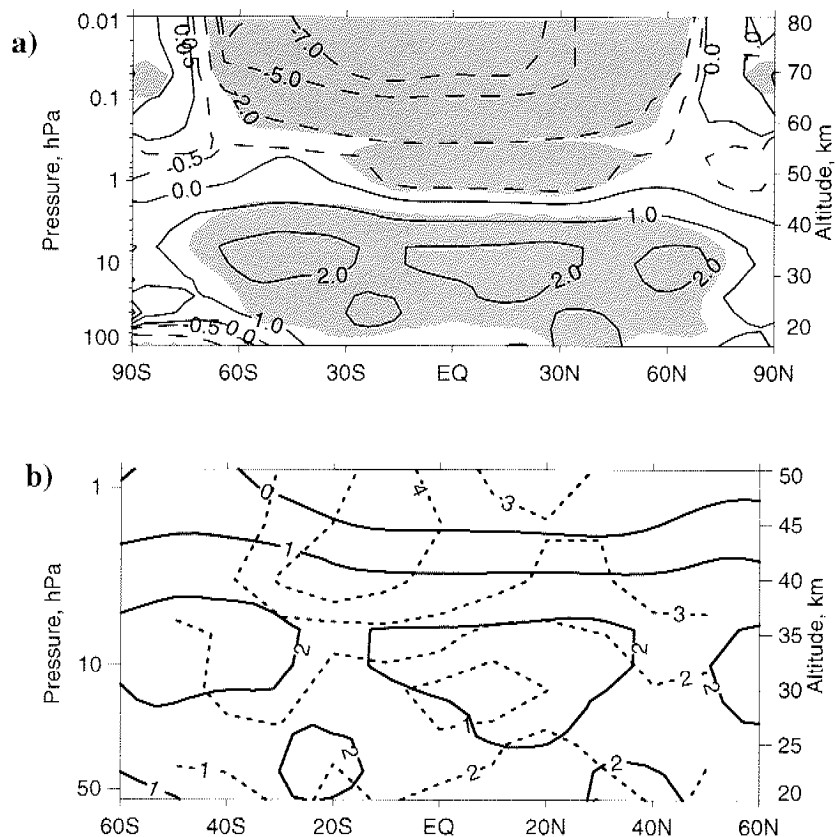
Figure 3.1: *Annual mean zonal mean solar signal (%) in the ozone. (a) Simulated signal, (b) simulated (solid contours) and observed (dotted contours, SAGE I/II from (SPARC, 1998]) signals. The shading marks regions with statistically significant solar signal at the 95 % confidence level.*

3.2.4 Stratospheric temperature and wind response

Figure 3.2 a shows annual mean tropical temperature response simulated with and without the $dT/dt(O_2,O_3)$ parameterization. Figure 3.2 b compares the SOCOL results with three observational data sets as well as with the results of MAECHAM/CHEM. Clearly there is considerable scatter in the data. Notwithstanding the data scatter, SOCOL gives a reasonable description of the stratospheric and mesospheric temperature response. The solar signal in the temperature calculated by SOCOL is more pronounced than that obtained by MAECHAM/CHEM, because Tourpali *et al.*, (2003) used the original MAECHAM4 radiation code without special attention to $\sigma^{abs}(O_2,O_3)$ has been used (see Section 2). Given that the stratospheric ozone distributions in the two coupled chemistry climate models are similar, this comparison suggests that the primary temperature changes are caused by the direct radiation heating. To confirm this we have performed an additional 1-year long run for the solar maximum conditions with the $\sigma^{abs}(O_2,O_3)$ parameterization switched off. Figure 3.2a depicts the

temperature response for this short run together with the results from the first year of the standard run and ensemble mean. The results indicate that the model without $\sigma^{abs}(O_2,O_3)$ tends to underestimate the temperature response.
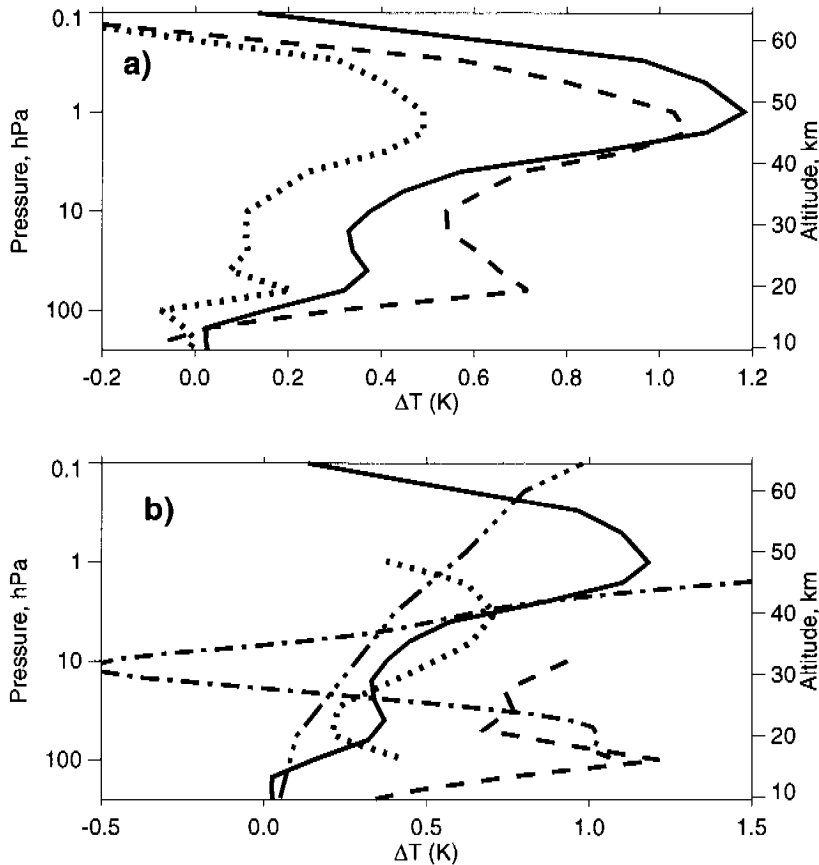

Figure 3.2: *Annual mean difference in the tropical (23°S-23°N averaged) temperature (K) between solar maximum and solar minimum calculated with SOCOL: a) ensemble average including $\sigma^{abs}(O_2,O_3)$ and dT/dt(O_2,O_3) parameterizations describing the UV absorption by ozone and oxygen (solid curve); a 1-year long run without UV absorption (dotted curve); the first year of the standard run (dashed line); b) the result from SOCOL (solid) in comparison with SSU/MSU (dotted) from Hood and Soukharev (2000), CPC reanalysis (dash-dot) from Hood (2003), NCEP reanalysis (dashed) from Labitzke (2002), and MAECHAM/CHEM simulations (dash-dot-dot) from Tourpali et al. (2003).*

Figure 3.3 depicts the simulated solar signal in the annual mean zonal mean temperature and zonal wind in the stratosphere. For the temperature we obtained statistically significant warming in most of the stratosphere by up to 1.2 K at the stratopause in the tropics, and more than 1.5 K in the high-latitude upper stratosphere. In comparison with the analysis of temperature observations by SSU/MSU4 (Hood and Soukharev, 2000), the simulated signal is located ~ 10 km higher and is ~30% larger. However, the observational basis is not strong, and in comparison with other data (e.g. NCEP and CPC data) the model underestimates

54

strength of the signal in the lower stratosphere. In the mesosphere the solar signal in tempera-
ture is positive and reaches up to 1.5 K over the southern high latitudes and in the tropics.

A pronounced simulated dipole vertical structure develops over the poles in the tem-
perature field, which is associated with an acceleration of the Polar Night Jet (PNJ) by up to 2
m/s in the Southern Hemisphere (SH) and 1.5 m/s in Northern Hemisphere (NH), see Figure
3.3 b. This effect is statistically significant in the SH, where the model noise is lower than in
the NH. The results also show a statistically significant strengthening of the easterly winds in
the SH tropics and in the NH extra-tropics (between 30° and 60°N). This supports a study of
Haigh (1996), who argued that an increase in stratospheric temperatures during solar maxi-
mum conditions leads to a strengthening of easterly winds, which penetrate into the tropical
upper troposphere.

3.2.5 Tropospheric temperature and wind response

The analyses of the solar signal in the troposphere suggest the existence of an 11-year period
oscillation during the last eight decades. Van Loon and Shea (1999) estimated the magnitude
of the solar signal in the zonally averaged temperature in the layer 750-200 hPa to be 0.15-0.2
K for the NH, and according to Gleisner and Thejll (2003) there is a maximum of the solar
signal of 0.45 K around 250 hPa at mid-latitudes. Haigh (1996, 1999) also showed changes in
the troposphere due to solar variability and explained them by a shift of the Hadley circula-
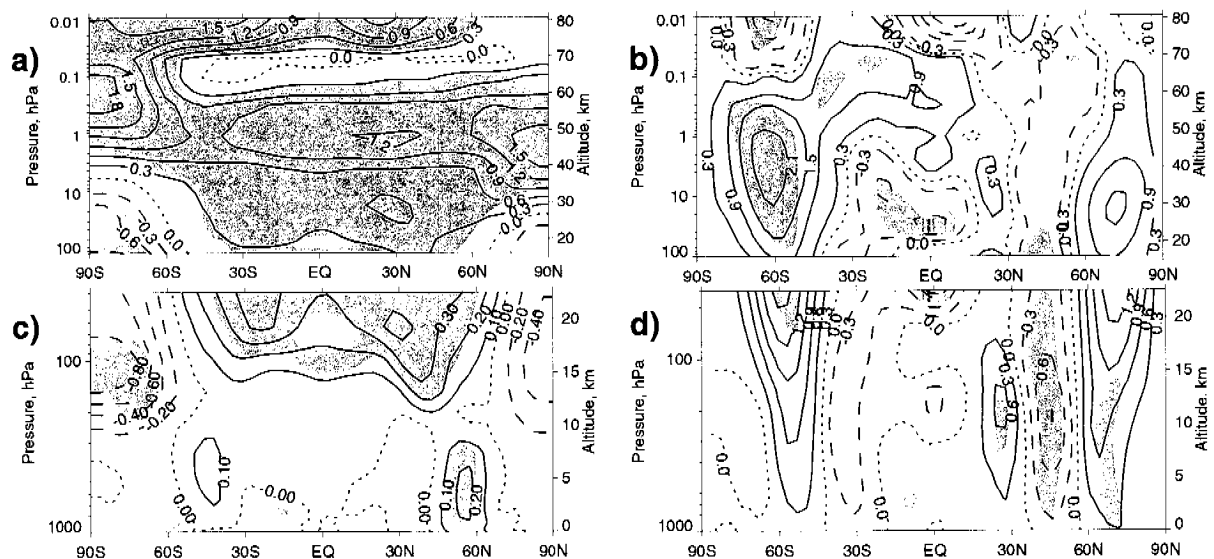tion.

Figure 3.3: *Annual mean zonal mean difference of solar maximum relative to solar minimum
in temperature (in K, a and c) and zonal wind (in m/s, b and d). The shading marks regions
with statistically significant solar signal at the 95% confidence level.*

Figures 3.3c and 3.3d suggest that changes in solar fluxes via the reported changes in the stratosphere lead to statistically significant changes in the simulated tropospheric temperature and zonal wind. In the northern lower troposphere the magnitude of the temperature response from solar maximum to solar minimum exceeds 0.2 K. The zonal mean zonal wind variations reveal a banded structure with easterly and westerly anomalies, in accordance with Haigh (1999). In contrast to the NH stratosphere (Figure 3.3b) the signal is statistically significant in the NH troposphere (Figure 3.3d).

Figure 3.4 presents the simulated solar signal in the surface air temperature. Our results reveal a statistically significant warming of the annual mean surface air by up to 1 K over North America and 1.2 K over Siberia. The pattern in Figure 3.4 resembles surface temperature changes during positive AO phases (Thompson and Wallace, 1998), which implies downward propagation of the solar signal via intensification of the PNJ.
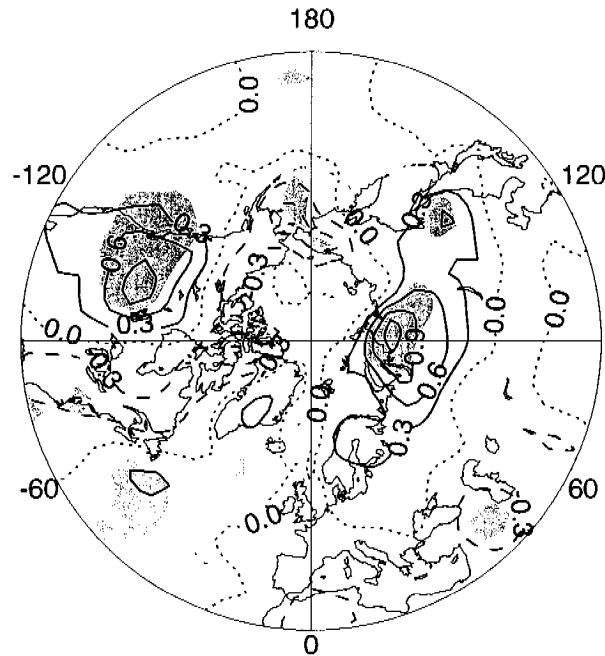
Figure 3.4: *Annual mean solar signal in surface air temperature for the Northern Hemisphere.*

3.2.6 Conclusions

We evaluated the solar signal in the atmosphere with a new chemistry-climate model SOCOL, which utilizes a parameterization of the primary solar forcing taking proper account of the heating rates due to oxygen and ozone absorption in the middle atmosphere. Our results reveal that a correct representation of the direct heating rate is an essential prerequisite for the simulation of the solar signal in the stratosphere. The simulation suggests more pronounced solar

signal in the stratospheric temperature fields compared to previous work implying the necessity of the MAECHAM4/5 radiation code improvement.

In the stratosphere below 38 km the simulated ozone response is in a reasonable agreement with observations, however in the upper stratosphere it is underestimated. A small ozone response in the upper stratosphere is theoretically expected, therefore probably some physical-chemical processes are still missing or the data analysis is not complete. We obtain an acceleration of the PNJ during solar maximum presumably due to an increase in the meridional temperature gradient. The intensification of the polar vortices leads to the formation of vertical dipole structures in the annual mean zonal mean temperature response over both poles, deceleration of the meridional circulation and warming in the lower tropical stratosphere. This warming is in agreement with SSU/MSU4 data, but it is substantially underestimated in comparison with NCEP and CPC data sets. The introduction of the solar flux variations into the model leads to a statistically significant signal in the annual mean surface air temperature of up to 1.2 K over North America and Siberia. This pattern is typical for the positive phase of arctic oscillation and suggests an enhanced stratosphere-troposphere coupling including downward propagation of the UV-triggered signal. Thus, while the simulated solar signals in the stratosphere are in accordance with theoretical expectations a solid validation of the SOCOL results is difficult because of a considerable disagreement between the existing observational analyses.

Further investigation of this solar-climate link and proper attribution of the underlying physical mechanisms are required, including overcoming the steady-state assumption (implying perpetual solar maximum or/and solar minimum conditions), because the solar signal is transient by nature.

3.2.7 Acknowledgments

3.2.8 References

Egorova, T., E. Rozanov, V. Zubov, and I. Karol, Model for Investigating Ozone Trends (2003), *Atm. and Ocean. Phys.*, **39**, 277-292.

Gleisner, H., and P. Thejll (2003), Patterns of tropospheric response to solar variability, *Geophys. Res. Lett.*, **30**(*13*), 1711, doi: 10.1029/2003GL017129.

Haberreiter, M. et al. (2002), Towards a spherical code for the evaluation of solar UV-bands that influence the chemical composition in the stratosphere, in: *ESA SP-508*, p. 209.

Haigh, J. (1996), The impact of solar variability on climate, *Science*, **272**, 981-984.

Haigh, J. (1999), A GCM study of climate change in response to the 11-year solar cycle, *Q. J. R. Met. Soc.*, *125*, 871-892.

Hood, L. and B. Soukharev (2000), The solar component of long-term stratospheric variability: observations, model comparison, and possible mechanisms, in Proceed. *II SPARC General Assembly*.

Hood, L. L. (2003), Effects of solar UV variability on the stratosphere. AGU monograph, in press.

Huang, T. and G. Brasseur (1993), Effect of long-term solar variability in a two-dimensional interactive model of the middle atmosphere, *J. Geophys. Res.*, **98**, 20,413-20, 427.

Kodera, K. and Y. Kuroda (2002), Dynamical response to the solar cycle, *J. Geophys. Res.*, **107**, 4749, doi:10.1029/2002JD002224.

Labitzke, K. et al. (2002), The global signal of the 11-year solar cycle in the stratosphere: observations and models, *J. Atm. Sol. Terr. Phys.*, **64**, 203-210.

Lee, H. and A. Smith (2003), Simulation of the combined effects of solar cycle, quasi-biennial oscillation, and volcanic forcing on stratospheric ozone changes in recent decades, *J. Geoph. Res.*, *108*, 4049, doi:10.1029/2001JD001503.

Manzini, E. and N. McFarlane (1998), The effect of varying the source spectrum of a gravity wave parameterization in the middle atmosphere general circulation model, *J. Geophys. Res.*, **103**, 31523-31539.

Manzini, E., N. McFarlane, and C. McLandress (1997), Impact of the Doppler Spread Parameterization on the simulation of the middle atmosphere circulation using the MA/ECHAM4 general circulation model, *J. Geophys. Res.*, **102**, 25751-25762.

Matthes, K. et al. (2003), GRIPS solar experiments intercomparison project: initial results, *Pap. Meteor. Geophys.* **54**, 380-395.

Reid, G. C. (2000), Solar variability and the Earth's climate: Introduction and overview, *Space Science Reviews*, **94**, 1-11.

Rozanov, E. et al. (2002), Estimation of the ozone and temperature sensitivity to the variation of spectral solar flux, in: *ESA SP-508*, p. 181.

Rozanov, E. et al. (2004), Atmospheric Response to the Observed Increase of Solar UV Radiation from Solar Minimum to Solar Maximum Simulated by the UIUC Climate-Chemistry Model, *J. Geophys. Res.*, **109**, D01110, doi:10.1029/2003JD003796.

SPARC assessment of trends in the vertical distribution of ozone (1998), WMO Rep. 43, pp.210-213, Geneva.

Strobel, D. F. (1978), Parameterization of the atmospheric heating rate from 15 to 120 km due to O_2 and O_3 absorption of solar radiation, *J. Geophys. Res.*, **83**, 6225-6230.

Thompson, D., and J. Wallace (1998), The arctic oscillation signature in the wintertime geopotential height and temperature fields, *Geophys. Res. Lett.*, **25**, 1297.

Tourpali, K., C. Schuurmans, R. van Dorland, B. Steil, and C. Brühl (2003), Stratospheric and tropospheric response to enhanced solar UV radiation: A model study, *Geophys. Res. Lett.*, **30**, 1231, doi: 10.1029/2002GL016650.

van Loon, H. and D. J. Shea (1999), A probable signal of the 11-year solar cycle in the troposphere of the northern hemisphere, *Geophys. Res. Lett.*, **26**, 2893-2896.

3.3 Chemical effects

Influence of solar 11-year variability on chemical composition of the stratosphere and mesosphere simulated with a chemistry-climate model

T. Egorova[1,2], E. Rozanov[1,2], V. Zubov[3], W. Schmutz[2], and Th. Peter[1]

Abstract. An understanding of observed global chemistry and climate changes caused by solar activity changes is a high priority in modern geosciences. Here we discuss the influence of the ultraviolet spectral irradiance variability during solar cycle on chemical composition of the stratosphere and mesosphere with chemistry-climate model that fully describe interactions between chemical and thermodynamical processes. We have performed several 20-year long steady-state runs and found a significant influence of solar irradiation on the chemical composition in the stratosphere and mesosphere. An enhanced photolysis during solar maximum results in destruction of methane, nitrous oxide and CFCs providing an increase in the chemical activity of the atmosphere with more pronounced effects in the mesosphere. In the mesosphere an increase of HO_x caused by more intensive water vapor photolysis results in significant ozone depletion there. More intensive methane oxidation gives statistically significant rise to the stratospheric humidity. The influence of dynamical perturbations has been identified over high latitude areas. The response of OH is found to be in a good agreement with observation data. The response of the other species is hard to validate, because of the lack of theoretical and observational studies.

3.3.1 Introduction

In the last IPCC assessment solar forcing has been considered as one of the main players in climate change during last several centuries with very low confidence of scientific under-standing (IPCC, 2001). Therefore, further studies on solar-climate connection issue are necessary. Solar irradiance variability may influence climate by several mechanisms (see e.g. Reid, 2000). One of the most physically solid mechanisms involves changes in solar ultraviolet flux and subsequent modulation of ozone, heating rates and dynamics in the entire atmosphere. The variability of the UV irradiance during 11-year solar cycle has larger magnitude then the variability of the visible and near infrared radiation. According to Lean et al. (1997) solar UV variability may contribute up to ~ 30% of the overall total solar irradiance change. Variations

---

[1] Institute for Atmospheric and Climate Science ETH, Zürich, Switzerland
[2] Physical-Meteorological Observatory/World Radiation Center, Davos, Switzerland
[3] Main Geophysical Observatory, St.-Petersburg, Russia

of solar radiation may directly affect chemical composition of the stratosphere and meso-sphere, because the specie distributions depend on the intensity of the photolysis reactions. The dynamical perturbations caused by solar flux variability could also be important, because transport process also play substantial role in regulating the chemical state of the atmosphere.

Effect of long-term variability on the chemical composition of stratosphere and meso-sphere has been studied for many years first with 1-D and 2-D models of the middle atmos-phere (e.g, Brasseur and Simon,1981; Brasseur et al., 1983; Garcia et al, 1984; Kiselev and Rozanov, 1985; Dyominov et al, 1989). Due to absence of the accurate satellite measurement all these studies suffer from the substantial overestimation of the solar ultraviolet irradiance variability which leaded to an exaggerated solar signal in atmospheric species. The availabil-ity of the satellite measurements allowed better simulations of the long-term (as well as short-term) solar irradiance variability influence on the atmospheric chemistry (e.g., Huang and Brasseur, 1993; Haigh, 1994; Fleming et al., 1995; Khosravi et al., 2002, Lee and Smith, 2003). Fleming et al. (1995) gave excellent overview of previous observational analysis and theoretical studies performed with 2-D models on the ozone response to solar 27-day and 11-year ultraviolet variations. All these investigations were concentrated mainly on ozone and odd hydrogen species response to increased UV flux. Substantial deviation of the simulated ozone response to the solar flux variability from analysis of observations (e.g., Hood et al., 1993) inspired application to this problem of 3D chemistry-climate models, which enable more accurate (in comparison with 2-D models) representation of the dynamical and transport response in the atmosphere to the imposed solar forcing. The results of the simulations with state-of-the-art CCMs have been recently presented in several publications: Labitzke et al. (2002), Tourpali et al. (2003), Rozanov et al. (2004) and Egorova et al. (2004). However, these more complicated models were also not able to mimic the ozone response obtained from the analysis of the observations (Hood, 2004). To determine the causes of these disagree-ments it is necessary to analyze the response of the other atmospheric species to the solar flux variability during solar activity cycle. The comparison of the simulated response with the analysis of the satellite observations would potentially allow defining the missing processes in the models or problems with data analysis. Unfortunately, at the moment there are only a few attempts to extract solar response for the other species (except ozone), but they will appear for sure in the nearest future when the longer time series of the measurements will emerge. The aim of this paper is to document the response of several important atmospheric species to the 11-year solar variability simulated with CCM SOCOL (Egorova et al., 2004). It should be noted that the solar signal in many species presented here has not been studied with a CCM

before. We believe, that these results will form a good basis for future comparisons with observation data analysis.

The paper organized as follows. In section 3.3.2 we briefly describe our CCM SOCOL and experimental set-up. In section 3.3.3 we show the chemical response of some atmospheric species to the enhanced solar UV radiation. Summary of the findings and conclusions are given in section 3.3.4.

3.3.2 Model and experiments

CCM SOCOL couples the MAECHAM4 spectral GCM (Manzini and McFarlane, 1998; Manzini et al., 1997) with a chemistry-transport model MEZON (Egorova et al., 2003). Detailed description and validation of CCM SOCOL is presented by Egorova et al. (2005).

We have performed two 20-year long steady-state simulations for the present day distributions of sea surface temperature, sea ice, greenhouse gases and ozone destroying substances: one simulation for solar maximum and the other for solar minimum conditions, applying two solar UV spectral irradiance distributions obtained from satellite measurements. Visible solar irradiance for the solar maximum case was increased by 0.16%. These solar fluxes have been used in SOCOL to calculate the radiation fluxes, heating and photolysis rates. For dynamical variables and ozone, the solar response has been presented by Egorova et al. (2004). There we obtained an acceleration of the polar night jets during solar maximum presumably due to an increase in the meridional temperature gradient. The intensification of the polar vortices leads to the formation of vertical dipole structures in the annual mean zonal mean temperature response over both poles, slight deceleration of the meridional circulation and warming in the lower tropical stratosphere. To investigate separate influence of UV and visible radiation on the global atmosphere we have carried out two additional 20-year long steady state simulations with observed spectral solar fluxes: solar maximum where only UV radiation has been increased and solar maximum where only Visible radiation has been increased. The results of these simulations will be presented here as the difference between solar maximum and solar minimum cases together with their statistical significance estimated with known two-sided t-Student test. The shaded areas on all figures mark where the obtained signal is statistically significant at the 95% confidence level.

3.3.3 Results

3.3.3.1 Ozone

UV mechanism of solar-climate connections is based on the ozone changes caused by the UV variability. Figure 3.5 shows the ozone changes due to only UV (a), only Visible (b) and both UV and Visible (c) radiation enhancement from solar minimum to solar maximum case. More
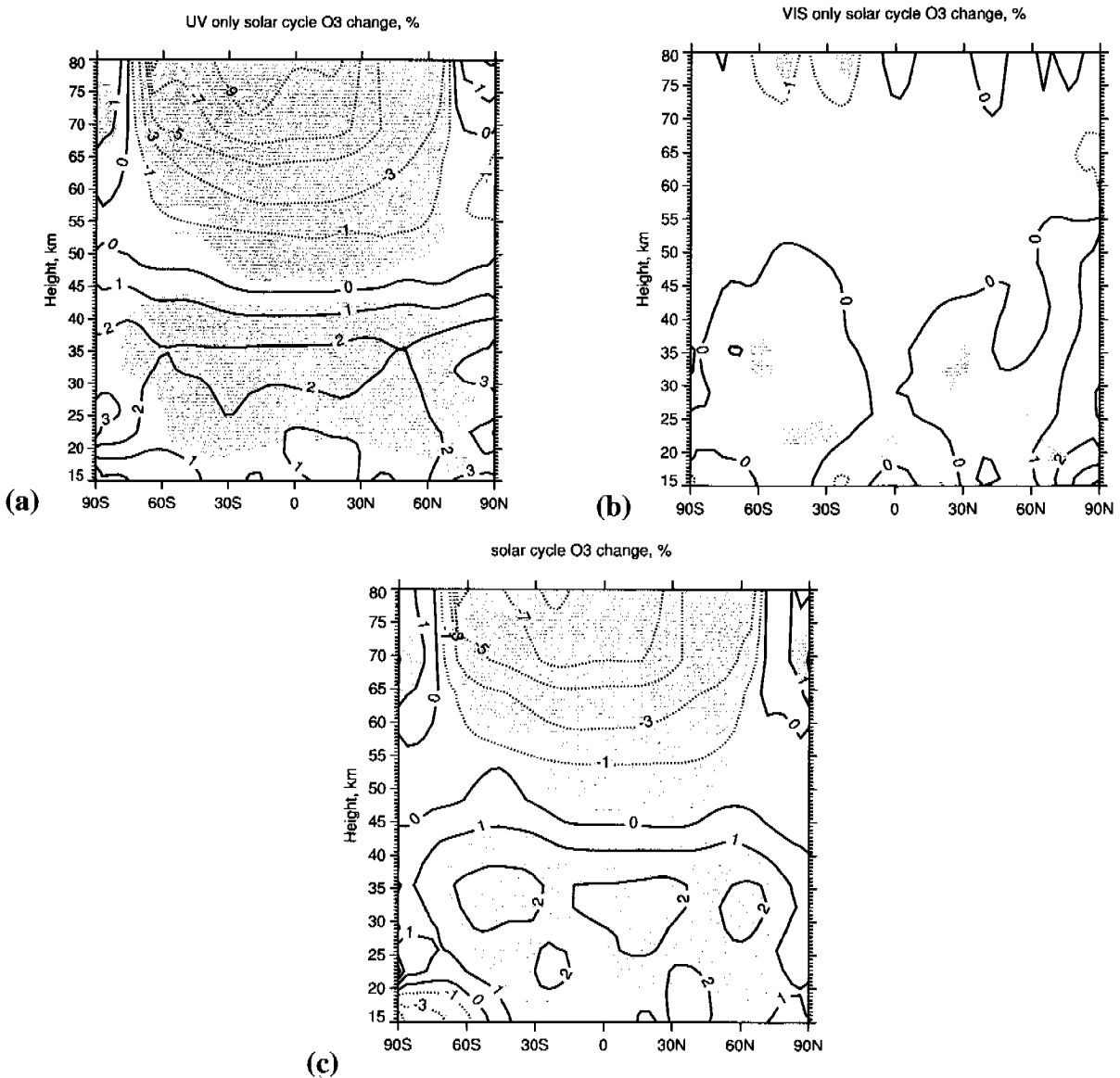
Figure 3.5: *Annual mean zonal mean ozone changes due to 11-year solar forcing: a) for UV radiation variation, b) for Visible radiation variation, c) for UV and Visible radiation variations. Shaded areas mark 95% statistically significant changes.*

intensive solar UV irradiation during solar maximum reduces ozone by about 1-3% in the lower mesosphere and up to ~ 10% in the upper mesosphere mainly due to intensified water vapor photolysis in the Lyman-α line and subsequent increase of odd hydrogen (HO_x) produc-

tion. Those results are in good quantitative agreement with the results obtained for the meso-sphere with 2D model by Khosravi et al. (2002). In the stratosphere ozone increases about 2%, manly because of an intensification of the oxygen photolysis in the Herzberg continuum and Schumann-Runge band which is in agreement with the results of 2-D models (e.g., Huang and Brasseur, 1993) and CCMs (e.g., Rozanov et al., 2004 and Tourpali et al., 2003). The analysis of the ozone response in case (c) and its comparison with observations have been presented in more details by Egorova et al. (2004). As it has been expected there is almost no response in the stratosphere and mesosphere in the case of Visible radiation perturbation only because the atmosphere is almost transparent for visible radiation and the variability of visible radiation during solar activity cycle is rather small. As it can be seen from the Figure 3.5 the ozone changes due to combine influence are caused essentially by the UV perturbations. Therefore, further analysis of solar variability on chemical composition of the middle atmosphere will be for the model run where both UV and Visible radiation have been introduced. As was shown before (see Egorova et al. 2004) the simulated by CCM SOCOL ozone response to the solar UV enhancement differ substantially from the solar signal in the ozone extracted from the satellite data in the upper stratosphere and in the tropical middle stratosphere. As has been suggested by Lee and Smith (2003) a successful simulation of the negative ozone response in the middle stratosphere can be achieved when the solar signal is extracted by multiple regression analysis from the results of transient model run forced by solar irradiance, QBO and volcanic aerosol.

3.3.3.2 Source gases (CH_4, N_2O, H_2O, CF_2Cl_2)

Here we present the response of source gases (CH_4, N_2O, H_2O, CF_2Cl_2) to the increase of the solar irradiance from the minimum to the maximum of the 11-year solar activity cycle. Their mixing ratio in the stratosphere and mesosphere is regulated by vertical transport from the troposphere, horizontal transport by the meridional circulation and by photochemical processes. In the middle atmosphere these species play significant role as sources of chemically active species participating in the catalytic ozone destruction. Methane, nitrous oxide and CF_2Cl_2 have no photochemical sources in the middle atmosphere and can be destroyed by photolysis and by reaction with several active radicals (OH, $O(^1D)$ and Cl). Water vapor is destroyed by the photolysis and reaction with $O(^1D)$, however it can be also formed as a result of methane oxidation chain. Photolysis rates of CH_4 and H_2O diverge by a factor of two over the solar cycle due to the variation in the Schumann-Runge bands at 175-205 nm and Lyman-α irradiation near 121.5 nm (Brasseur and Solomon, 1986). The photolysis rates of the other

species vary with slightly smaller magnitude. Therefore, a substantial reduction of these species in the upper stratosphere and mesosphere is theoretically expected.

Figure 3.6 shows substantial and statistically significant decrease of the simulated CH_4, N_2O, H_2O and CF_2Cl_2 in the mesosphere by about 10-35% caused by more intensive photolysis during solar maximum. In the middle stratosphere CH_4, N_2O, and CF_2Cl_2 decrease by about 5-30% depending on the species over the high latitudes while over the tropical and middle latitudes the changes are only marginally statistically significant.
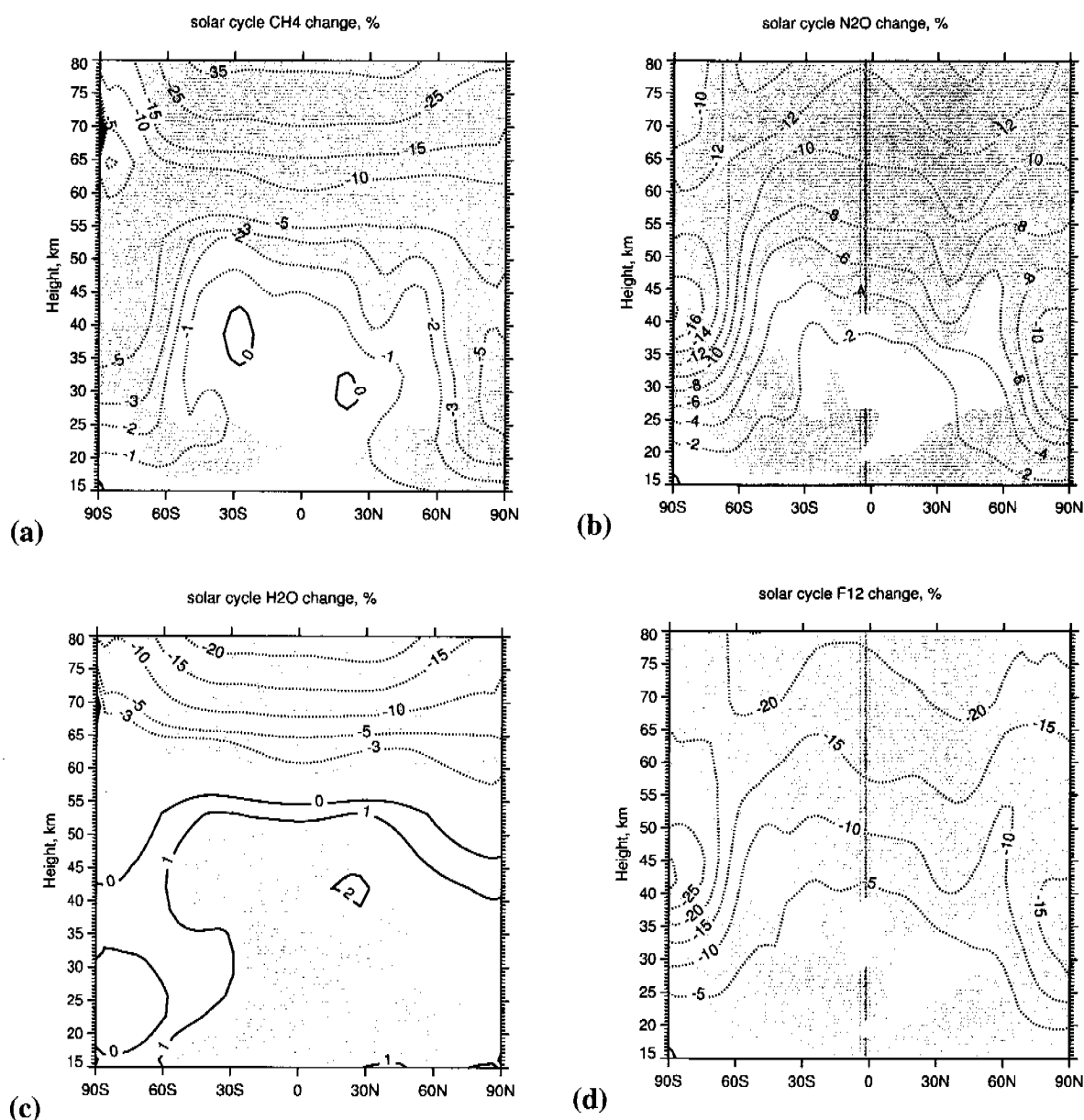

Figure 3.6: *Annual mean zonal mean changes due to 11-year solar variability: (a) for CH_4, (b) for N_2O, (c) for H_2O and (d) for CF_2Cl_2. Shaded area marks 95% statistically significant changes.*

Simulated negative changes over the high latitude areas in the middle stratosphere reflect presumably above mentioned, dynamical changes (see section 3.3.2). Deepening of the polar vortices simulated by our model provides a strengthening of the transport barriers, which slows down horizontal transport of the species toward poles and intensify sinking motion inside vortices. The dynamical nature of the changes in the high-latitude area is confirmed by the simulated asymmetry of the response. It is larger in the southern hemisphere, where the acceleration of the zonal wind is more pronounced (see Egorova et al., 2004). A statistically significant increase of H_2O in the tropical stratosphere (1-2 %) can be attributed to enhanced CH_4 oxidation by the hydroxyl radical below 50 km ($CH_4 + OH \rightarrow CH_3 + H_2O$) and partially by the simulated warming of the tropical UTLS (Egorova et al., 2004), which lead to increase of the water vapor at the entry point and its subsequent transport to the stratosphere. The comparison of our results in the upper stratosphere and mesosphere with previous publications reveals that the magnitude of the response is substantially smaller. At 50 km and 75 km in the tropics our model shows about ~6% and 12% decrease of N_2O. The solar signal in N_2O simulated by Garcia et al. (1984) and Dyominov et al.(1989) exceeds our estimation by two and three-four times. The solar signal in CF_2Cl_2 at the stratopause simulated by Brasseur and Simon (1981) exceeds our estimation by five times. Our estimation of water vapor increase in the stratosphere agree with the results of Dyominov et al.(1989), but again the magnitude is about 2 times smaller. In the mesosphere the decrease of water vapor by up to 40% has been simulated by Garcia et al.(1984) and Brasseur et al.(1983) while our model shows only of about 20% decrease. All these differences are explained by the overestimated solar irradiance variability applied in these simulations.

3.3.3.3 Reservoir and radical species

We present here the solar signal in two reservoir species – nitrous acid (HNO_3) and hydrochloric acid (HCl). Figure 3.7 shows that HCl, which is an inert reservoir for active chlorine, increases below 30 km over tropical and middle-latitude area due to additional chlorine produced from an intensified CFCs destruction during solar maximum.

Hydrochloric acid has small positive changes in the mesosphere and upper stratosphere and decreases over high latitudes due to stronger polar vortices during solar maximum. The latter is similar to the behavior of source gases discussed earlier. The simulated decrease of the solar signal in HCl with altitude simply reflects the rising profile of HCl mixing ratio. Nitrous acid increases in the upper mesosphere due to enhanced HO_x and NO_2 (see below) and according to the reaction $NO_2 + OH + M \rightarrow HNO_3 + M$. This effect is statistically signifi-

cant, but not important because there is essentially no nitric acid at these altitudes. In the tropical upper stratosphere HNO_3 destruction (up to 3%) prevails mostly due to enhanced photolysis.
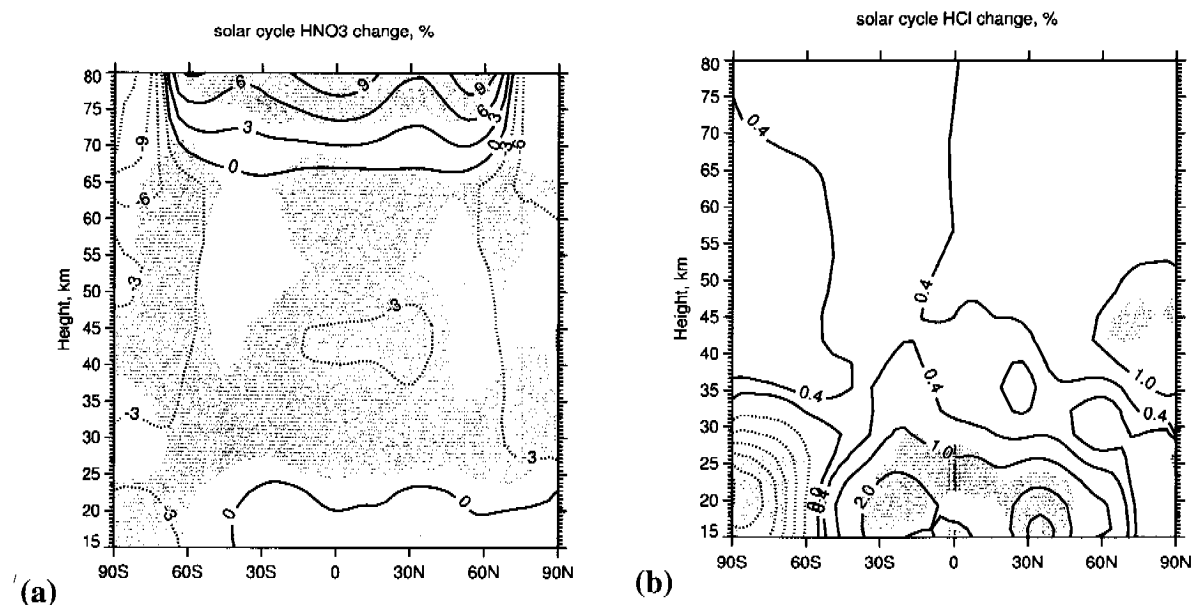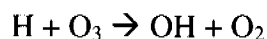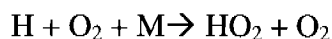

Figure 3.7: *Annual mean zonal mean changes due to 11-year solar variability: a) for HNO_3, b) for HCl. Shaded area marks 95% statistically significant changes.*

The simulated changes of some important radicals (OH, HO_2, NO_2 and ClO) between solar maximum and solar minimum are presented in Figure 3.8. Concentrations of hydroxyl (OH) and peroxy (HO_2) radicals are increased in the mesosphere for the solar maximum case due to enhanced photolysis of CH_4 and H_2O and subsequent formation of HO_x:

$$H_2O + h\nu \ (\lambda<200 \text{ nm}) \rightarrow H + OH$$

$$CH_4 + h\nu \rightarrow CH_3 + H$$

$$H + O_2 + M \rightarrow HO_2 + O_2$$

$$H + O_3 \rightarrow OH + O_2$$
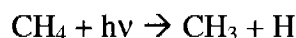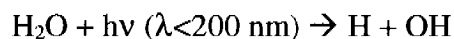
In the stratosphere enhanced ozone mixing ratio and photolysis rates lead to the increase of excited atomic oxygen ($O(^1D)$) and HO_x cause the following reactions with CH_4 and H_2O:

$$O_3 + h\nu \rightarrow O_2 + O(^1D)$$

$$H_2O + O(^1D) \rightarrow 2OH$$

$$CH_4 + O(^1D) \rightarrow CH_3 + OH$$

67
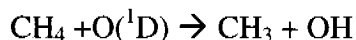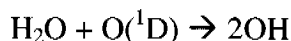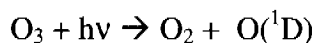
The magnitude of the HO_x changes in the stratosphere is smaller than in the mesosphere, because the variability of the solar UV irradiance responsible for ozone destruction and production of $O(^1D)$ is substantially smaller during solar activity cycle than the variability in Schumann-Runge bands and Lyman-α line (Rottman et al., 2004). The simulated change of the column amount of OH from solar minimum to solar maximum case is around 4% over $40^{\circ}N$, which is in a relatively good agreement with observation data analysis published by Canty and Minschwaner (2002).

Response of NO_2 exhibits almost no changes in the stratosphere, but statistically significant increase in the mesosphere. This increase can be explained by the enhanced concentration of HO_2, which helps to form NO_2 via reaction ($NO+HO_2 \rightarrow OH + NO_2$). This source of NO_2 plays the most important role in the mesosphere, because NO is a dominant representative of NO_y group there. The simulated increase of the NO_2 should be taken with precaution, because in the experiment considered here the model was not set-up to take into account either additional sources of NO_y from the thermosphere or its variability during solar activity cycle as proposed by Garcia et al.(1984). This mechanism is believed to be important for chemistry not only in the mesosphere, but also in the stratosphere (Huang and Brasseur, 1993).

Figure 3.8 d shows statistically significant decrease of ClO in the mesosphere and increase in the stratosphere in the tropics and in the high latitudes. In the mesosphere it is explained by the fact that the production of ClO from the reaction ($Cl + O_3 \rightarrow ClO + O_2$) is suppressed by ozone reduction (see Figure 3.6). In the stratosphere the increase of ClO is the result of intensification of the CFCs destruction due to more intensive photolysis. The model estimates of the ClO changes are in a good agreement with theoretical prospects.

3.3.4 Conclusions

In this paper we document the response of several important atmospheric species (CH_4, N_2O, H_2O, CF_2Cl_2, OH, HO_2, NO_2 and ClO) to the observed increase of the solar irradiance from minimum to maximum of the 11-year solar activity cycle simulated with state-of-the-art CCM SOCOL. The response of ozone, temperature and dynamics to solar irradiance variability have been analyzed by Egorova et al. (2004) and here we concentrate only on chemical aspect of the issue. Our results confirm that solar variability has significant influence on the chemical composition of the stratosphere and mesosphere. We found substantial changes in the concentration of several source gases as well as reservoir and radical species that are responsible for ozone destruction in the atmosphere. Enhanced photolysis rates during solar maximum lead to

additional destruction of methane, nitrous oxide and CFCs providing an increase in the chemical activity of the atmosphere with more pronounced effects in the mesosphere. In the mesosphere an increase of HO_x caused by more intensive water vapor photolysis results in substantial ozone depletion there. More intensive methane oxidation gives statistically significant rise to the stratospheric humidity. The application of the fully coupled CCM allow tracing of dynamical changes influence, which appear as a pronounced decrease of source gases
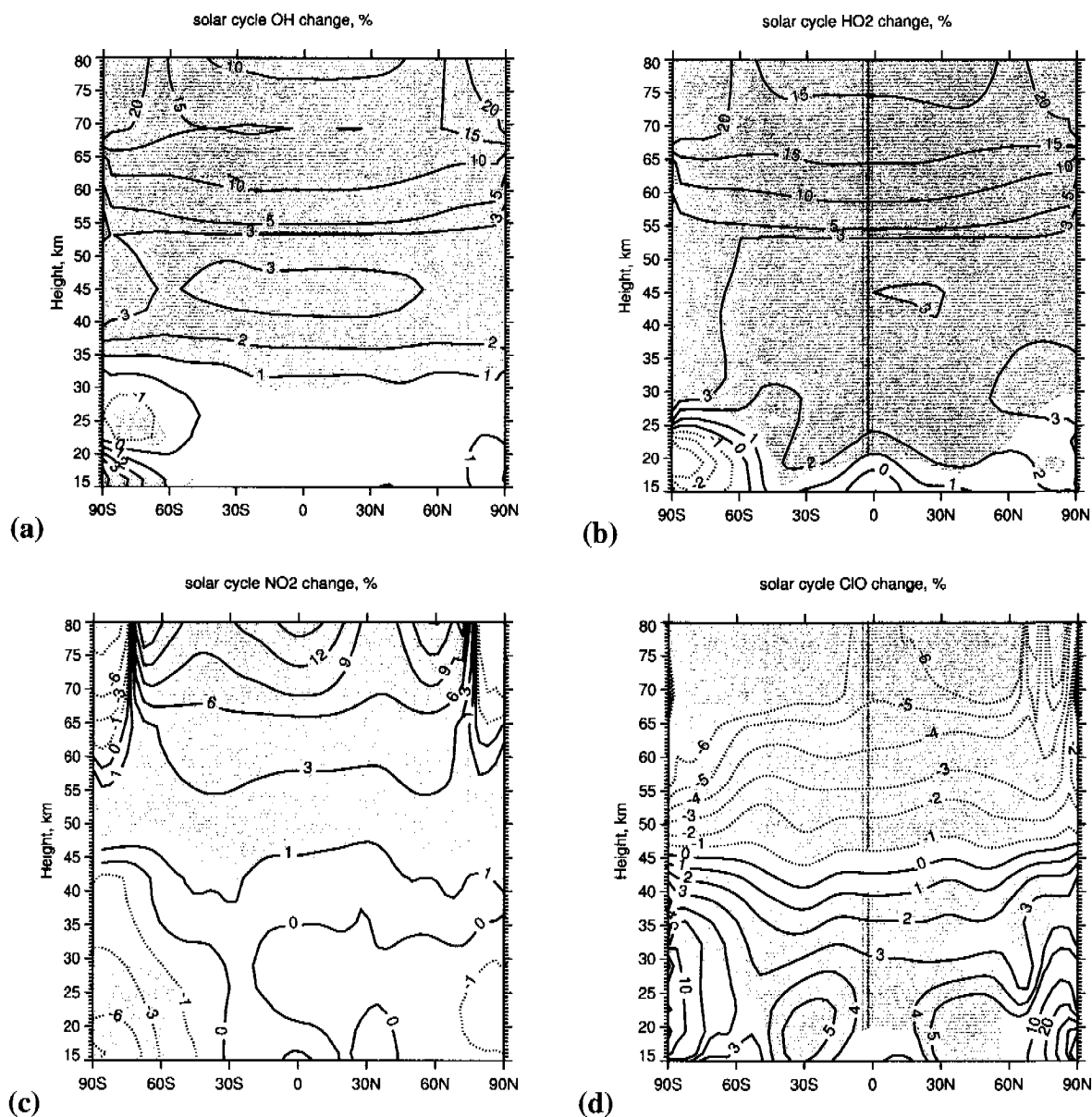

Figure 3.8: *Annual mean zonal mean changes due to 11-year solar variability: (a) for OH, (b) for HO_2, (c) for NO_2 and (d) for ClO. Shaded area marks 95% statistically significant changes.*

over the high latitude area. However, from our CCM results it is impossible to distinguish between chemical and dynamical influence with high level of confidence. An additional run of the same model in off-line mode (i.e. with prescribed dynamics and temperature) may provide the solar signal solely due to chemical processes and subsequent comparison with interactive run can help to elucidate the dynamical contribution. It should be also noted that the model is not capable of simulating transport effects properly because of the steady-state approach used in this study. It is particularly true for long-lived trace species, which have transport times of several years within the middle atmosphere. We will address this issue using the results of our ongoing transient runs. However, we think that the presentation of the solar signal using steady-state approach is necessary step forward in our understanding of the atmospheric response to the solar irradiance variability. It helps to comprehend the chain of physical and chemical processes responsible for the formation of the solar signal in the atmosphere and provide a basis for future analysis of the solar signal obtained from the transient simulations.

Simulated response of the hydroxyl radical is in a reasonably good agreement with theoretical prediction and observation data presented by Canty and Minschwaner (2002). The ozone response does not agree well with the solar signal in ozone extracted from observational data (Egorova et al., 2004). The responses of the other species to solar flux variability (while they are close to the theoretical expectations and qualitatively agree with previous estimations) are hard to validate, because almost no observational studies are available at the moment. We hope that in the nearest future such studies will appear and we will have reliable data to validate our model results. This investigation will help to answer the question why simulated ozone response is far from the observational evidences and which process could be missing in the model.

3.3.5 Acknowledgements

3.3.6 References:

Brasseur, G., and Simon P. C. (1981). Stratospheric chemical and thermal response to long-term variability in solar UV irradiance, *J. Geophys. Res.*, **86**, 7343-7362.

Brasseur, G., Solomon, S. (1986). Aeronomy of the middle atmosphere: Chemistry and physics of the stratosphere and mesosphere. Second edition, D.Reidel Publishing company, Dordrecht, Holland.

Canty, T., Minschwaner, K. (2002). Seasonal and solar cycle variability of OH in the middle atmosphere. *J. Geophys. Res.* **107**(D24), 4737,doi:10.1029/2002JD002278.

Egorova, T., Rozanov, E., Zubov, V., Karol, I. (2003). Model for Investigating Ozone Trends. *Atmos. and Ocean Phys.* **39**, 277-292.

Egorova, T., Rozanov, E., Manzini, E., Haberreiter, M., Schmutz, W., Zubov, V., Peter, T. (2004). Chemical and dynamical response to the 11-year variability of the solar irradiance simulated with a chemistry-climate model, *Geophys. Res. Lett.* **31**, L06119, doi:10.1029/2003GL019294.

Egorova, T., Rozanov, E., Zubov, V., Manzini, E., Schmutz, W., Peter, Th. (2005). Chemistry-climate model SOCOL: A validation of the present-day climatology. *Atmospheric Chemistry and Physics*, accepted.

Fleming, E.L., Chandra, C., Jackman, C.H., Considine, D.B., Douglass, A.R. (1995). The middle atmospheric response to short and long term solar UV variations: analysis of observations and 2D models results. *J. Atm. Terr. Phys.* **57**, 333-365.

Garcia, R., S. Solomon, R. G. Roble, and D. W. Rusch (1984). A numerical study of the response of the middle atmosphere to the 11 year cycle, Planet. Space Sci., **32**(4), 411-423.

Intergovernmental Panel of Climate Change (2001). *Climate Change 2001: The Scientific Basis*, 881pp., Cambridge Univ. Press, New York.

Haigh, J.D. (1994). The role of stratospheric ozone in modulating the solar radiative forcing of climate. *Nature*, **370**, 544-546.

Hood, L.L., Jirikowic, J., McCormack, J.P. (1993). Quasi-decadal variability of the stratosphere: Influence of long-term solar ultraviolet variations. *J. Atmos. Sci.* **50**, 3941-3958.

Hood, L. L. (2004). Effects of solar UV variability on the stratosphere. In *Geophysical Monograph* **141**: Solar Variability and its Effects on Climate, *AGU*, 283-303.

Huang, T., Brasseur, G. (1993) Effect of long-term solar variability in a two-dimensional interactive model of the middle atmosphere. *J. Geophys. Res.* **98**, 20,413-20, 427.

Kiselev, A., and E. Rozanov (1985). Radiative-photochemical modeling of the ozone mechanism of the Sun – Earth connections, VNIIGMI-WDC publication No. 452gm, p. 54-65 (in Russian).

Khosravi, R., Brasseur, G., Smith, A., Rusch, D., Walters, S., Chabrillat, S., Kockarts, G. (2002). Response of the mesosphere to human-induced perturbations and solar variability calculated by a 2-D model. *J. Geophys. Res.* **107**, 4358, doi:10.1029/2001JD001235.

Labitzke, K., Austin, J., Butchart, N., Knight, J., Takahashi, M., Nakamoto, M., Nagashima, T., Haigh, J., Williams, V. (2002). The global signal of the 11-year solar cycle in the stratosphere:observations and models. *J. Atmos. Sol. Terr. Phys.* **64**, 203-210.

Lean, J, Rottman, G.J., Kyle, H.L., Woods, T.N., Hickey, J.R., Puga, L.C. (1997). Detection and parameterization of variations in solar mid- and near-ultraviolet radiation (200-400 nm), *Geophys. Res. Lett.*, **102**, 29939-29956.

Lee, H. and A. Smith (2003). Simulation of the combined effects of solar cycle, quasi-biennial oscil;ation, and volcanic forcing on stratospheric ozone changes in recent decades, *J. Geoph. Res.*, **108**(D2), 4049, doi:10.1029/2001JD001503.

Manzini, E., McFarlane, N. (1998). The effect of varying the source spectrum of a gravity wave parameterization in the middle atmosphere general circulation model. *J. Geophys. Res.* **103**, 31523-31539.

Manzini, E., McFarlane, N., McLandress, C. (1997). Impact of the Doppler Spread Parameterization on the simulation of the middle atmosphere circulation using the MA/ECHAM4 general circulation model, *J. Geophys. Res.* **102**, 25751-25762.

Reid, G. C. (2000). Solar variability and the Earth's climate: Introduction and overview. *Space Science Reviews* **94**, 1-11.

Rottman, G., Floyd, L., Viereck, R. (2004). Measurement of the solar ultraviolet irradiance. In *Geophysical Monograph* **141**: Solar variability and its effects on climate, *AGU*, 111-125.

Rozanov, E.V., Schlesinger M.E., Egorova T.A., Li B., Andronova N., Zubov V.A.(2004). Atmospheric response to the observed increase of solar UV radiation from solar minimum to solar maximum simulated by the UIUC climate-chemistry model. *J. Geophys. Res.* **109**, D01110, doi:10.1029/2003JD003796.

Tourpali, K., Schuurmans, C., van Dorland, R., Steil, B., Brühl, C. (2003). Stratospheric and tropospheric response to enhanced solar UV radiation: A model study. *Geophys. Res. Lett.*, **30**(5), 1231, doi: 10.1029/2002GL016650.

3.4 Seasonal and geographical distribution analysis

Seasonal and geographical variations of solar induced changes

in ozone, temperature and zonal wind

T. Egorova[1,2] et al.

Abstract. In this paper seasonal and geographical variation of solar-induced changes in the atmospheric parameters have been analyzed, separate influence of UV and visible radiation are have been studied and seasonal behavior of simulated zonal mean zonal wind and temperature changes with corresponding data of observational analysis have been compared. In the mesosphere a negative ozone anomaly has been obtained throughout the year at the tropical latitudes. In the stratosphere ozone response is positive and maximizes at 50 hPa in the tropics up to 4% from November to February. Temperature changes over the tropics in the stratosphere are positive with maximum response at 1 hPa of about 1 K. Over the high latitudes the sign of the temperature response depends on season. Zonal wind anomaly appears in June around 50°S and propagates with time poleward and maximizes in November reaching 12 m/s. We consider geographical distribution of solar-induced changes in geopotential height, temperature and zonally averaged zonal wind at different atmospheric levels for December, surface air temperature for winter over the Northern Hemisphere and total ozone column. The response of total ozone to solar irradiance changes has been obtained in the tropics throughout the year and comprise of an increase by 3-5 DU. In southern high latitudes the model simulates a total ozone decrease by up to 20 DU in November caused by the vortex intensification. The study of separate influence of UV and visible radiation has shown that UV radiation influence dominates in the stratosphere and plays a role in surface air temperature changes. The pattern of the simulated zonal wind and temperature anomalies has some resemblance with the analysis of observations but differ in timing and magnitude. Obtained results in this work support the idea of a solar UV influence on the dynamical state of the atmosphere.

3.4.1 Seasonal variation of Sun-induced changes in ozone, temperature and zonal wind

Figure 3.9 shows the seasonal evolution of solar-induced zonal mean ozone mixing ratio differences in percent ($[O_3]_{solmax}-[O_3]_{solmin})/[O_3]_{solmin}$ on the 0.1, 10 and 50 hPa levels. Shaded areas mark statistical significance on the 95 % confidence level. In the mesosphere (Fig. 3.9a) a negative ozone anomaly has been obtained throughout the year at the tropical latitudes, mainly due to photolysis of H_2O at very short wavelengths, mainly by the solar Lyman-α line

---

[1] Institute for Atmospheric and Climate Science ETH, Zürich, Switzerland
[2] Physical-Meteorological Observatory/World Radiation Center, Davos, Switzerland

at $\lambda = 121.6$ nm, which yields additional production of ozone-destroying HO_x radicals. Over the high latitudes at 0.1 hPa model results show also a negative response during the summer, but a positive response during wintertime. This positive response might be connected to more intensive downward transport for the solar maximum conditions from the area of tertiary ozone mixing ratio maximum that situated in the mesosphere over high latitudes (Marsh et al., 2001) and well reproduced by SOCOL. A reason for the summer negative feedback at high latitudes is the same as for the tropical area. At 10 hPa (Fig. 3.9b) we find a statistically significant solar-induced ozone increase, which is due to a more intensive photolysis of molecular oxygen at $\lambda < 242$ nm and subsequent ozone production. The ozone solar signal maximizes at 50 hPa (Fig. 3.9c) in the tropics of both Southern and Northern hemispheres, reaching about 4 % from November to February. In the lower stratosphere, the retrieved ozone changes are connected mainly to circulation changes (acceleration of stratospheric jets and deceleration of meridional transport during boreal winter, see Fig. 3.11). There are statistically significant positive changes over southern high latitudes with a maximum ozone response of about 6 % from January to May, but only during March, April and May the changes in ozone mixing ratio here are statistically significant.

Figure 3.10 presents the seasonal dependence of zonal mean temperature changes due to 11-year solar irradiance variability at 1, 10 and 50 hPa. Over the tropics a positive signal is obtained throughout the tropical stratosphere with the maximum response at 1 hPa of about 1 K. Over the northern high latitudes there are no statistically significant changes in temperature during boreal winter. Over the southern high latitudes the signal appears at 1 hPa as positive response to 11-year solar irradiance variability for all seasons except for the austral winter. Below 1 hPa at southern high latitudes the response has different sign: for SON it is negative and for DJF it is positive, revealing seasonal changes in the circulation. The simulated temperature response has a dipole structure in the meridional direction during SON when the intensification of PNJ dominates, and is accompanied by more intensive downward motions in the upper stratosphere and subsequent compression heating. Hence the stratosphere warms at 1 hPa. Conversely, it cools at 10 hPa and below due to radiative processes and the decrease of the horizontal heat transport due to a stronger and more isolated vortex. Similar features of the seasonal evolution of the temperature solar signal can be seen over the northern high latitudes, however not statistically significant.

Figure 3.11 presents the seasonal development of the solar-induced changes in zonal mean zonal wind. The maximum of the response has been obtained in the Southern Hemisphere for September, October, November and December, which display a statistically sig-

nificant intensification of PNJ during solar maximum by about 10-12 m/s at all considered levels of the simulated atmosphere. The zonal wind anomaly appears in June around 50°S, reflecting the intensification of the subtropical jet in the upper stratosphere caused by an in
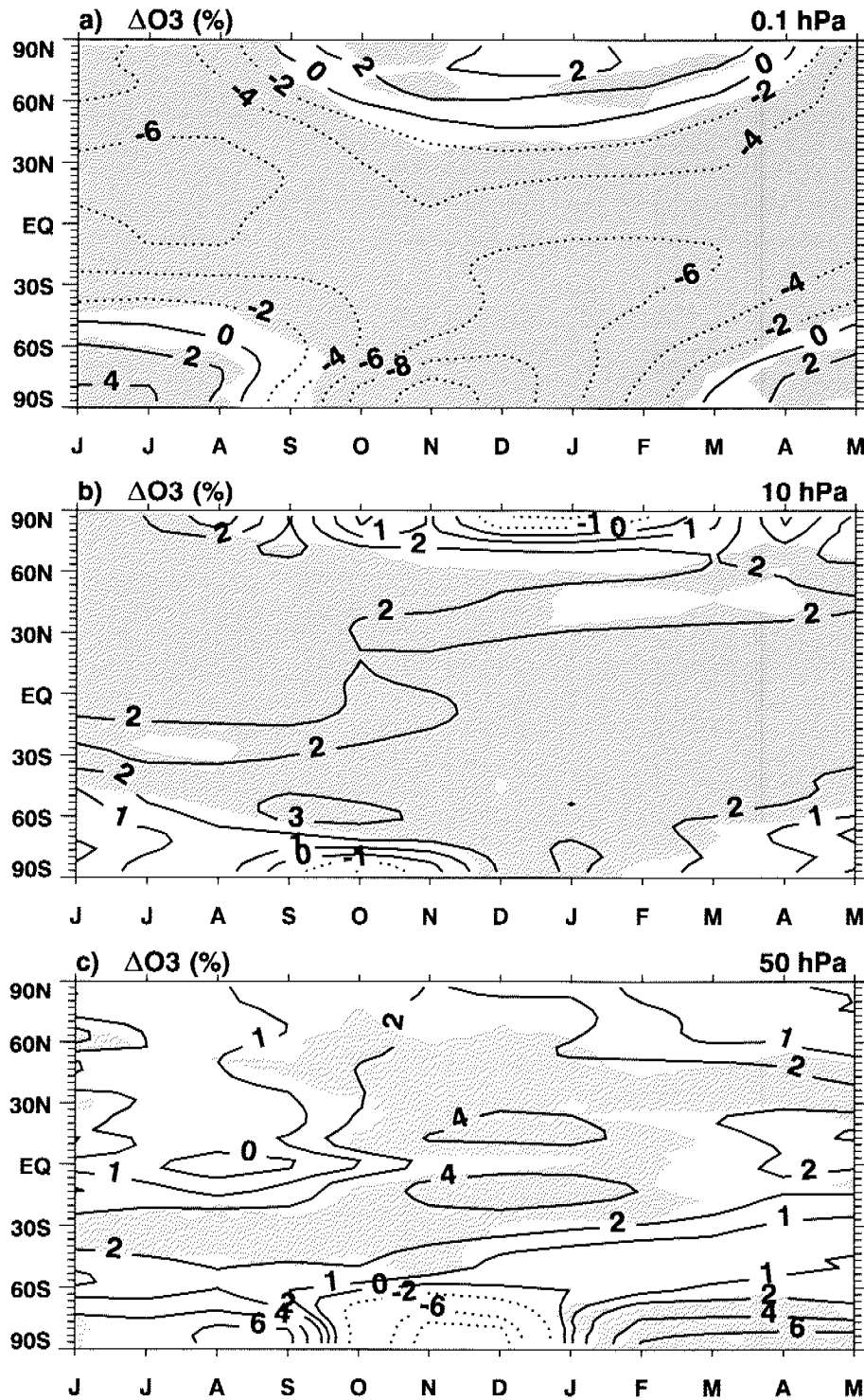
Figure 3.9: *Seasonal dependence of solar-induced ozone mixing ratio changes ($[O_3]_{solmax}$-$[O_3]_{solmin}$)/$[O_3]_{solmin}$ (%): (a) at 0.1 hPa; (b) at 10 hPa; (c) at 50 hPa. Shading marks statistical significance at the 95-%-level of confidence.*
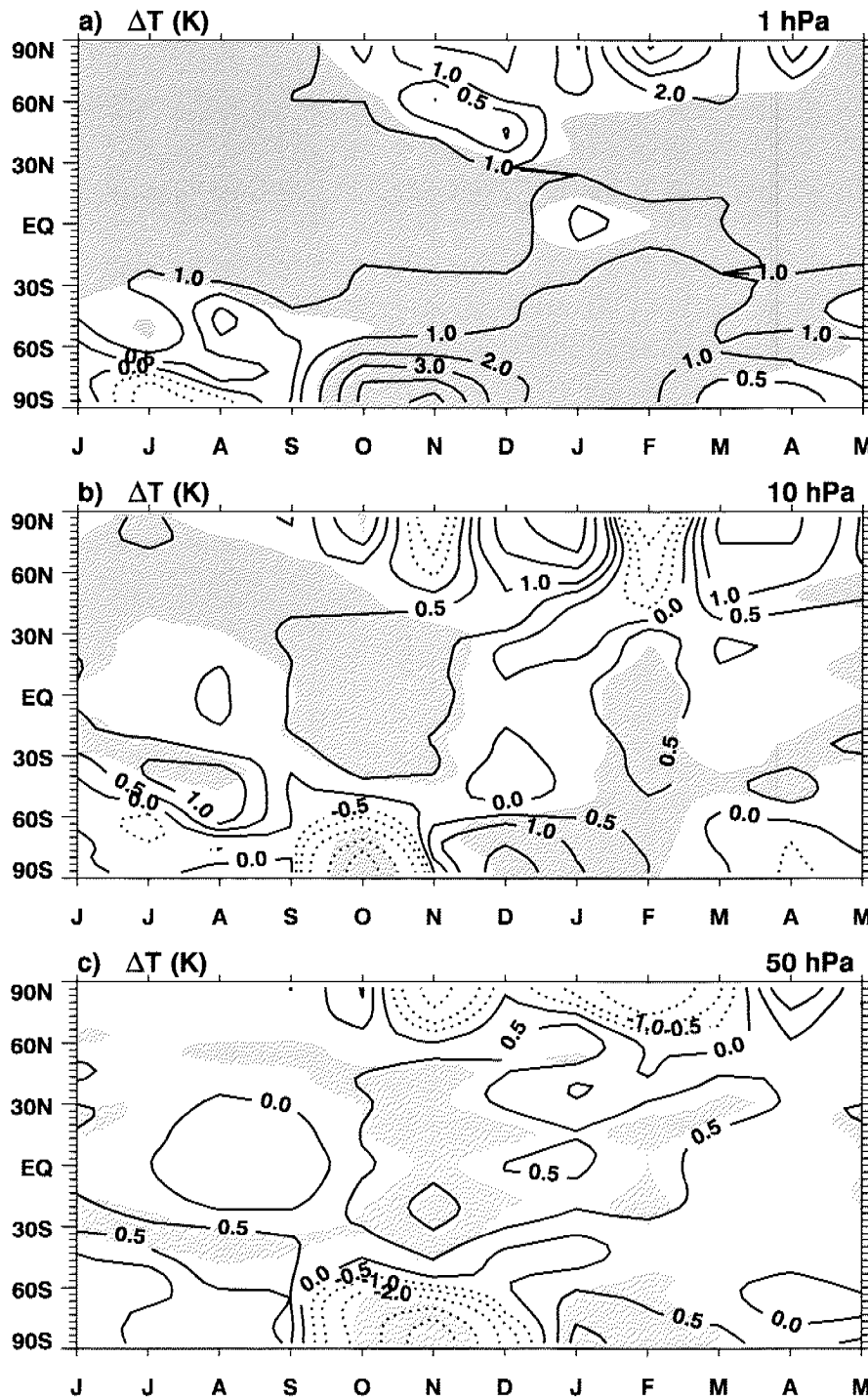
Figure 3.10: *Seasonal dependence of solar-induced temperature changes (T_{solmax}- T_{solmin})/T_{solmin} (K): (a) at 1 hPa; (b) at 10 hPa; (c) at 50 hPa. Shading marks statistical significance at the 95-%-level of confidence.*

crease in the latitudinal temperature gradient. With the course of time it propagates poleward and maximizes in November. Over the northern high latitudes the solar signal appears to be significant at only 80 % confidence level (not shown). During boreal winter and spring the zonal wind response changes the sign from positive to negative values at 1 hPa over the
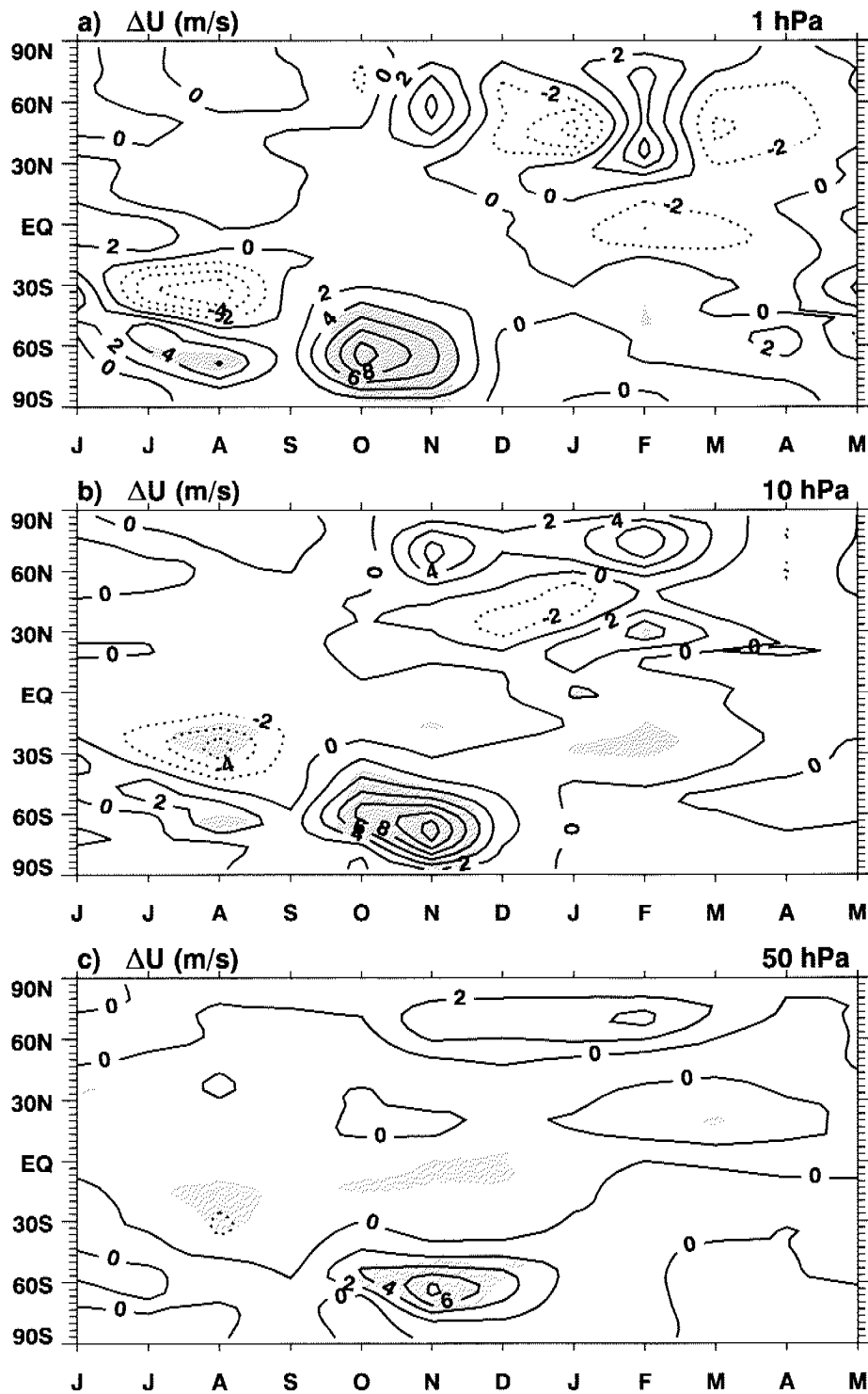
Figure 3.11: *Seasonal dependence of solar-induced zonal wind changes (u_{solmax}-u_{solmin})/u_{solmin} (m s^{-1}): (a) at 1 hPa; (b) at 10 hPa; (c) at 50 hPa. Shading marks statistical significance at the 95-%-level of confidence.*

northern high latitudes. The intensification of the vortex occurs manly during November and February. At the lower levels the zonal wind changes are positive and imply strengthening of polar vortex, but with only marginal significance (at 80 % level).

3.4.2 Geographical distribution of the solar-induced changes

As shown above, the solar-induced warming of the tropical stratosphere shifts temperature gradients in the meridional direction with subsequent alteration of the pressure and zonal wind fields. In this section the geographical distribution of solar-induced changes in several atmospheric parameters are considered. Figure 3.12 presents the geographical distribution of the solar-induced changes in geopotential height (GPH), temperature and zonal wind for December at different levels. The geographical distribution of the geopotential height changes has a structure with positive and negative values that can be seen from 0.1 to 850 hPa. Positive values maximize at 1 hPa (not shown) and have 550 gpm magnitude over North Canada and Alaska as well as negative values over the Northern Russia and Europe with 350 gpm magnitude. At lower levels the negative anomaly is shifted to the North Pole. It is seen that the negative anomaly of the geopotential height moves poleward and downward in accordance with the analysis of observations (Kodera and Kuroda, 2002).

Solar-induced changes in temperature also display a dipole structure and reach + 5 K at 10 hPa over Northern Canada and their minimum with – 3 K over Northern Russia and Europe, but the latter are statistically not significant. In accordance with the temperature changes at 10 hPa statistically significant positive (6 m/s) and negative (9 m/s) changes have been obtained in the zonal wind over the same areas. Solar-induced changes of GPH are consistent with changes in temperature and zonal wind presented in the Figure 3.12. Therefore we conclude that the obtained changes due to enhanced solar irradiance are physically reasonable and should be significant not only in the stratosphere but also in the troposphere.

Figure 3.13 presents simulated changes in the surface air temperature for boreal winter (mean for December, January and February) over the Northern Hemisphere. The obtained changes result in shifts of surface temperature gradients across the continents. Over the north of Europe and Russia, and north of Canada and U.S. the model suggests positive changes up to 1.5 K, and over Greenland and Asia the model produces negative (up to 2.5 K) response to enhanced solar irradiance. The similarity to the annual-mean Figure 3.4, but with more pronounced perturbations, is evident.
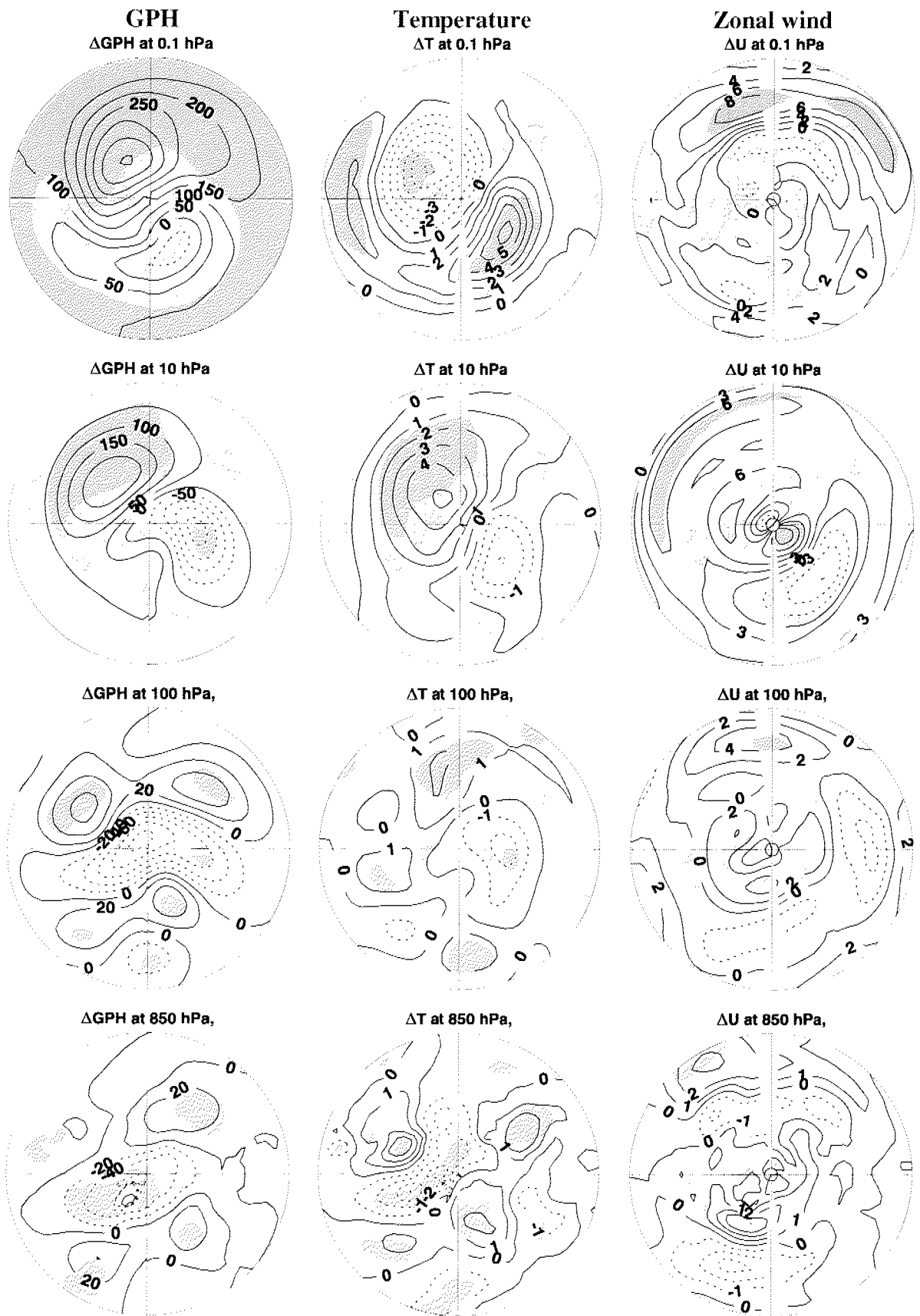
Figure 3.12: *Geographical distribution of solar-induced changes in geopotential height (m), temperature (K) and zonal wind (m/s) for various atmospheric model levels for December.*

ΔTs, DJF

Figure 3.13: *Geographical distribution of solar-induced changes in surface air temperature (in K) over the Northern Hemisphere in boreal winter (DJF) simulated by SOCOL.*

3.4.3 Solar-induced changes in total ozone

Figure 3.14 presents the seasonal cycle of solar-induced changes in total ozone. It can be seen that the total ozone changes reflect the changes of the meridional circulation in the lower stratosphere from solar maximum to solar minimum. The most pronounced and statistically significant response of total ozone to solar irradiance changes has been obtained in the tropics ($30°N$-$30°S$) throughout the year, which is equivalent to an increase of 3-5 DU. In the period
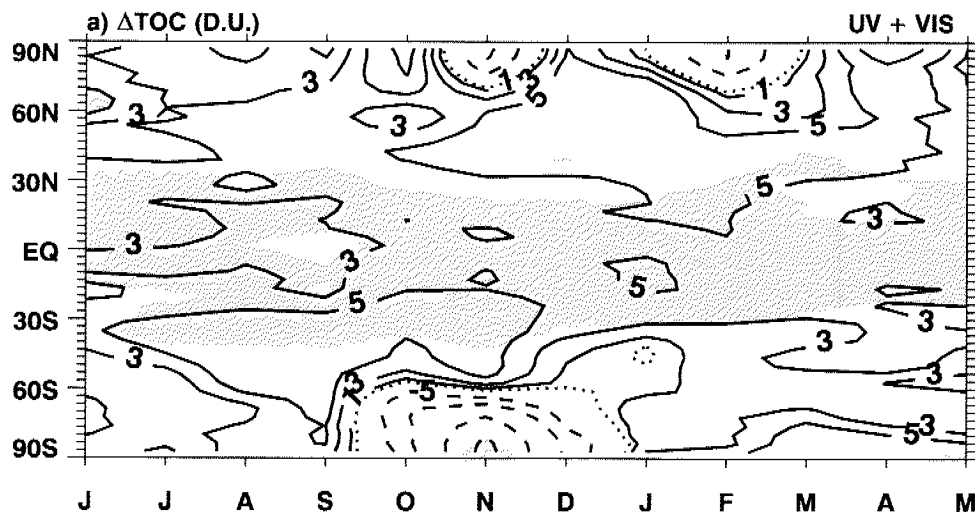
Figure 3.14: *Seasonal development of solar-induced changes in total ozone column (in DU).*

October-December over the southern high latitudes the model simulates a total ozone decrease by up to 20 DU, which is connected to the indirect influence of solar irradiance changes on total ozone through changes in dynamics. During solar maximum conditions, the ozone hole is deeper because of polar vortex is stronger. Over the northern high latitudes negative changes also take place, but they are not statistically significant.

Figure 3.15 illustrates the geographical distribution of solar-induced changes in total ozone (in %) for February over the NH and for November over the SH, when the response of total ozone to solar irradiance changes reaches the maximum. In the NH the negative signal maximizes over Pole and Northern Canada, positive one is over Scandinavia, Europe and Northern Russia (±5%). Only in the SH the total ozone changes are statistically significant (shading) and take place over Antarctica (-15 %) and over Atlantic sector (+7 %).
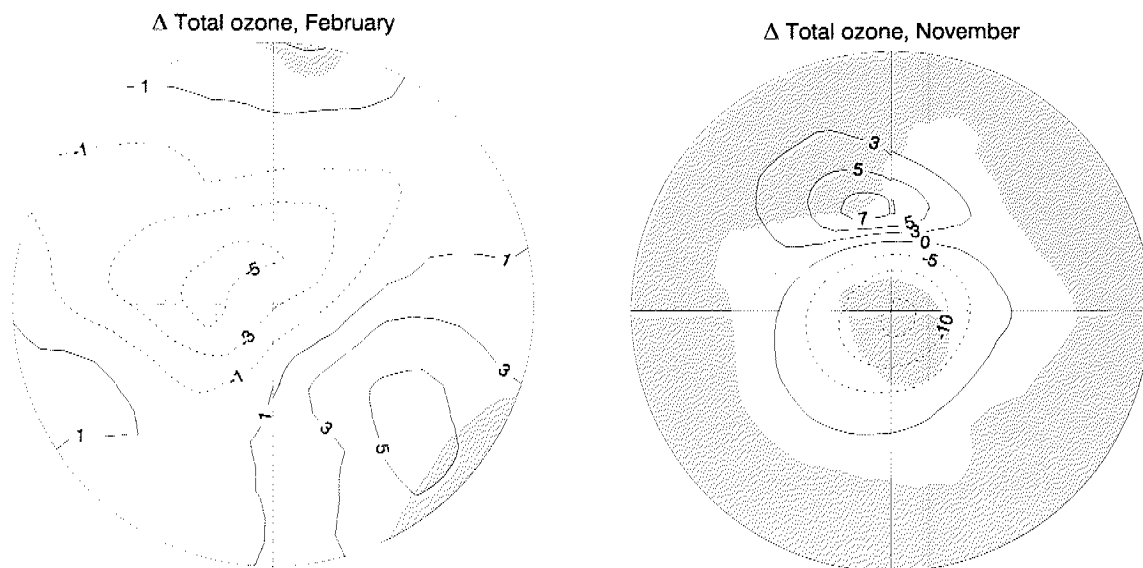
Figure 3.15: *Geographical distribution of solar-induced changes in total ozone for February in the Northern Hemisphere and for November in the Southern Hemisphere.*

The simulated annual mean total ozone response is presented and compared with two sets of satellite data (WMO, 2003) in Figure 3.16. The comparison shows that the model matches the observed total ozone changes from 50°S to 60°N within the uncertainty of the observational analysis. The total ozone changes simulated by the CCM are close to zero over the high latitude in annual mean response. The decrease from middle latitudes to the poles in the both hemispheres is in accordance with the simulated intensification of the PNJs during solar maximum conditions.

81
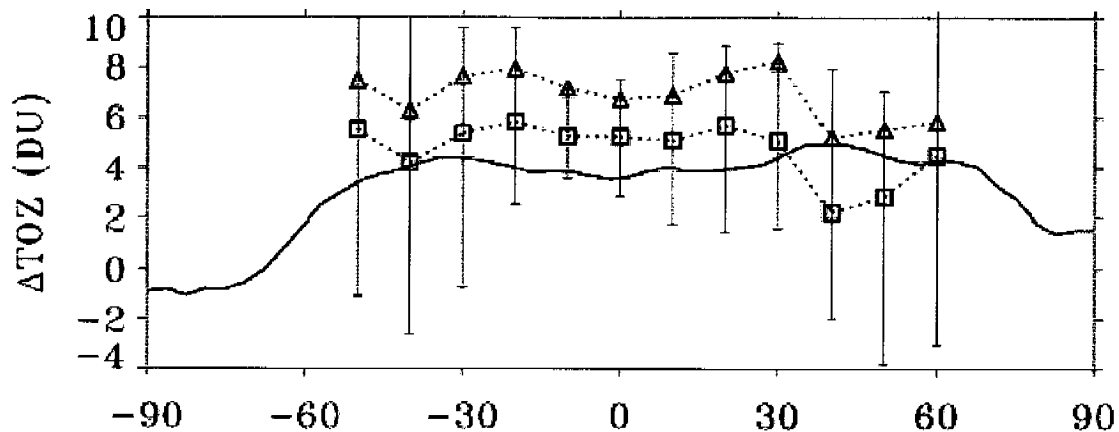
Figure 3.16: *Comparison of the simulated annual mean total ozone response with observations. The solid line represents the simulated total ozone changes by SOCOL. Two other lines are from observational data sets: SBUV/SBUVII (dotted line with open squares) and merged satellite data (dotted line with open triangles) according to WMO (2003).*

3.5 Separate influence of UV and Visible radiation

3.5.1 Introduction

In this section we present the separate influence of UV and visible radiation variability during the 11-year solar cycle on the Earth's atmosphere as simulated with the CCM SOCOL. The wavelength dependence of the absorption of solar radiation in the atmosphere suggests to inspect the influence of UV and visible (VIS) radiation variations on the atmosphere separately. The UV radiation is absorbed mostly in the mesosphere and stratosphere; VIS radiation is predominantly absorbed in the lower troposphere and at the surface. The land surface is able to absorb visible radiation and additional heating (according to MA-ECHAM4 surface parameterization) may be transported to the lower troposphere also over the sea. Given these different atmospheric responses, changes caused by UV and VIS can potentially amplify or weaken each other. To investigate these effects during the 11-year solar cycle separately, two additional 20-year long steady-state simulations using prescribed SST/SI have been performed, applying the following combination of solar visible and UV irradiance: in one simulation only observed UV changes, and in the other only VIS changes have been introduced. A detailed description of the performed experiments is presented in Section 3.3.2.

3.5.2 Annual mean

Here a preliminary analysis of the separate influences of UV and VIS variability during 11-year solar cycle on the zonal mean zonal wind and surface air temperature is presented. Figure 3.17 represents the influence of UV and VIS radiation on annual mean zonal mean zonal

wind. In the "VIS only" case a significant signal above the tropopause has been obtained that results in an intensification of the easterlies in the tropics. In the "UV only" case a significant positive signal has been obtained in the upper stratosphere over the middle latitudes of the both hemispheres. The zonal mean pattern in the zonal wind is different for UV and VIS radiation except in the northern high latitudes, where a small weakening of vortex in the both cases has been obtained. In case of combined effects we obtained the intensification of PNJ in the both hemispheres.
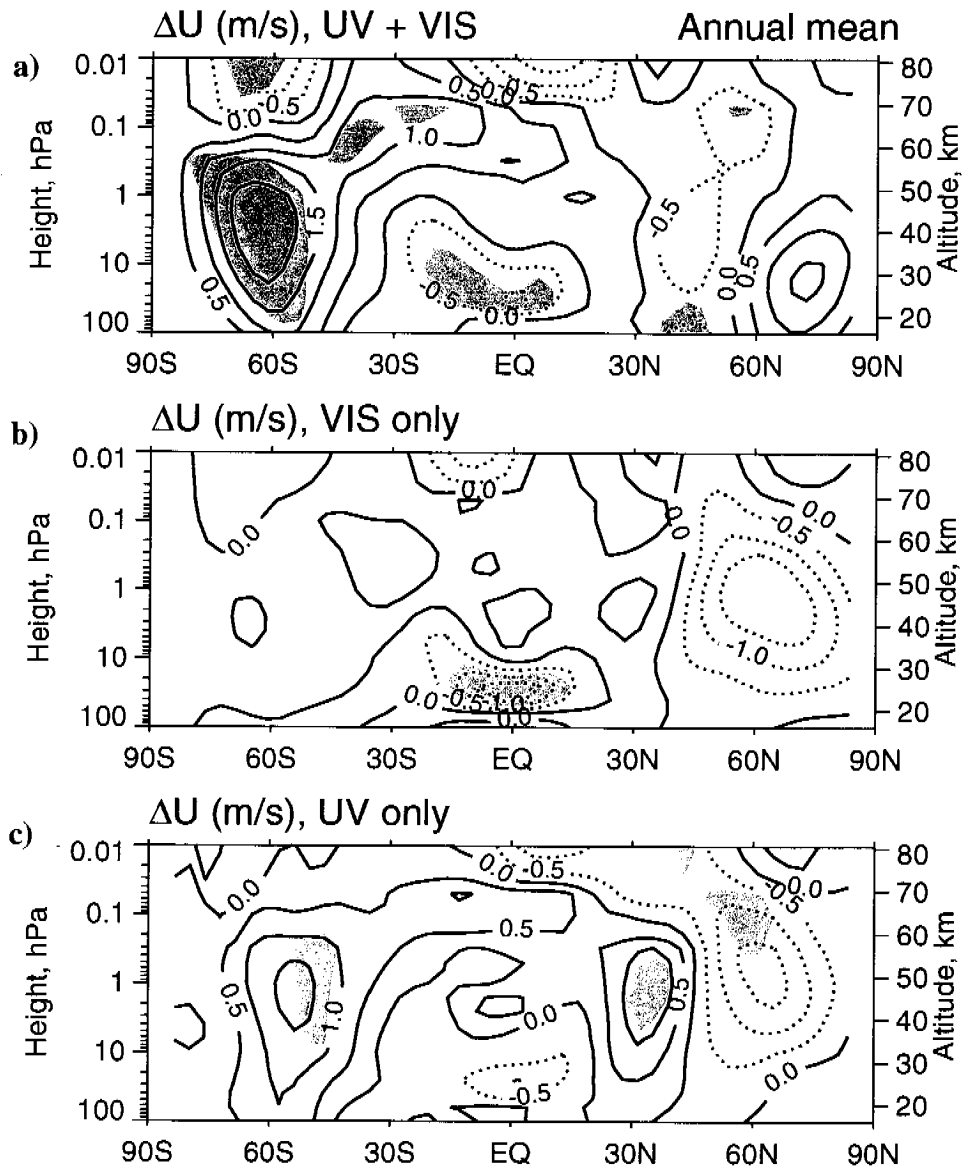
Figure 3.17: *The annual mean zonal mean signal in zonal wind (ms^{-1}) due to variations during 11-year solar cycle: (a) combined influence of UV and visible radiation; (b) due to visible only; (c) due to UV only. The shading marks regions with statistically significant signal at the 95 % confidence level.*

a) ΔTs (K), Ann.mean, UV+VIS

b) ΔTs (K), Ann.mean, VIS

c) ΔTs (K), Ann.mean, UV
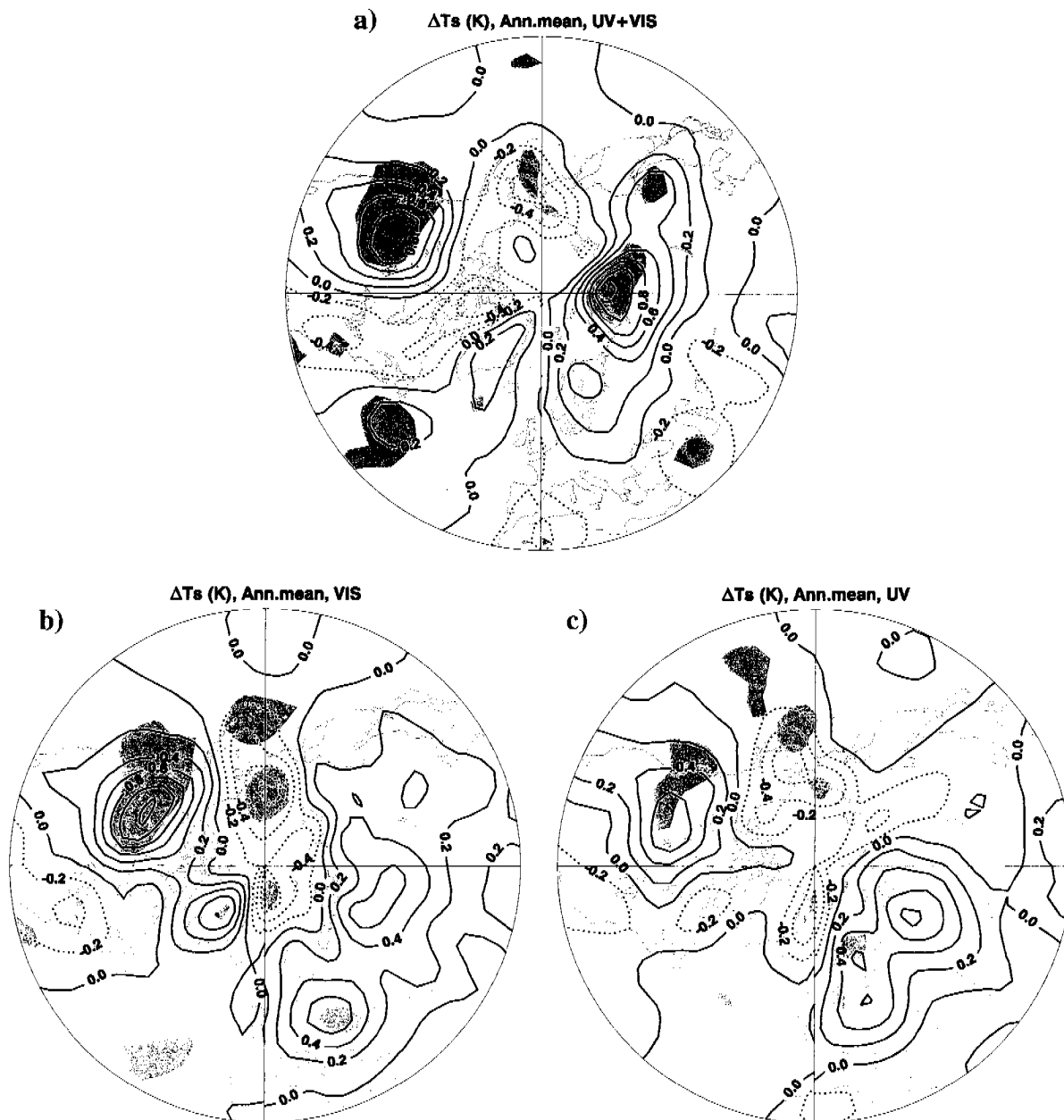
Figure 3.18: *Geographical distribution of the annual mean surface air temperature changes over the Northern Hemisphere due to VIS and UV radiation. The shading marks regions with statistically significant signal at the 95 % confidence level. Contour interval is 0.2 K.*

Figure 3.18 demonstrates the geographical distribution of the VIS and UV radiation influence on the annual mean surface air temperature. UV radiation alone produces some effect on the surface air temperature (Figure 3.18c), which is in general smaller than the "VIS only" influence (Fig. 3.18b) over North America and has comparable effects over Europe and Russia. The annual mean pattern of the signal distribution is very similar for the both cases. However, as will be shown later, UV and VIS radiation dominate in different geographical

regions during different seasons. The combined effect exhibits larger amplitude of the signal over the North of the Russian Federation and smaller amplitude over North America.
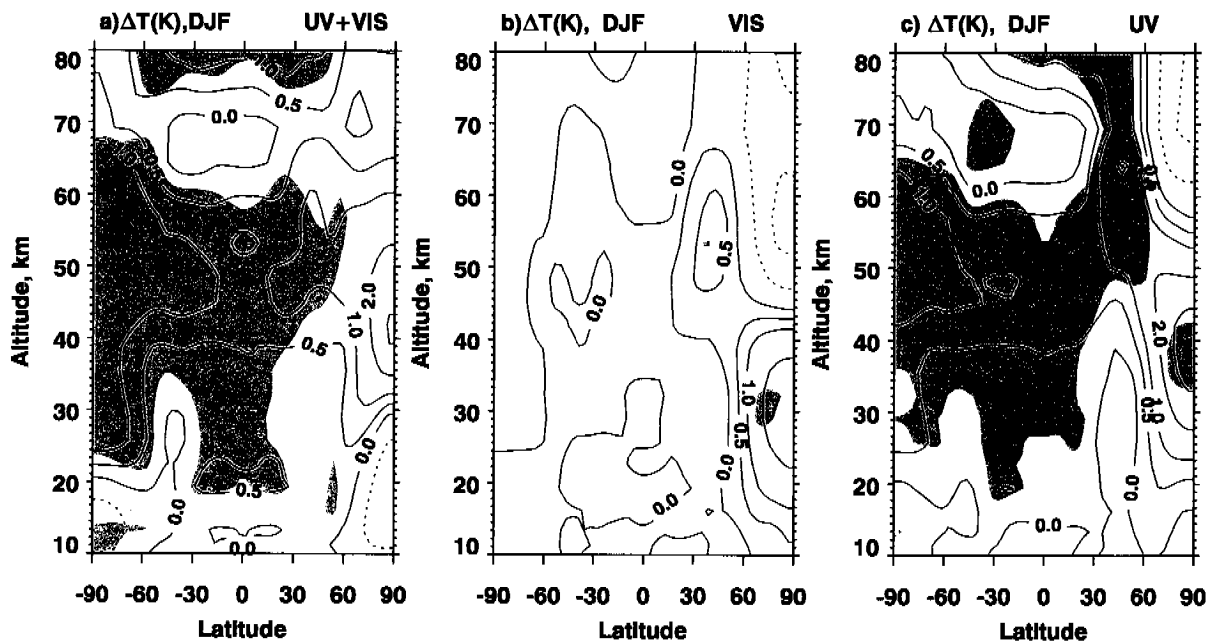
Figure 3.19: *The zonal mean signal in temperature (K) during 11-year solar cycle: (a) due to combined influences of UV and VIS; (b); due to VIS variability only; (c) due to UV variability only averaged for DJF . The shading marks regions with statistically significant signal at the 95 % confidence level.*

3.5.3 Seasonal mean

Figure 3.19 presents 11-year-cycle-induced winter mean (DJF) zonal mean changes in temperature for all three cases: UV+VIS, VIS and UV only. As can be seen from this figure only UV radiation is able to significantly influence stratospheric temperatures. For the "UV only" case (Figure 3.19c) and combined influence (Figure 3.19a) positive changes have been obtained in the upper stratosphere. Positive changes have been also found in the lower tropical stratosphere for the combined influence case and have dynamical origin. Similar, but more pronounced warming has been found in the analysis of observations for annual means by Labitzke (2001).

Figure 3.20 presents the corresponding changes in the zonal mean zonal wind for the winter in the stratosphere (upper panel of Figure 3.20) and troposphere (lower panel of Figure 3.20). As for the annual mean signal different zonal mean patterns have been obtained for the winter in all three experiments, but with larger magnitude of the zonal wind response. For the "UV only" case (Figure 3.20c) the positive anomaly is shifted to the tropics, for "UV + VIS" the positive anomaly developed in high latitudes (Figure 3.20a) that associated with the

changes of the lower part of the stratospheric jet(Figure 3.21a). For the "VIS only" case there are no statistically significant changes in the stratosphere (Figure 3.20b), however the core of PNJ has shrunken (Figure 3.21b). In case of "UV only" a shift towards to the equator of the stratospheric jet core has happened (Figure 3.21c). UV + VIS anomaly envelopes not only the stratosphere but also troposphere (Figure 3.20d). In case of only UV influence tropospheric anomaly is separated from anomaly in the stratosphere (Figure 3.20f) and mainly formed due to expansion of the tropospheric jet boundary to the North Pole (Figure 3.21b). These results show that UV solar variations may quite substantially alter stratospheric and tropospheric jets, in particular their boundaries in middle latitudes by indirect mechanism through ozone and oxygen absorption in the upper stratosphere. The reason for the smaller influence of VIS changes on the stratospheric dynamical patterns is that visible radiation is not efficiently absorbed, quite in contrast to UV radiation.
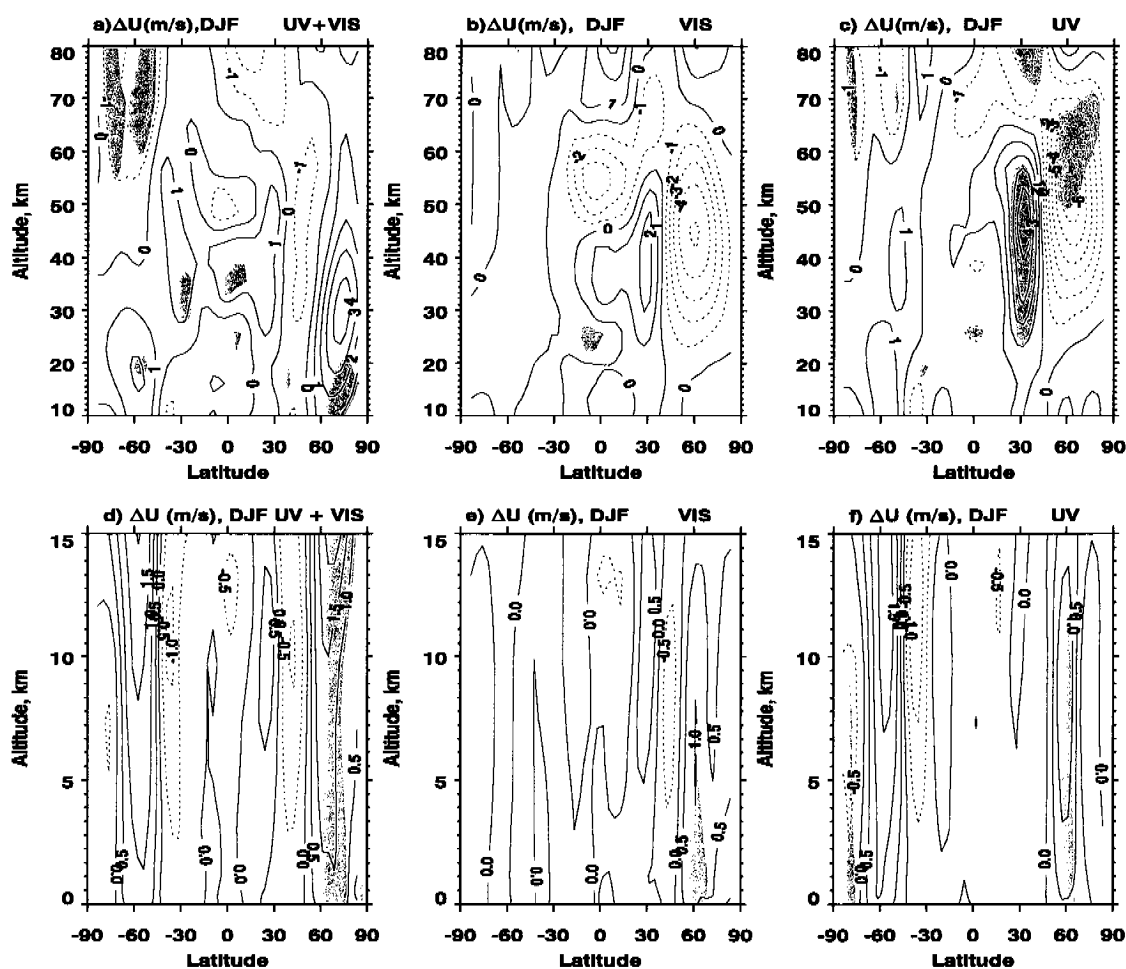
Figure 3.20: *Winter mean zonal mean signal in zonal wind (ms^{-1}) during 11-year solar cycle for the stratosphere (a, b, c) and troposphere (d, e, f): (a, d) combined influence of UV and VIS variability; (b, e) VIS variability only; (c, f) UV variability only. The shading marks regions with statistically significant signal at the 95 % confidence level.*

86
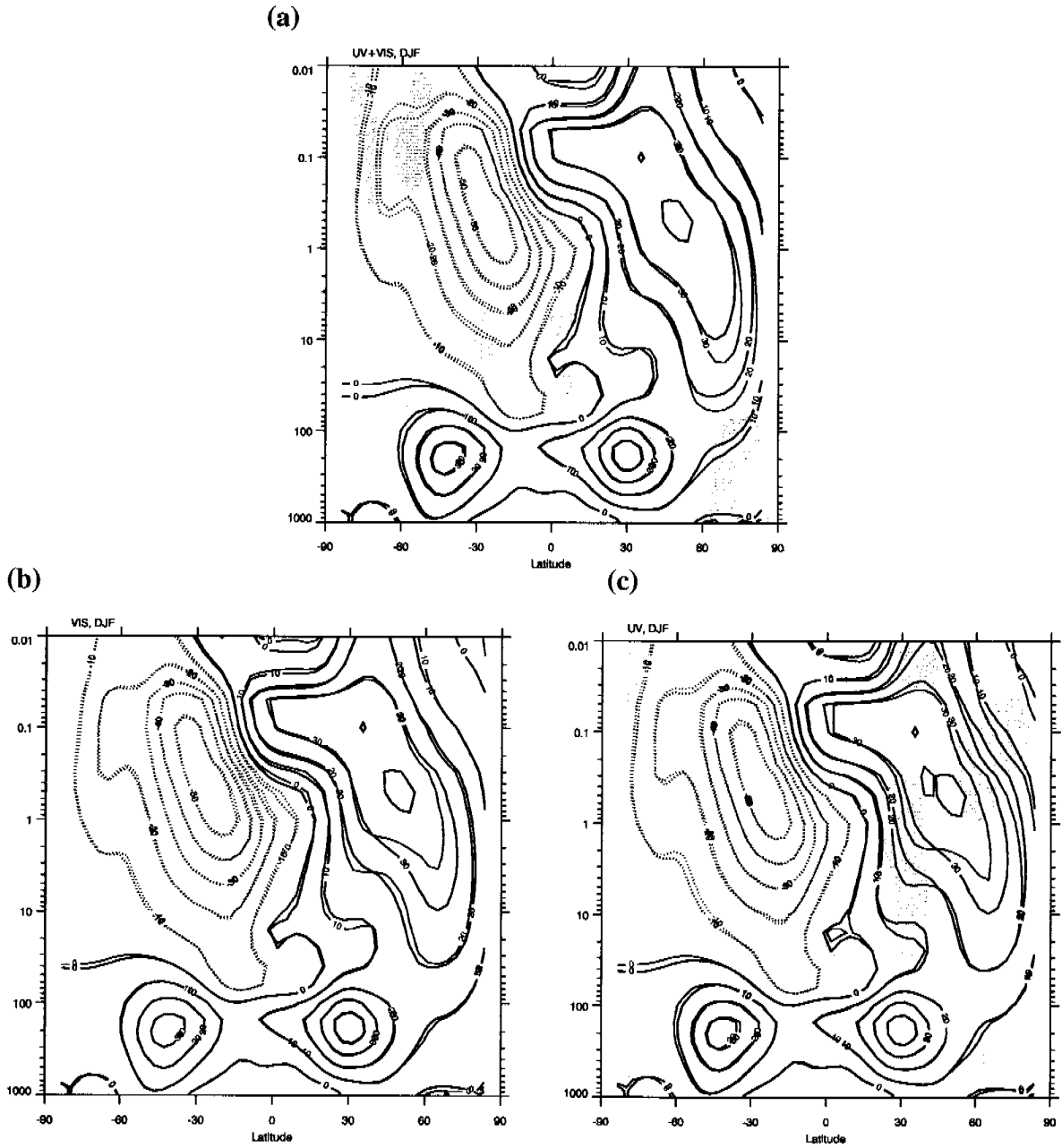
Figure 3.21: *Distribution of zonal mean zonal wind for DJF: (a) VIS + UV case; (b) VIS only case; (c) UV only case. Black isolines represent distribution for solar minimum, red lines for solar maximum.*

Fig. 3.22 presents changes in the surface air temperature for the winter season and shows that the influences of UV and VIS radiation superimpose non-linearly. For the winter season the VIS influence is dominating (Figure 3.22b) and their combined influence gives a slightly reduced magnitude of the signal (Figure 3.22a). The opposite result is found for autumn (Figure 3.23) when the UV dominates changes of surface air temperature. For the winter model results show air surface temperature pattern close to the pattern typical for positive phase of AO as for annual mean values. The causes of such statistically significant pattern are

87

the changes of meteorological quantities during solar maximum in winter. During solar maximum the model shows lower than during solar minimum atmospheric pressure over the Arctic and eastern North America (see geographical distribution of geopotential height, temperature and wind at 100 hPa on Fig. 3.12). It leads to stronger westerly winds at northern latitudes, which results in colder air over Arctic and warmer temperatures over western United States for solar maximum. Over the central Atlantic higher atmospheric pressure and stronger westerly winds during the solar maximum lead to warmer temperatures over the northern Europe, and model results show warmer surface air temperature over the North Europe and Asia. For the fall model shows somewhat different pattern of surface air temperature changes for all three considered cases. It might be explained by different monthly response of zonal wind for the considered cases. However, Fig. 3.22 supports the idea that changes in UV radiation alone are able redistribute surface air temperature and shows that it's influence prevail during transitional seasons.

3.5.4 Conclusion

The effects of variations in solar irradiance during the 11-year solar cycle using a chemistry-climate model has been investigated. Two additional 20-year long steady-state simulations have been performed using observed spectral solar fluxes, which allow separation of the ultraviolet (UV) and visible (VIS) radiation influence on the atmosphere. For the simulation in which only the visible radiation was enhanced, a significant response in zonal wind has been obtained in the tropical stratosphere. The analysis of the surface air temperature response shows that the VIS and UV radiation dominate in different geographical regions during the year, but produce similar annual mean pattern.

The described results have been obtained from the SOCOL steady-state runs with fixed SST/SI distribution. Such a limitation hampers the ability of the model to simulate the response of the tropospheric temperature and dynamics to the solar variability; therefore the obtained results should be taken with caution. It is very desirable to repeat our experiments using the model with interactive ocean dynamics or applying SOCOL in transient mode driven by the observed SST/SI distribution as well as by other known forcing mechanisms to simulate long-term changes in the atmosphere. In the latter case the comparison of the surface air temperature behavior in the two model runs (with solar irradiance variability switched on and off) with observational data would allow to determine the contribution of the solar irradiance variability to the surface air temperature changes over the land with higher confidence.
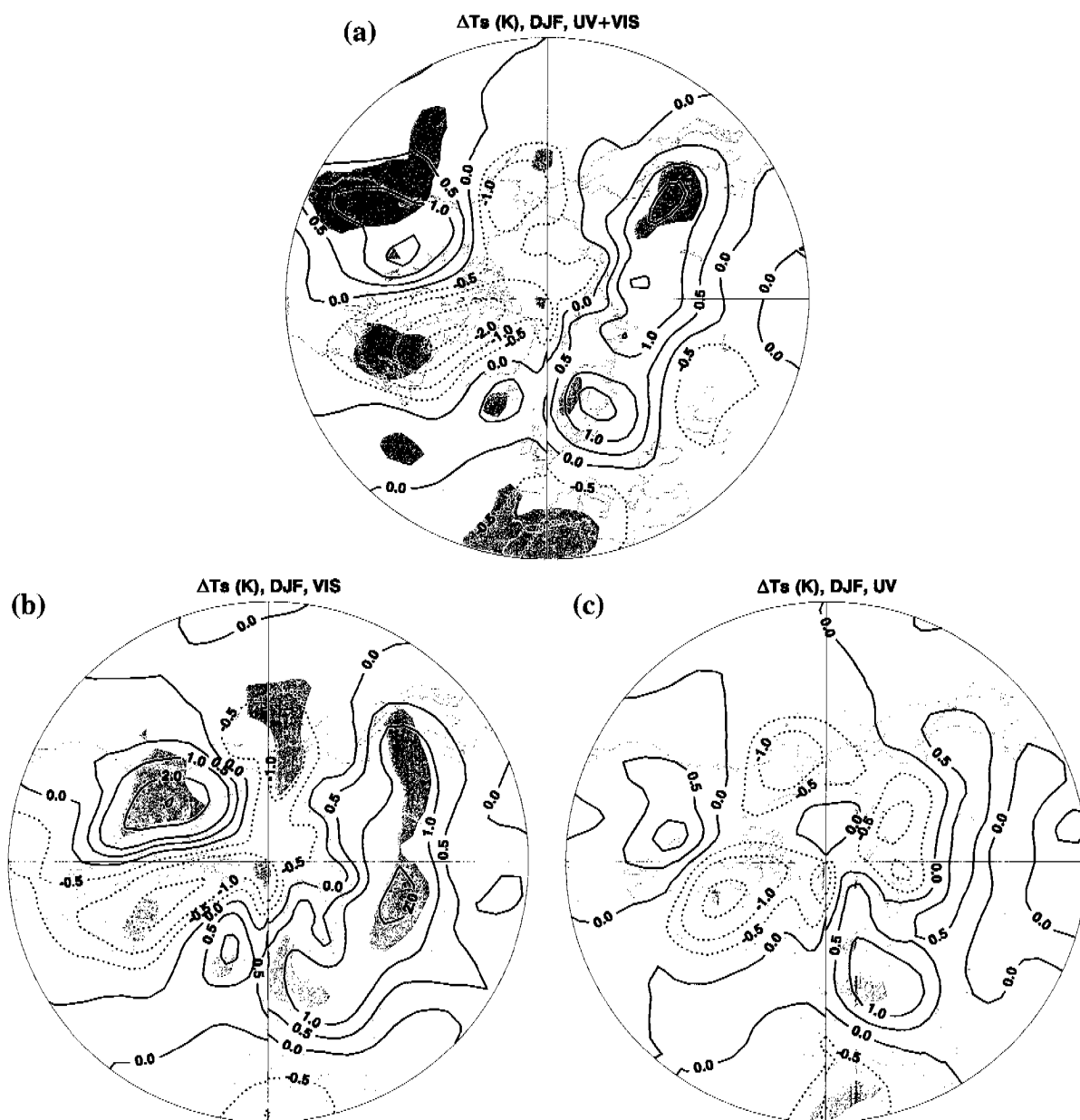
Figure 3.22: *Geographical distribution of surface air temperature changes (K) for DJF: (a) UV+VIS case; (b) VIS only case; (c) UV only case.*
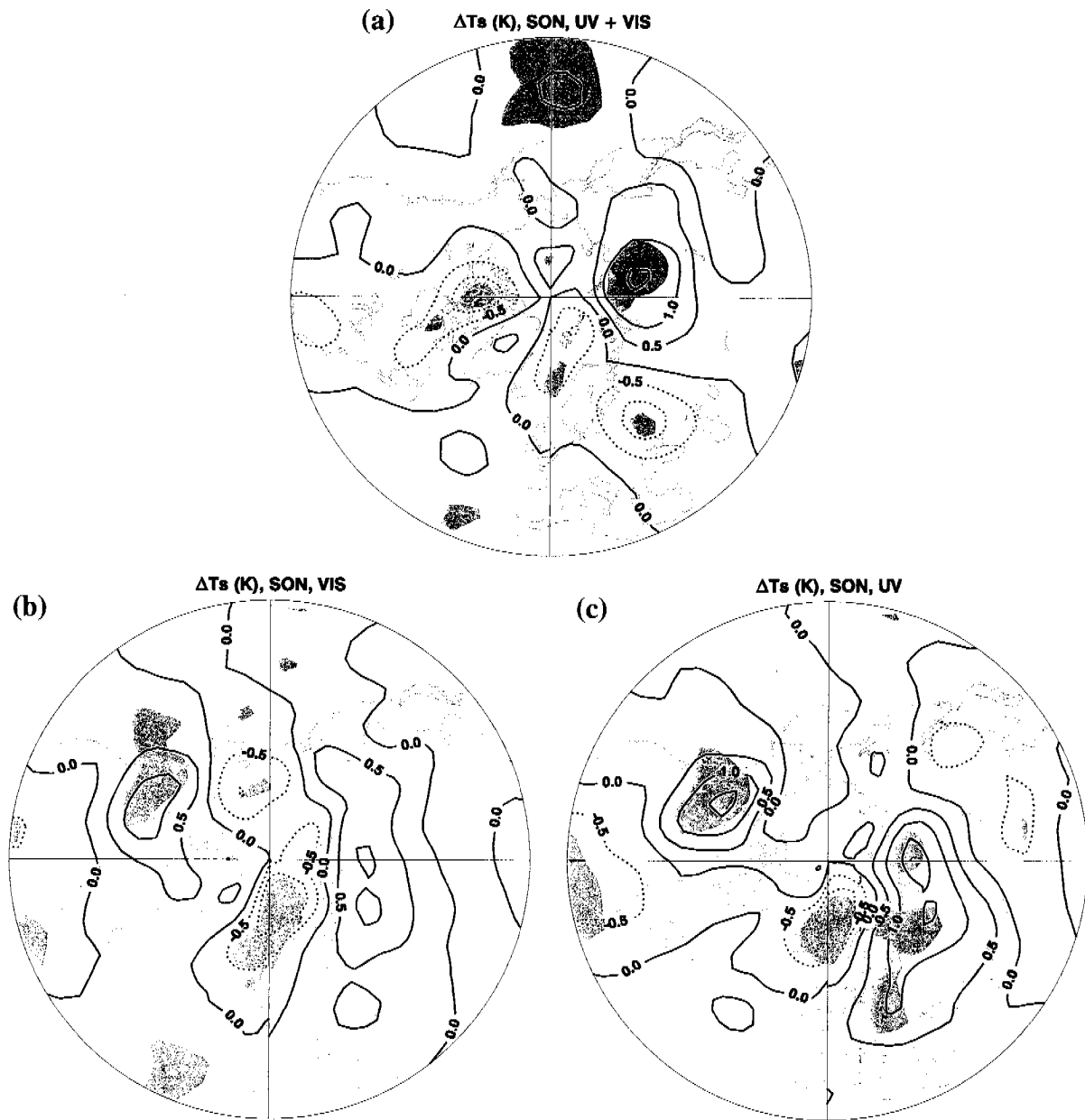
Figure 3.23: Same as Figure 3.22, but for SON.

3.6 Comparison of solar effects simulated by SOCOL and obtained from observational analysis

Hines (1974), Hood *et al.* (1993), Haigh (1996, 1999), Kodera (1996), Shindell *et al.* (1999) and Kodera and Kuroda (2002) have established a possible mechanism of solar influence, which can be tested with numerical models. The mechanism is based on solar radiative heating due to absorption of solar UV by ozone in the upper stratosphere and stratopause area. The absorption and subsequent temperature increase creates a large temperature gradient during the winter with consequently induced strong westerly jet. In this section the possible mechanism is verified with results of SOCOL simulations, which are compared with analyses of NCEP and ERA-40 data.

3.6.1 Zonally averaged zonal wind

Figure 3.24 shows development of zonal mean zonal wind solar-induced anomaly from November to February (a) simulated by the CCM SOCOL, (b) in comparison with NCEP (formerly NMC) data, and (c) ERA-40 analysis data. NCEP data composite analysis includes the period from 1979-1998, which covers two solar cycles. Here the solar maximum and minimum phases is defined with equal periods of four years: 1979-1987 and 1988-1991 for solar maximum; 1984-1987 and 1994-1997 for solar minimum (Kodera and Kuroda, 2002). ERA-40 data composite analyses cover the period 1979-2001, which includes 11 year of solar maximum and 9 years of solar minimum phases. The data have been obtained by applying the December-January-averaged 10.7-cm radio flux (Gray *et al.*, 2004). In general both data sets as well as the model exhibit a strong positive anomaly that moves poleward and downward with time, indicating a colder and more stable vortex during years within the solar maximum phase. However there are some noticeable differences in the zonal averaged zonal wind anomaly between NCEP and ERA-40 data. For example, in January both data sets show a quite intensive anomaly, but the position of its maximum is located in the middle latitudes and at 1 hPa for ERA-40 and in high latitudes and at 10 hPa for NCEP. The magnitude of the maximum also substantially deviates: 30 ms^{-1} for ERA-40 and 12 ms^{-1} for NCEP. The simulated solar-induced anomaly of the zonal mean zonal wind has a magnitude of only 2 ms^{-1} and its location close to NCEP data for the same month. In November the simulated anomaly is 6 ms^{-1} and moves poleward and downward. In December the anomaly becomes less intensive (only 2 ms^{-1}), moves further downward and propagates to the troposphere. In January the

situation stays quite the same as in December, but in February the anomaly intensifies and reaches 6 ms^{-1}, which is not in agreement with the data. In the data, the zonal wind anomaly changes the sign from positive to negative and in the model this happens one month later (in March) and is less intensive (not shown). An easterly anomaly starts to develop in December and then it intensifies in January in the upper stratosphere of subtropical and middle latitudes. This suggests a more frequent occurrence of stratospheric warming events during solar maximum (e.g., Gray et al., 2004).

3.6.2 Zonally averaged temperature

In Figure 3.25 the latitude-height distribution of zonal mean temperature differences is shown for the same time period in comparison with corresponding NCEP and ERA-40 analyses. Model temperature anomalies of different sign occur in high latitudes during winter and are of dynamical origin. In the tropical and subtropical stratosphere there is a significant positive temperature anomaly (about 1 K). The strongest effect on the meridional temperature gradient has been obtained in November and February. A positive anomaly developing in November over high latitudes moves downward in December. In January a stratospheric positive anomaly moves to middle latitudes and merges with the positive high latitudes anomaly. At the tropopause, a negative anomaly over high latitudes starts to develop in January. It reaches -4 K in February and forces the positive anomaly to move into the upper stratosphere. The meridional gradient in February enhances and leads to intensification of the PNJ (see Figure 3.24 a).

3.6.3 Conclusion

The comparison of the seasonal development of the simulated zonally averaged zonal wind anomalies with corresponding analyses of observations supports the idea of a solar influence on the dynamical state of the atmosphere through solar heating, which can be reproduced qualitatively with the numerical model. In general the pattern of the simulated zonal wind and temperature anomalies has some resemblance with the analyses of observations but differ in timing and magnitude. In the CCM SOCOL a strong PNJ exists from November to February, which is for one month longer and has smaller amplitude than the observational analyses suggest. Therefore, there is a need for some additional amplifying mechanism to reach observed magnitude of the solar influence.

(a) SOCOL   **(b) NMC**   **(c) ERA-40**
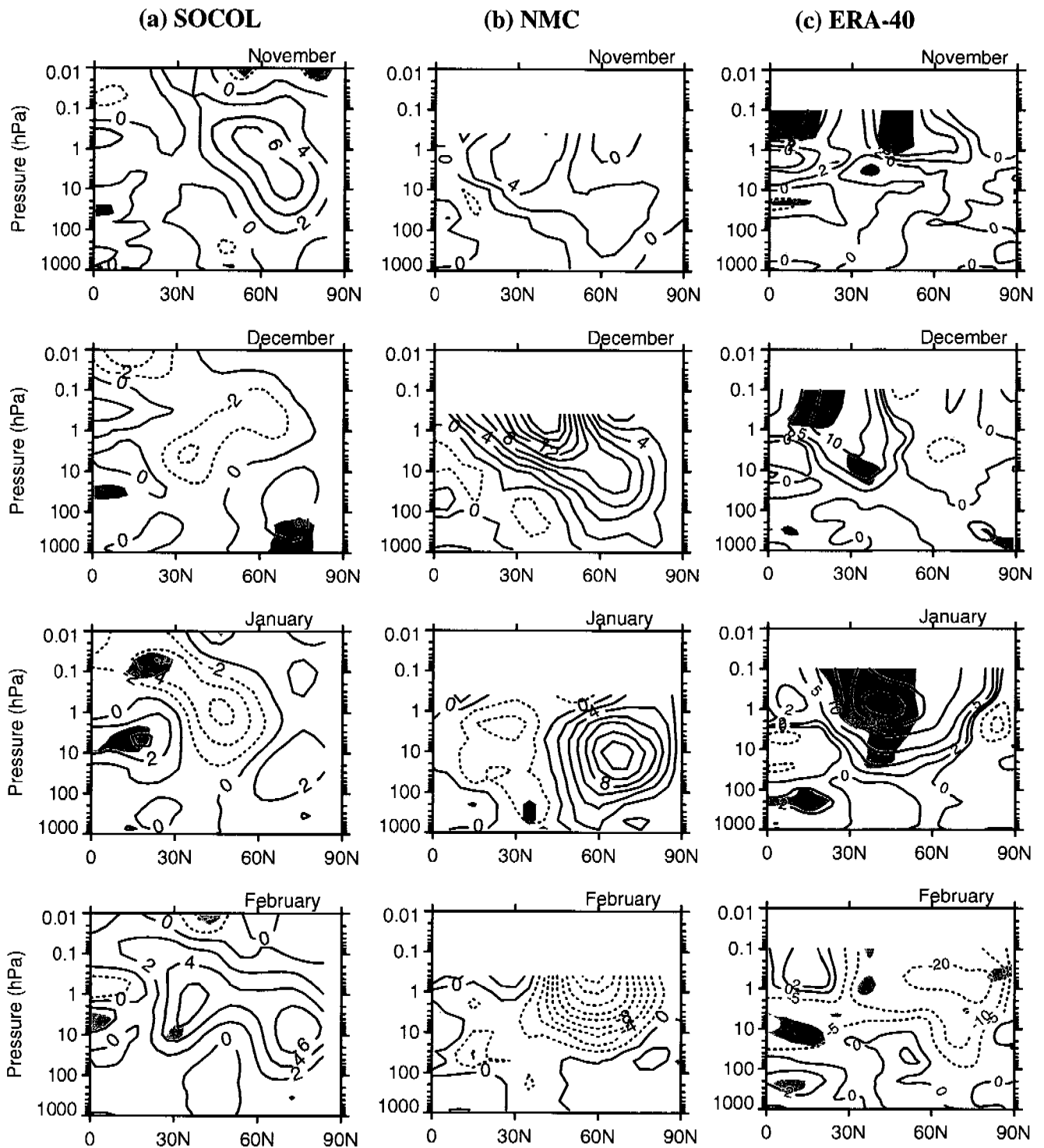
Figure 3.24: *Monthly averaged latitude-height profiles of solar-induced changes in zonally averaged zonal wind (ms^{-1}) for the Northern Hemisphere from November to February: (a) simulated by SOCOL; (b) analysis of NCEP data (Kodera and Kuroda, 2002); (c) analysis of ERA-40 data (Gray et al., 2004). The light and dark shading indicate statistical confidence of the obtained solar signal at the 80 % and 95 % levels using a standard Student's t-test. Data were obtained from private communication with K. Kodera and S. Crooks.*
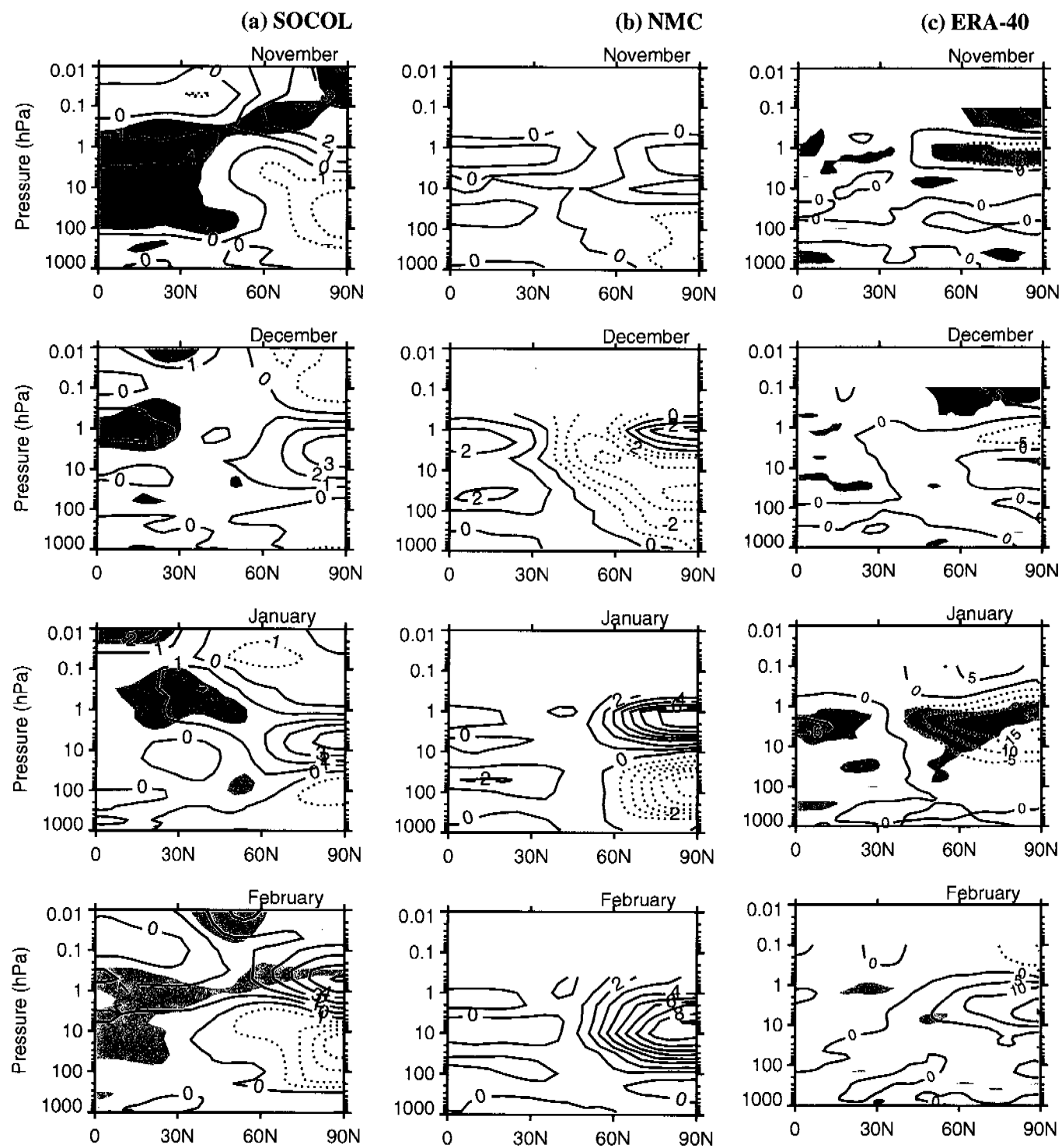
Figure 3.25: *Same as Fig. 3.24 but for the zonally averaged temperature solar-induced anomaly. Contour interval for (a) and (b) is 1 K, for (c) is 5 K.*

References:

Haigh, J.D. (1996). The impact of solar variability on climate, *Science*, *272*, 981-984, 1996.

Haigh, J. (1999). A GCM study of climate change in response to the 11-year solar cycle, *Quart. J. Roy. Meteorol. Soc.*, **125**, 871-892.

Hines, C. O. (1974). A possible mechanism for the production of Sun-weather correlations, *J. Atmos. Sci*, **31**, 589-591.

Hood, L.L., J. Jirikovich & J. P. McCormack (1993). Quasi-decadal variability of the stratosphere: Influence of long-term solar ultraviolet variations, *J. Atmos. Sci.*, **50**, 3941-3958.

Gray, L., Crooks S., Pascoe Ch., Sparrow S., Palmer M. (2004). Solar and QBO influences on the timing of stratospheric sudden warmings, *J. Atmos. Sci.*, **61**, 2777-2796.

Kodera, K. (1996). On the origin and nature of the interannual variability of the winter stratospheric circulation in the northern hemisphere, *J. Geophys. Res.*, **100**, 14077-14087.

Kodera, K. and Kuroda Y. (2002). Dynamical response to the solar cycle, *J. Geophys. Res.*, **107**, 4749, doi:10.1029/2002JD002224.

Labitzke, K. (2001). The global signal of the 11-year sunspot cycle in the stratosphere: Differences between solar maxima and minima, *Meteorol, Z.*, **10**, 83-90.

Marsh, D., Smith A., Brasseur G, Kaufmann M., Grossmann K. (2001). The existence of a tertiary ozone maximum in the high-latitude middle mesosphere, *Geophys. Res. Lett.*, **28**, 4531-4534.

Shindell, D., D. Rind, N. Balachandran, J. Lean, and P. Lonergran (1999). Solar cycle variability, ozone, and climate, *Science*, **284**, 305-308.

World Meteorological Organization (WMO), Scientific Assessement of Ozone Depletion: 2002, Rep. 47, Global Ozone Res. and Monitoring Project, Geneva, 2003.

Seite Leer /
Blank leaf

4. Study of 27-day long solar variability

4.1 Introduction

Different aspects of sun-climate relationship issues are under permanent evaluation during at least two hundred years (e.g., Hoyt and Schatten, 1997). The interest to this problem is driven by the necessity to understand the role of solar activity in the climate changes. During last several decades the growing amount of different observation data allowed to establish several important features of the atmospheric response to the decadal scale solar variability (Hood, 2004 and references therein), which then were applied for the validation of the solar signal simulated with different atmospheric models. Despite of substantial progress in the atmospheric modeling and application of rather sophisticated model tools the agreement of the simulated atmospheric response to decadal scale solar variability with the solar signal in different atmospheric quantities obtained from the statistical analysis of the observations cannot be qualified as successful (Tourpali *et al.*, 2003; Matthes *et al*, 2003; Hood, 2004; Rozanov *et al.*, 2004; Egorova *et al.*, 2004). Partially, it can be explained by the fact that the applied models suffer from the absence of some important physical or chemical mechanism of solar-climate connections. On the other hand it can be a result of difficulties with extraction of the solar signal from rather short and noisy time series. At the moment, the decadal scale solar signal in the stratosphere can be extracted only from about 25 years of satellite observation, which covers less then three full solar cycles. Moreover, the solar signal in these time series was perturbed by the influence of major volcanic eruptions and anthropogenic changes. All these factors could lead to substantial inaccuracy of the obtained solar signal and its deviation from the simulated results.

An alternative way to validate the simulated solar signal is to compare the sensitivity of the model to the solar irradiance variability on the shorter time scales. It is well known that during solar rotation cycle the solar UV flux undergoes substantial variability, which magnitude is comparable with the changes of solar irradiance from the minimum to the maximum of the 11-year solar activity cycle (Rottman, 2004). The solar rotation cycle in the irradiance reflects the heterogeneity of the solar spots distribution across the Sun surface and should be the most intensive during the solar activity maximum. The variability of the solar irradiance during solar rotation cycle has clear implications for the stratosphere and mesosphere, where an enhanced UV radiation during more active periods increases the radiation heating and photolysis rates altering atmospheric temperature and species

distributions. The effects of the solar irradiance variability during solar rotation cycle have been intensively studied by the statistical analysis of the satellite measurement and the results of the simulations with numerical models of different complexity. The results of the analysis of different satellite observations have been widely presented (see Hood, 1986; Keating *et al.*,1987; Hood *et al.*, 1991; Chen *et al.*,1997; Hood and Zhou, 1998; Hood, 1999; Hood, 2004 and references therein). The results of the statistical analysis allowed to establish that the ozone and temperature in the tropical stratosphere and mesosphere have detectable response to the solar irradiance variability during solar rotation cycle.

The ozone response is found to be negatively correlated with solar irradiance in the mesosphere around zero phase shift. In the stratosphere the ozone mixing ratio increases in phase with the solar irradiance. The stratospheric ozone response reaches its maximum around 35-40 km depending on the data set used and/or considered period of time. It has been pointed out by Hood and Zhou (1998) that the results of statistical analysis strongly depend on the time period considered. For the first 500 days of the record they obtained very weak correlation (up to 0.2) between the ozone and solar irradiance, while the correlations during second sub-period exceed 0.5. The ozone response to solar irradiance variability during Sun rotation cycle simulated with 1-D and 2-D models (Hood *et al.*, 1991; Chen *et al.*, 1997; Summers *et al.*,1990; Zhu *et al.*, 2003) is found to be in a reasonably good agreement with observation analysis. In particular, it has been shown that the anti-correlation between ozone and solar irradiance in the mesosphere is driven by the increased photolysis of the water vapor in Lyman-alpha line and subsequent enhancement of the hydrogen radicals, which destroy the ozone. The increase of the ozone in the stratosphere during more active Sun has been explained by the enhanced photolysis of oxygen in Herzberg continuum resulting in the additional ozone production. The issue of the time evolution of the simulated responses has not been considered because applied models are rather linear and the solar signal does not depend much on the period considered.

The correlations of the tropical temperature changes with the solar irradiance during solar rotation cycle obtained from the observations are about 0.2-0.3 and substantially weaker then for the ozone. It reflects longer relaxation time scale for the temperature and probably the presence of the internal short-time temperature variability in the atmosphere. The obtained sensitivity of the temperature has two maximums: first one is located near the stratopause (Hood, 1986; Hood and Zhou, 1998) and the second one in the mesosphere around 75 km (Chen *et al.*, 1997). As for the ozone Hood and Zhou (1998) found that the results of statistical analysis are not robust and depend strongly on the time period considered. For the

two parts of the record cross-correlations between the temperature and solar irradiance look differently showing rather different time lags. The temperature response to solar irradiance variability simulated with 1-D and 2-D models (Hood *et al.*, 1991; Chen *et al.*, 1997; Zhu *et al.*, 2003) can be considered as rather successful near the stratopause, while all models failed to match observational data in the mesosphere.

It was shown by Chen *et al.* (1997) that the temperature response is much better simulated with interactive 2-D model in comparison with 1-D model. It emphasizes that correct description of the non-linear dynamical processes plays important role in the simulation of the temperature response to the short-time solar irradiance variability. 1-D and 2-D models are also difficult to apply for a study of the robustness of the obtained correlations, i.e. their dependence of the time period established by Hood and Zhou (1998). These kind of models robustly reproduce rather identical features of the solar response for any period of integration simply because the lack of non-linear dynamics in the model equations. Therefore, the application of more sophisticated model tool is necessary to elucidate the dependence of the solar signal on the time period under consideration. The causes of the time varying response reflects different meteorological state of the atmosphere during considered periods and this problem can be addressed only with model whose variability is close to the real, i.e. with CCM based on primitive hydro-dynamical equations.

At the moment there is only one simulation with CCM (Williams *et al.*, 2001), but the authors paid no attention to the robustness of the obtained solar signal and, moreover, their model has no representation of the Lyman-alpha line in photochemical code, which is extremely important to reproduce the solar signal in the mesosphere. Here CCM SOCOL (Egorova *et al.*, 2004, 2005) has been applied that represent main physical-chemical processes in the atmosphere from the ground up to mesopause to study the solar signal of solar irradiance variability during Sun rotation cycle.

Here the analysis is concentrated on inter-annual variability of the solar signal during sun rotation cycle and evaluation how well the model reproduces known and robust features of the solar signal in the stratosphere and mesosphere.

4.2 Experiment set-up

Nine one-year long model runs have been carried out for 1992 conditions. The sea surface temperature and the sea ice distributions have been taken from Gleckler (1996), which is climatology of the last 20 years. The stratospheric aerosol, greenhouse gas and ozone destroying substances concentrations, and the sources of NO_x, CO are the same as in

99

(Rozanov *et al.*, 1999, 2001). The coefficients for photolysis and heating rates calculations in the model are re-calculated every day using the solar energy spectrum obtained by the SUSIM instrument onboard of the UARS satellite for the year 1992. The radiation in visible and near-infrared parts of the spectrum was kept unchanged. From the described simulation daily and zonal mean values have been stored for temperature, total ozone and mixing ratio of the species considered in the chemical part of the model, which allows analyzing the response of these quantities to the solar irradiance variability during sun rotation cycle. The analysis of the results has been followed the procedure applied by Hood (1986), Hood and Zhou (1998) to facilitate the comparison of our results with the satellite data. Zonal mean data have been averaged over tropical latitudes (over latitude belt 20°S-20°N). Then the anomalies have been calculated relative to the mean values during considered period of time and the time series have been smoothed using standard program from IDL package with 35 days smoothing windows to eliminate the variability with longer time scales. The same procedure has been applied to the solar irradiance at 205 nm. Then standard Fourier transformation have been applied to calculate discrete power spectrum and spectral coherency between different simulated quantities and solar irradiance at 205 nm. Also cross-correlations of the simulated time series have been calculated with the solar flux at 205 nm to estimate the time lag of the response and the sensitivity of these quantities to the solar irradiance variability. For the analysis time series of ozone, temperature and hydroxyl have been chosen. The temperature and ozone are necessary for the comparison with the observations. Hydroxyl is of interest for consideration because of its relative short life time and expected high and robust correlations with solar irradiance in the upper stratosphere and mesosphere.

4.3 Results

4.3.1 Cross-correlation functions

Fig. 4.1 represents the results of the Fourier analysis of the UV daily solar irradiance for 1992 at 205 nm, which has been used to drive the model. The figure shows that the solar rotation cycle with period of about 28 days dominates the spectrum. Although, the solar irradiance possesses variability mostly with smaller periods, the spectral power of the variability due to Sun rotation exceed other variability by about 40%. The variability of the solar irradiance is not homogenous during the year. Wavelet analysis of the variability (not shown) revealed that the power spectrum is the most pronounced during the first 3-4 months, while during the rest
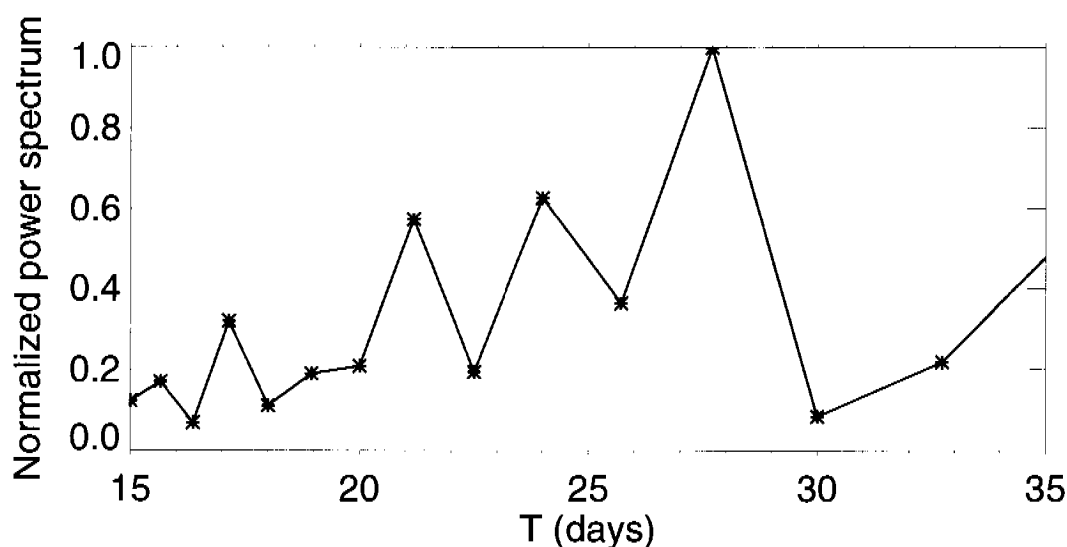
Figure 4.1: *Normalized power spectrum of the solar irradiance at 205 nm for 1992.*

of the year the variability associated with the Sun rotation is much smaller, probably related to the declining phase of solar activity.

Fig. 4.2 represents the cross-correlation function of the hydroxyl, ozone and temperature versus solar irradiance at 205 nm for the year 8. The hydroxyl shows rather high (> 0.8) and positive correlation with solar flux in the upper stratosphere and mesosphere at zero time lag. This can be expected because the hydroxyl production is dominated by the photolysis of water vapor and ozone, which are in turn directly connected to the solar irradiance. Elevated level of the hydroxyl in the mesosphere provide additional sink for the ozone, therefore, the ozone response in the mesosphere is negative for zero phase lag. An enhancement of the solar irradiance leads to the increase of the oxygen photolysis providing additional source for ozone therefore, the ozone response in the mesosphere is negative for zero phase lag. An enhancement of the solar irradiance leads to the increase of the oxygen photolysis providing additional source for ozone. This mechanism starts to dominate below ~60 km and, therefore, the ozone correlations in the upper and middle stratosphere turn into positive. This ozone increase prevents the penetration of the UV radiation further down, which results in the relative decrease of the ozone and oxygen photolysis followed by decrease of ozone, exited atomic oxygen and hydroxyl production. It explains the appearance of negative response for the hydroxyl below ~ 40 km and ozone below ~30 km. The correlation between ozone and solar irradiance reaches maximum at almost zero phase lag from 50 to 80 km reflecting the rather small ozone life time. Below 50 km the phase lag increases gradually in the stratosphere and reaches 5 days around 35 km, which is in reasonable agreement with observations (Hood, 2004). For this particular year the correlation

of the temperature with solar irradiance exceeds 0.4 and has maximuma in the upper mesosphere and in the stratosphere. The response of the temperature for the maximum correlation is positive with phase lag around 5-10 days in the mesosphere and 15-18 days in the stratosphere. The obtained warming is a result of the direct heating by the increased UV irradiance and indirect heating due to increased ozone in the stratosphere. Time lag depends on relaxation time and internal frequencies. As it was shown analytically by Zhu et al. (2003) the time lag for the maximum correlation depends on the frequency of the applied forcing (in our case solar irradiance variability during 27-day solar rotation cycle) and relaxation time for the quantity under consideration. The relaxation time for hydroxyl is very small, because of the hydroxyl life-time is short, therefore there is almost no time lag between time series of hydroxyl mixing ratio and solar irradiance. For the ozone the relaxation time increases toward the lower stratosphere together with an increase of the life-time. Accordingly, the time lag increases from almost zero shift in the mesosphere and upper stratosphere to 4-5 days in the middle stratosphere. The relaxation time for the temperature also decreases with altitude, because the density increase providing for an increase of the time lag from 4-5 days in the upper part of the model domain to 10-20 days in the middle stratosphere.

Figure 4.2. *Cross-correlation function of the hydroxyl (left panel), ozone (central panel), temperature (right panel) versus the solar irradiance at 205 nm for the year 8 in the latitude band 20°S-20°N.*

The analysis of the other years of the ensemble run reveal that the presented results for year 8 are very robust for the hydroxyl, while it is not exactly the case for the ozone and especially for the temperature. Fig. 4.3 illustrates the cross-correlation function between the ozone, temperature and solar irradiance obtained from the results of the year 2. The ozone

102

cross-correlation function for year 2 looks similar to those for year 8, but it should be noted that the maximum correlation substantially lower. For the temperature the cross-correlation function appears to be different. First of all, the obtained correlations are very weak reaching at most 0.2. Moreover, the time lag in the stratosphere is by about 5 days smaller then for the year 8.

Fig. 4.4 illustrates the maximum correlation between hydroxyl, ozone and temperature and solar irradiance at 205 nm calculated for each year of the run. The results confirm that the hydroxyl reveals high and robust correlations with solar irradiance in the upper stratosphere and mesosphere. It can be expected because the hydroxyl production is dominated by the photolysis of water vapor and ozone, which are directly connected to the solar irradiance. The pattern of the ozone and temperature correlations is more complicated because their behavior is not completely controlled by the radiation processes depending on the transport and non-linear dynamics in the atmosphere. In the mesosphere above ~50 km, where the life time of the ozone is smaller and dynamical processes are less important, the correlation between ozone and solar irradiance exceeds 0.5 and does not substantially changes from year to year.

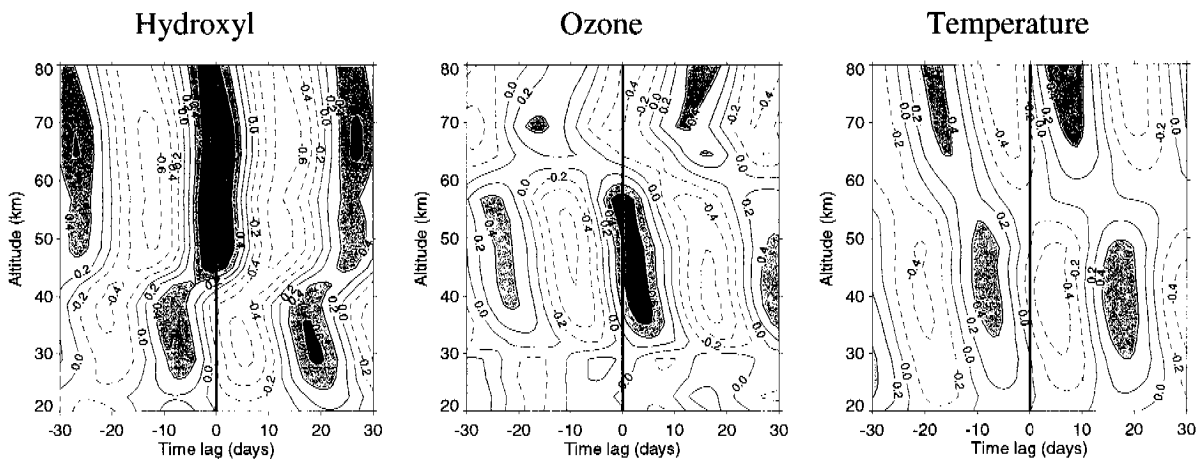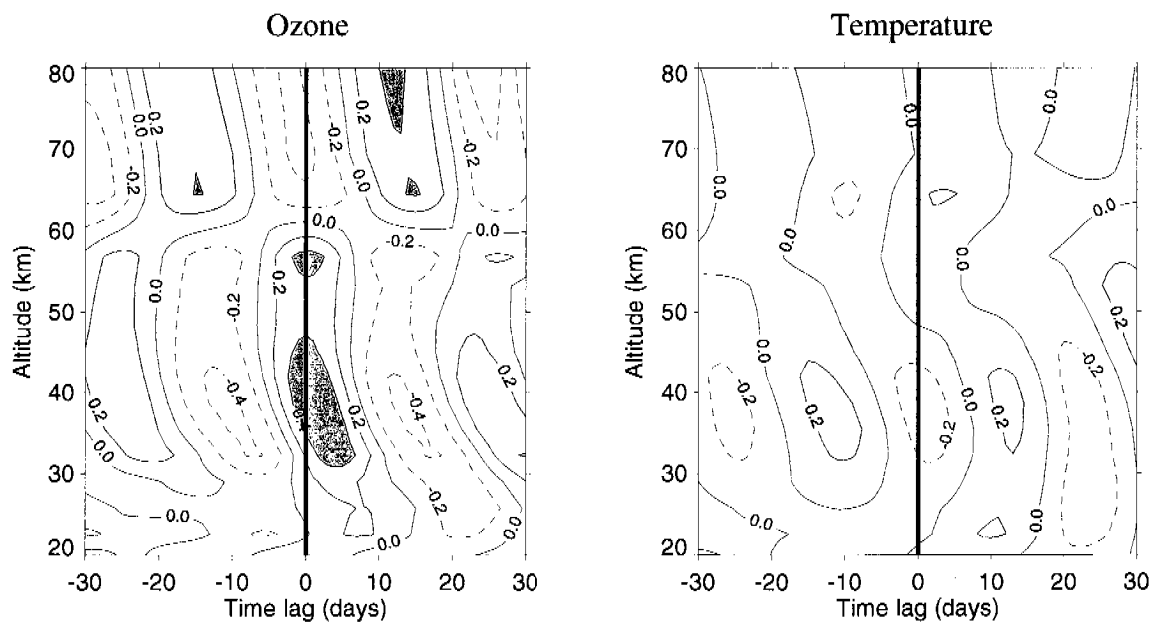**Figure 4.3.** *Cross-correlation function of the ozone (left panel) and temperature (right panel) versus the solar irradiance at 205 nm for the year 2.*

In the upper stratosphere the correlation is still reasonable, but the dependence on the dynamical state of the atmosphere becomes noticeable. For example, around 40 km the correlation exceeds 0.6 for the years 5, 6, and 8, while for year 4 the correlation is rather small

(less than 0.3). In the lower stratosphere the correlation is rather low and rarely reaches 0.3. The correlation between temperature and solar irradiance is found to be significant only during some particular years. For example, during years 5 and 8 the temperature variability correlates with the solar irradiance rather well (0.4-0.5), while during the other years the typical correlation is only about 0.2. It should be noted that the temperature behavior in the upper mesosphere and stratosphere looks synchronized, if the correlation between temperature and solar irradiance is high in the stratosphere then it is also high in the upper mesosphere.

4.3.2 Comparison with observations

To compare our results with observations the sensitivity of the hydroxyl, ozone and temperature have been calculated to 1% increase of the solar irradiance at 205 nm. Following Hood (1986), Hood and Zhou (1998) the calculations have been performed using regression of the considered quantities on the solar irradiance with the time lag corresponding to the maximum positive correlation. The sensitivities of the hydroxyl, ozone and temperature are presented in Fig. 4.5 for all years of the experiment. The sensitivity of the hydroxyl does not depend much on the year of the experiment and reaches 2.4% per 1% of solar irradiance variability at 205 nm in the middle mesosphere. The simulated hydroxyl sensitivity is in a good agreement with the results of 2-D model of Chen et al. (1997), however, it is impossible to justify the results because of the lack of observational evidences.
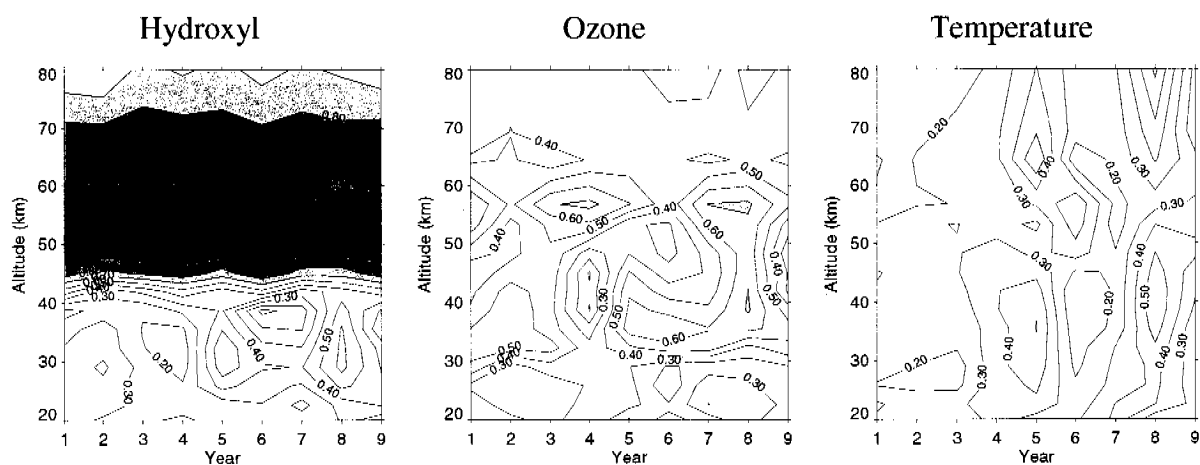

Figure 4.4. *Maximum of the cross-correlation function between the hydroxyl (left panel), ozone (central panel), temperature (right panel) and the solar irradiance at 205 nm for the lags from −30 to 30 days.*

The sensitivity of the ozone is rather robust in the mesosphere reaching 1% in the upper mesosphere and in the lower stratosphere, which typical value of about 0.2%. In the middle and upper stratosphere the ozone sensitivity is not homogeneous. During the years with high correlation between ozone and solar irradiance the sensitivity is higher (up to 0.8%), while for some years the ozone sensitivity can be as low as 0.2%. The temperature sensitivity in the stratosphere also depends on the correlation function. It is higher for the years when the correlation between temperature and solar irradiance is high (see Fig. 4.4). Typically, the sensitivity of the temperature is of about 0.1-0.2 K, but for several years its value can reach 0.4 K in the upper mesosphere and around 40 km.
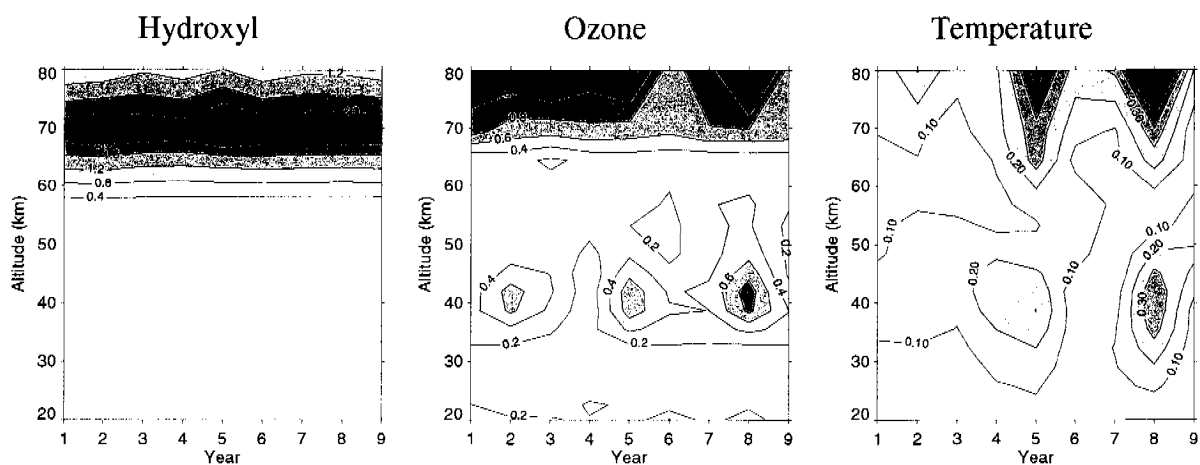
Figure 4.5. *The sensitivity of the hydroxyl (left panel), ozone (central panel), temperature (right panel) to 1 % change of 205 nm solar flux for the maximum correlation. Sensitivity is shown in percents for hydroxyl and ozone, temperature sensitivity is given in K.*

As it has been shown earlier (see Fig. 4.5) the ozone sensitivities for different years of the ensemble run are rather compact in the mesosphere and lower stratosphere. The simulated sensitivities are in a good agreement with observation in the mesosphere up to 70 km. At higher altitude the model still shows rather high sensitivity, while the observed sensitivity tends to decrease with altitude. In the lower stratosphere below 30 km the simulated sensitivity is close to the observations. The model mimics well the minimum sensitivity at 25 km and slight increase toward the tropopause. The ensemble mean ozone sensitivity in the rest of the stratosphere is in a perfect agreement with SBUV and SME data. However, the simulated ensemble mean is overestimated in comparison with MLS data between 40 and 50 km. As was mentioned by Hood and Zhou (1998), smaller sensitivity obtained from the MLS data can be due to the fact the night time measurements dominates the record. It should be

noted, that, however, some years of the ensemble run also shows smaller sensitivity in this area. Therefore, it could mean that smaller sensitivity obtained from MLS data is a result of the different atmospheric state during considered period. The ozone sensitivity in this area shows substantial inter-annual variability. Around 40 km the years with closer correlation between ozone and solar irradiance reveal substantially higher sensitivity up to 0.9% per 1% change of the solar irradiance at 205 nm, while there is one anomalous year with a very small (~0.1%) sensitivity. The temperature sensitivities are even more scattered in comparison with the ozone. They are compact only between 20 and 30 km and in the mesosphere where the agreement with observations is reasonable. The simulated ensemble mean sensitivities are at the maximum near 42 km, which by about 5-8 km lower then the maximum sensitivity in the observation data. The position of the simulated maximum is determined by the 3 ensemble members characterized by higher correlation between the temperature and solar irradiance variability. The sensitivity derived from these runs is about 0.3-0.4 K. There are also four ensemble runs, which results are rather close to the observations and two runs with very low sensitivity. In the mesosphere the temperature sensitivities derived from the MLS and SME data sets do not agree well. The temperature sensitivity obtained from MLS data (Chen *et al.*, 1997) is as twice as higher in comparison with SME data published by Hood *et al.* (1991). The simulated temperature sensitivities for different runs of the ensemble also can be also divided into two groups. Two runs are close to the MLS data and the other seven runs (and ensemble mean) are closer to SME data. It should be noted that none of the simulated sensitivities decreases toward mesopause.

4.4 Conclusions

In this study the Chemistry-Climate Model *SOCOL* has been used to study the atmospheric response to the solar irradiance variability during Sun rotation. Applied model has state-of-the art representation of the climate processes, chemistry, transport and non-linear dynamics in the middle atmosphere, which allows addressing the problem of internal variability of the simulated effects. An ensemble simulation has been carried out which comprising of 9 1-year long runs driven by the spectral solar irradiance prescribed on the daily basis using UARS SUSIM measurements for year 1992. Ensemble members differ slightly by initial state of the atmosphere only, while the representation of all physical and chemical processes as well as external forcing is identical for all runs. Therefore, the difference in the atmospheric response for different ensemble members reflects only internal

variability caused by non-linearity of the model. The robustness of the atmospheric response to the short-time solar irradiance variability has been studied on the basis of the observation data (e.g., Hood and Zhou, 1998), but not with a state-of-the-art CCM. The correlation of zonal mean hydroxyl, ozone and temperature averaged over the tropics with solar irradiance time series have been analyzed. The choice of these quantities has been made to represent different relaxation/life time scales.
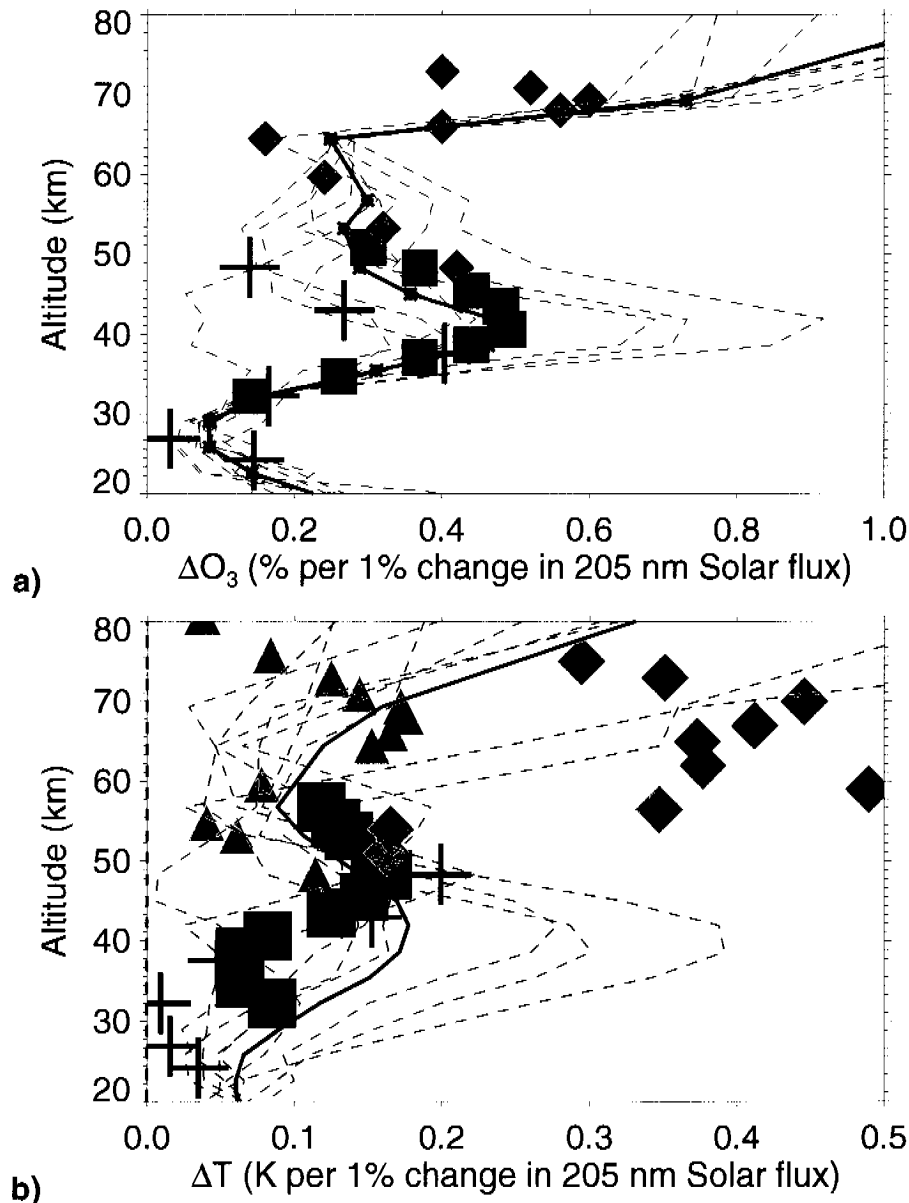
Figure 4.6. *Ozone (a) and temperature (b) sensitivity to 1 % change of 205 nm solar flux for the maximum correlation. Simulated sensitivity is shown by solid line (ensemble mean) and dotted lines (ensemble members). Observed sensitivities are from MLS (Hood and Zhou, 1998; crosses), SBUV (Hood, 1986; squares), SME (Hood et al., 1991; diamonds) for the ozone and from MLS (Hood and Zhou, 1998; crosses), SAMS (Hood, 1986; squares), SME (Hood et al., 1991; triangles) and MLS (Chen et al., 1997; diamonds) for the temperature.*

The correlations between the hydroxyl and solar irradiance are very robust and almost the same for all years of the ensemble run. The correlation of the hydroxyl with the solar irradiance changes is positive in the upper stratosphere and mesosphere due to enhanced photolysis rates during more active period at the Sun surface. The simulated sensitivity of the hydroxyl to the solar irradiance changes is in a good agreement with previous estimations (e.g., Chen et al., 1997), which confirms that the model correctly treats chemical processes in the middle atmosphere. The correlations of the ozone with solar irradiance are significant and robust in the mesosphere, which can be also explained by relatively short ozone life time there. For zero phase lag the response of the ozone to the increase of the solar irradiance is negative reflecting enhancement of hydroxyl radical destroying the ozone. The simulated ozone sensitivity is in a reasonable agreement with observation data. In the lower stratosphere the ozone-solar irradiance correlations are stable but very weak. In the stratosphere the ozone correlation with solar irradiance is relatively stable, however for two years of the ensemble the correlation is rather weak. The ensemble mean sensitivity of the ozone to the solar irradiance changes is in a very good agreement with observation data, however, there is a substantial scatter of its magnitude among different members of the ensemble. The temperature correlations with solar irradiance are not robust, because its variability strongly depends on non-linear dynamics and transport in the atmosphere. The correlation is found to be significant (>0.5) only for two years of the ensemble. The ensemble mean temperature sensitivity is in a reasonable agreement with observation data only above 50 km. In the stratosphere the maximum of the temperature sensitivity appears to be by 5 km lower then in the observations. The temperature sensitivity has substantial variability and depends on the year of the ensemble run. There are some years of the ensemble, which resemble the observation data more closely then ensemble mean. The simulated temperature sensitivity in the mesosphere could help to explain substantially different results of the observation analysis in the mesosphere. The model also shows higher sensitivity for two years of the ensemble and lower sensitivity for the other seven years of the ensemble. Therefore, the difference in the observed sensitivity can be explained by different atmospheric state during the considered periods of time.

In general, it may be concluded that the model successfully simulates the ozone response to the solar irradiance variability during the Sun rotation cycle, but the simulated temperature response is not robust. The physical nature of this is not clear yet. It looks like the temperature (and part of the ozone) daily fields possess their own internal variability, which is not stable and can differ from year to year reflecting different dynamical state of the system.

The imposed forcing (in our case solar irradiance) interacts with this internal variability, which leads to the shift of the spectrum of the resulting temperature variability. Depending of the internal variability the resulting power of 27-day component of the spectrum can be amplified or decreased. This process is clearly seen in the obtained results and due to controlled conditions of the experiment it cannot be explained by any physical reasons. If the model's non-linear behavior is real it implies that the sensitivity of the temperature to the solar irradiance variability extracted from the observation data could reflect rather the internal sate of the atmosphere instead of the response of the temperature to the external forcing. Therefore, the model validation based on the temperature sensitivity should be taken with precautions. Obviously, more extended data analysis and numerical experiments with sophisticated non-linear models are necessary to address this issue.

4.5 References

Chen, L., J. London, and G. Brasseur (1997). Middle atmospheric ozone and temperature responses to solar irradiance variations over 27-day periods, *J. Geophys. Res.*, **102**, 29957-29979.

Egorova, T., E. Rozanov, E. Manzini, M. Haberreiter, W. Schmutz, V. Zubov, and T. Peter (2004). Chemical and dynamical response to the 11-year variability of the solar irradiance simulated with a chemistry-climate model, *Geophys. Res. Lett.*, **31**, L06119, doi:10.1029/2003GL019294.

Egorova, T., E. Rozanov, V. Zubov, E. Manzini, W. Schmutz, and T. Peter (2005). Chemistry-Climate Model SOCOL: a validation present-day climatology. Submitted to: *Atmospheric chemistry and Physics*.

Gleckler, P. E. (1996). AMIP Newsletter: AMIP-II guidelines, *Lawrence Livermore Natl. Lab*, Livermore, Calif.

Hood, L. (1986). Coupled stratospheric ozone and temperature responses to short-term changes in solar ultraviolet flux: an analysis of Nimbus 7 SBUV and SAMS data, *J. Geophys. Res.*, **91**, 5264-5276.

Hood, L., Z. Huang, and W. Bougher (1991). Mesospheric effects of solar ultraviolet variations: further analysis of SME IR ozone and Nimbus 7 SAMS temperature data, *J. Geophys. Res.*, **96**, 12989-13002.

Hood, L., and S. Zhou (1998). Stratospheric effects of 27-day solar ultraviolet variations: an analysis of UARS MLS ozone and temperature data, *J. Geophys. Res.*,**103**, 3629-3638.

Hood, L. (1999). Effects of short-term solar UV variability on the stratosphere, *J. Atm. Sol.-Terr. Phys.*, **61**, 45-51.

Hood, L. L. (2004). Effects of solar UV variability on the stratosphere. *Geophys. Monogr. Ser.*, **141**, edited by J. Pap et al., AGU, Washington, D.C.

Hoyt, D.V., Schatten K.H. (1997). The role of the Sun in climate change, Oxford University Press, Inc., New York, p.279.

Keating, G., J. Nicholson, D. Young, G. Brasseur, and A. De Rudder (1987). Response of middle atmosphere to short-term solar ultraviolet variations, 1, Observations, *J. Geophys. Res.*, **92**, 889-902.

Matthes, K. et al. (2003), GRIPS solar experiments intercomparison project: initial results, *Pap. Meteor. Geophys.* **54**, 380-395.

Rottman, G., Floyd, L., Viereck, R. (2004). Measurement of the solar ultraviolet irradiance. In *Geophysical Monograph* **141**: Solar variability and its effects on climate, *AGU*, 111-125.

Rozanov, E. V., M. E. Schlesinger, V. A. Zubov, F. Yang, and N. G. Andronova (1999). The UIUC three-dimensional stratospheric chemical transport model: Description and evaluation of the simulated source gases and ozone. *J. Geophys. Res.,* **104**, 11755-11781.

Rozanov, E. V., M. E. Schlesinger, and V. A. Zubov (2001). The University of Illinois, Urbana-Champaign three-dimensional stratosphere-troposphere general circulation model with interactive ozone photochemistry: Fifteen-year control run climatology, *J. Geophys. Res.,***106**, 27233-27254.

Rozanov, E., M. Schlesinger , T. Egorova, B. Li, N. Andronova, and V. Zubov (2004). Atmospheric Response to the Observed Increase of Solar UV Radiation from Solar Minimum to Solar Maximum Simulated by the UIUC Climate-Chemistry Model, *J. Geoph. Res.*, **109**, D01110, doi:10.1029/2003JD003796.

Summers, M., D. Strobel, R. Bevilacqua, X. Zhu, M. DeLand, M. Allen, and G. Keating (1990). A model study of the response of mesospheric ozone to short-term solar ultraviolet flux variations, *J. Geoph. Res.*, **95**, 22523-22538.

Tourpali, K., C. Schuurmans, R. van Dorland, B. Steil, and C. Brühl (2003), Stratospheric and tropospheric response to enhanced solar UV radiation: A model study, *Geophys. Res. Lett.*, **30**, 1231, doi: 10.1029/2002GL016650.

Williams, V., J. Austin, J. Haigh (2001). Model simulations of the impact of the 27-day solar rotation period on the stratospheric ozone and temperature, *Adv. Space Res.*, **27**, 1933-1942.

Zhu, X., J.-H. Yee, and E. Talaat (2003). Effects of short-term variability in a coupled model of photochemistry and dynamics, *J. Atm. Sci.*, **60**, 491-509.

5. Discussion

During the last two decades potential candidates responsible for solar-climate connections have been extensively discussed. There are at least three properties of the Sun, which may contribute to climate change on Earth (Reid, 2000): (1) variations in total irradiance, (2) variations in the ultra-violet spectral irradiance, and (3) variations in the solar wind and energetic particles.

The studies presented in this thesis focused on the effect of the spectral solar irradiance variation with emphasis on changes in solar spectral flux during the 11-year and 27-day solar rotation cycles. This includes the development of chemistry-climate model SOCOL and its validation against available observations (Chapter 2), studies of the annual mean 11-year solar signal and its seasonal behavior and separate influence of UV and visible radiation variability (Chapter 3), and study of the 27-day solar cycle (Chapter 4).

Before addressing the findings and identified deficits of the present thesis in more detail, the subsequent list provides a general overview over the important new results that have been achieved:

- a new global Chemistry-Climate Model (SOCOL) has been developed which is capable of reproducing the dynamical and chemical state of the atmosphere from the ground to 80 km;

- a climatology of observed temperature, zonal wind and chemical species distributions has been compiled to validate the model by means of a 40-year long run compared to the observed climatology, showing that SOCOL is capable of reproducing the main observed features of the dynamical and chemical state of the atmosphere with state-of-the-art quality;

- a new parameterization for heating rate due to absorption of the solar radiation by oxygen and ozone has been developed, which was absent in the original radiation code of the applied GCM (MA-ECHAM4);

- the temperature and ozone response of the atmosphere to the variable solar UV flux including the Lyman-α line has been simulated;

- it has been demonstrated that introducing the 11-year solar flux variations into the model yields changes not only in the stratosphere but also in the troposphere and near the surface, suggesting stratosphere-troposphere coupling (downward propagation); these changes appear to be significant, however require further investigation and proper attribution of physical mechanisms;

111

- the model suggests that solar UV irradiance alone is capable of changing the Earth's surface temperature and climate;

- the chemical response of the stratosphere and mesosphere to solar flux variability has been documented for a number of species;

- the response in the middle atmosphere has been derived for the variable solar UV flux on the time scale of the 27-day solar rotation cycle, and it has been shown that the simulated ozone response is robust and agrees well with the response retrieved from the satellite data; the temperature response is not robust, because the temperature behavior is defined not only by external forcing but also by non-linear dynamics in the atmosphere;

- it has been shown that this state-of-the-art modeling reveals a considerable gulf to the solar signal derived from satellite measurements, possibly due to inconsistencies of the retrieval procedures;

- we propose ways for further model development and study of the solar-climate connection (see end of this chapter).

5.1 Brief synopsis of results obtained

In the following more detail is given to some of the bullet points above.

5.1.1 CCM SOCOL

Forecasting the future ozone and climate changes are amongst the most pressing and challenging problems in contemporary environmental science. Earth's climate is determined by a variety of physical and chemical processes within a complex system reacting to the different external forcings, as well as by short-term and long-term internal variability (IPCC, 2001). Therefore, the projections of the atmospheric state can be made only by means of sophisticated modeling tools, which are able to represent all known atmospheric physical and chemical processes and their interactions.

In Chapter 2 we present the description of a new modeling tool, the CCM SOCOL, together with the validation of the simulated present-day climatology against a variety of observational data. An example of processes-oriented validation is also presented. While the model performance is quite satisfactory based on an overall inspection of simulated fields and on a proper statistical analysis, we have identified a number of weaknesses in the model that need to be addressed for a future improvement of the model. In particular, the analysis of the simulated zonal wind and temperature deviations shows that for an improvement it will be necessary to pay special attention to the tropopause region in the tropics and at high latitudes as

well as to the description of the processes in the upper stratosphere and mesosphere, where significant cold biases have been found in the model during summer. The simulated descent of the air is too strong in the polar stratosphere, leading to a significant underestimation of CH_4 and O_3 mixing ratios in this area. The tropopause region is cold biased by 5-10 K, which might be related to insufficient vertical resolution. An analysis of the water vapor zonal mean and seasonal distributions reveals an overestimation of stratospheric H_2O, despite the cold bias of the tropical tropopause. This overestimated H_2O is probably related to the transport of H_2O from the troposphere across the subtropical jet.

As a process-oriented part of the validation we have analyzed how SOCOL reproduces the imprint of the Arctic Oscillation (AO) onto the temperature and ozone fields. During boreal winter (DJF) a signature of the positive AO phase or strong northern polar vortex is clearly visible in the observed and simulated data. Therefore the applied approach can be used for the validation of CCMs. SOCOL reasonably well reproduces AO-like patterns of the inter-annual variability, which consist of a deepening of the polar vortex and an acceleration of the PNJ during positive AO phases. The model also captures the concomitant deceleration of the meridional circulation, the subsequent warming, and the ozone increase in the lower tropical stratosphere. The model also matches well a pronounced dipole-like temperature response over the northern high-latitudes. However, the simulated warming in the tropical lower stratosphere is underestimated by a factor of 2. In the upper stratosphere the model almost completely fails to reproduce the observed warming. The observed ozone response in the tropical lower stratosphere is confined mostly to the lowermost stratosphere while the simulated ozone response extends to the middle stratosphere. Moreover, the ozone response over the northern high-latitudes disagrees with observed ozone changes. Additional observation and simulation data should be analyzed in order to elucidate the causes of the noticeable disagreement between simulated and observed atmospheric imprints of the AO phase.

Despite of these model deficiencies, the overall performance of SOCOL as a modeling tool is reasonable and many features of the real atmosphere are simulated rather well. SOCOL has been ported for regular PC and shows good wall-clock performance. Thus, it can be used for studies of chemistry-climate problems by many research groups even without access to super-computer facilities.

5.1.2 Study of 11-year solar irradiance variability study

One of the many possible physical mechanisms that can be responsible for a solar-climate relationship has been studied in this work. The response of the Earth's atmosphere to the enhancement of the solar irradiance from the minimum to the maximum of the 11-year solar activity cycle has been simulated using SOCOL. Analysis of the simulated ozone, temperature, geopotential height and zonal wind responses to an imposed increase of solar irradiance during solar maximum conditions and their comparison with observations and some other model results provides valuable insights for process-oriented understanding.

5.1.2.1 Long-term annual mean solar signal

The atmospheric response to enhanced solar irradiance has been evaluated with a new chemistry-climate model SOCOL, which utilizes a parameterization of the primary solar forcing taking proper account of the heating rates due to oxygen and ozone absorption in the middle atmosphere. The results reveal that a sufficiently resolved physical representation of the direct heating rate is an essential prerequisite for the simulation of the solar signal in the stratosphere. The simulation suggests more pronounced solar signal in the stratospheric temperature fields compared to previous work (Tourpali et al., 2003), implying the necessity of an improvement of the MAECHAM4/5 radiation code.

In the stratosphere below 38 km the simulated ozone response is in a reasonable agreement with observations; however, in the upper stratosphere it is underestimated. A small ozone response in the upper stratosphere is theoretically expected, therefore probably some physical-chemical processes are still missing or the data analysis is not complete. An acceleration of the PNJ has been obtained during solar maximum presumably due to an increase in the meridional temperature gradient. The intensification of the polar vortices leads to the formation of vertical dipole structures in the annual mean zonal mean temperature response over both poles, deceleration of the meridional circulation and warming in the lower tropical stratosphere. This warming is in agreement with SSU/MSU4 data, but it is substantially disagrees in comparison with NCEP and CPC data sets. The introduction of the solar flux variations into the model leads to a statistically significant signal in the annual mean surface air temperature of up to 1.2 K over North America and Siberia. This pattern is typical for the positive phase of the AO and suggests an enhanced stratosphere-troposphere coupling including downward propagation of the UV-triggered signal. Thus, while the simulated solar signals in the stratosphere are in accordance with theoretical expectations a solid validation of the

SOCOL results is difficult because of a considerable disagreement between the existing observational analyses.

5.1.2.2 Long-term chemical solar-induced response

The response of several important atmospheric species (CH_4, N_2O, H_2O, CF_2Cl_2, OH, HO_2, NO_2 and ClO) to the observed increase of the solar irradiance during solar maximum simulated with SOCOL has been documented. The results confirm that solar variability has a significant influence on the chemical composition of the stratosphere and mesosphere. Substantial changes have been found in the concentration of several source gases as well as reservoir and radical species that are responsible for ozone destruction in the atmosphere. Enhanced photolysis during solar maximum leads to additional destruction of methane, nitrous oxide and CFCs providing an increase in the chemical activity of the stratosphere along with more pronounced effects in the mesosphere. In the mesosphere an increase of HO_x caused by more intensive water vapor photolysis results in substantial ozone depletion. More intensive methane oxidation gives rise to a statistically significant increase in stratospheric humidity. The application of the fully coupled CCM allows to trace dynamical changes caused by the solar influence. However, from the CCM results alone it is not possible to distinguish chemical and dynamical factors with a high level of confidence. An additional run of the same model in offline mode (i.e. with prescribed dynamics and temperature) may provide the solar signal solely due to chemical processes and subsequent comparison with interactive run can help to elucidate the dynamical contribution.

5.1.2.3 Seasonal and geographical distributions

The analysis of solar-induced changes of ozone shows a negative anomaly in the mesosphere and a positive anomaly in the stratosphere over the 60°S-60°N latitudinal belt throughout the year. Solar-induced changes in temperature also show a positive anomaly in the stratosphere throughout the year with maximum changes of ~ 1 K at 1 hPa. In the seasonal evolution of the zonal wind response, a statistically significant acceleration of PJN in the SH (at 95 % level of confidence) have been obtained. As is clear from Figure 3.11, the SH zonal wind anomaly moves poleward in the course of time (from July to November). In the NH, the model suggests an acceleration of the PNJ in February, but with lower significance (80 %), presumably because of higher interannual variability as compared to in the SH.

115

The analysis in Chapter 3 of the geographical distribution of solar-induced changes in geopotential height, temperature, zonal wind and total ozone fields has shown that simulated changes due to enhanced solar irradiance are physically consistent.

5.1.2.4 Separation of the influences of UV and Visible radiation

The analysis of two additional 20-year long steady-state simulations have been performed using observed spectral solar fluxes, which allow to separate the ultraviolet (UV) and visible (VIS) radiation impacts on the atmosphere. Zonal wind changes show that UV radiation is manly responsible for an acceleration of the stratospheric PNJs. Figure 3.21 suggests that both UV and visible radiation might substantially influence the PNJ during the NH winter season but in a different way. The simulation taking only VIS changes into account indicates a significant response in annual mean zonal wind (easterly intensification) in the tropical lower stratosphere. In the SH winter, UV changes lead to he strengthening of the PNJ core, while VIS does not strongly influence the PNJ.

From the analysis of surface air temperatures the following conclusions can be drawn. The influence of UV radiation alone should be detectable in the surface air temperature field, which is in a contrast to results presented by Rind *et al.* (2004). However, the effect of UV irradiance is generally smaller than that of perturbation by changes in the visible. The response of surface air temperature shows that the VIS and UV radiation dominate in different geographical regions during the different seasons but produce similar annual mean patterns.

5.1.3 Study of 27-day long solar variability

In Chapter 4 an alternative way to validate the simulated solar signal is presented, namely a comparison of the model sensitivity to the solar irradiance variability on a shorter time scale. The correlation between ozone and solar irradiance reaches a maximum between 50 and 80 km at almost zero phase lag reflecting a relatively short life time of ozone up there. Below 50 km the phase lag increases gradually in the stratosphere and reaches 5 days around 35 km, which is in reasonable agreement with observations (Hood, 2004 and references therein). The response of the temperature is positive with phase lag around 5-10 days in the mesosphere and 15-18 days in the stratosphere. The hydroxyl radical concentration reveals a high and robust correlation with solar irradiance in the upper stratosphere and mesosphere. This is to be expected because the hydroxyl production is dominated by the photolysis of water vapor and ozone, which are directly connected to the solar irradiance. The results for the ozone and temperature sensitivities have been compared with the sensitivities obtained from the different

satellite observations. The simulated ozone sensitivity is in reasonable agreement with observational data. The temperature correlation with solar irradiance is not robust, but shown substantial variability and depends on the year of the ensemble run.

5.2 Future perspectives for our studies solar-climate connections

The comparison of simulated results with observations reveals some significant points of disagreement. For example, in the middle stratosphere the observational data analysis performed by Hood (2004) suggests a statistically significant decrease of the ozone, which is in contrast to the model results and to theoretical expectations for the solar-signal influence. The simulated warming in the tropical upper stratosphere is about half that obtained from the observational data analysis, and the observed second maximum of the warming in the tropical lower stratosphere appears in the model only during the winter season.

These disagreements could have one or several of the following reasons:

- *QBO:* The CCM SOCOL does not simulate the QBO. Therefore, if the solar influence is realized through the alteration of the QBO, as has been suggested by Salby and Callaghan (2000), then at the present it is not possible to simulate properly the solar signal, especially in the tropical stratosphere.

- *Experimental set up:* Two time-slice (steady-state) model runs for average and average plus maximum-minus minimum solar activity have been performed, however, the solar signal is transient by nature. Thus it may be more appropriate to perform a transient simulation covering several 11-year cycles. The results of such a simulation and their analysis using statistical tools for fingerprint detection within the observational data could possibly be in better agreement with observations. Such applications of SOCOL are in a progress, however the transient experiments are out of the scope of this thesis.

- *EEP (energetic electron precipitation):* Fast particles might play a role, and the involved physical/chemical mechanisms are currently missing in the model. Energetic electron precipitation (EEP) events are among the potential candidates, because they can substantially alternate stratospheric chemistry and global climate. The EEP mechanism has been proposed by Callis *et al.* (1998 a, b). Normally neither protons nor electrons cannot penetrate to the atmosphere because they posses rather small energy. But electrons from the solar wind trapped in the outer radiation belt of the Earth magnetosphere are accelerated and can

penetrate into the atmosphere over the sub-auroral regions and deposit their energy up to 50 km with maximum at 105 km. They ionize neutral components providing a source of reactive nitrogen and hydrogen. During the cold season, EEP-induced NO_y may penetrate into the stratosphere destroying ozone and affecting entire atmosphere. Measurements show that EEP events are more frequent during the declining phase of the solar activity, when solar spots are closer to the solar equator and the solar wind is directed towards the Earth. This fact is supported by yearly values of electron precipitation events in the Murmansk region (Bazilevskaya et al., 2002). As the intensity of EEP is the most pronounced during declining phase of the solar activity cycle, i.e. closer to solar activity minimum, EEP and UV mechanisms should work in phase in the extra-polar stratosphere, but out of phase over the high-latitudes and in the troposphere. The polar vortices should intensify for solar maximum conditions due to enhanced solar irradiance, but weakened due to less intense EEP events. This partial compensation would imply that for the correct detection of the solar signal the time evolution of the EEP should be taken into account as explanatory variable within multiple regression analysis. It would be also of great interest to evaluate the effects of EEP using not only steady-state but transient simulations.

5.3 References

Bazilevskaya et al., (2002). "Physics of Auroral Phenomena", Proc. XXV Annual Seminar, Apatity, pp.125-128.

Callis, L.B., M. Natarajan, J.D. Lambeth, and D.N. Baker, Solar atmospheric coupling by electrons (SOLACE), (1998a), 2: Calculated stratospheric effects of precipitating electrons, 1979-1988, *J. Geophys. Res.*, **103**, 28421-28438.

Callis, L.B., M. Natarajan, D.S. Evans, and J.D. Lambeth, (1998b), Solar atmospheric coupling by electrons (SOLACE), 1: Effects of the May 12, 1997 solar event on the middle atmosphere, *J. Geophys. Res.*, **103**, 28405-28420.

Hood, L. L. (2004), Effects of solar UV variability on the stratosphere. Geophys. Monogr. Ser., **141**, edited by J. Pap et al., AGU, Washington, D.C.

Intergovernmental Panel of Climate Change, (2001) *Climate Change 2001: The Scientific Basis*, 881pp., Cambridge Univ. Press, New York.

Reid, G. C. (2000), Solar variability and the Earth's climate: Introduction and overview, *Space Science Reviews*, **94**, 1-11.

Rind D., Shindell D., Perlwitz J., Lerner J. (2004). The relative importance of solar and anthropogenic forcing of climate change between the Maunder Minimum and the present, *J. Clim.*, 17, 906-929.

Salby and Callaghan (2000), Connection between the solar cycle and the QBO: The missing link, *J. Clim.*, **13**, 2652-2662.

Tourpali, K., Schuurmans, C., van Dorland, R., Steil, B., Brühl, C. (2003). Stratospheric and tropospheric response to enhanced solar UV radiation: A model study. *Geophys. Res. Lett.*, **30**(5), 1231, doi: 10.1029/2002GL016650.

Acronyms and Abbreviations

ADEOS	Advanced Earth Observing Satellite
AO	Arctic Oscillation
AMIP	Atmospheric Model Intercomparison Project
CCM	Chemistry-Climate Model
CPC	Climate Prediction Center (NOAA), USA
CTM	Chemistry-Transport Model
DLR	Deutschen Zentrum für Luft- und Raumfahrt
ECMWF	European Center for Medium-range Weather Forecast
EEP	Energetic Electronic Precipitations
ERA-15	ECMWF re-analysis data from December 1978 to February 1994
ERA-40	ECMWF re-analysis data for 40 years
GCM	General Circulation Model
GHG	Green House Gases
GISS	Goddard Institute for Space Studies, USA
HRDI	High Resolution Doppler Imager
IPCC	Intergovernmental Panel on Climate Change
MA-ECHAM4	Middle Atmosphere version of the "European Center/Hamburg Model 4"
MEZON	Model for the Evaluation of oZONe trends
MPI	Max-Planck Institute for Meteorology, Germany
NAT	Nitric Acid Trihydrate
NCEP	National Center for Environmental Prediction (formerly NMC), USA
NH	Northern Hemisphere
NMC	National Meteorological Center, USA (now NCEP)
ODS	Ozone Depleting Substances
PC	Personal Computer
PMOD/WRC	Physical Meteorological Observatory in Davos and World Radiation Centre
PNJ	Polar Night Jet
PSC	Polar Stratospheric Clouds
SAGE	Stratospheric Aerosol and Gas Experiment
SH	Southern Hemisphere
SL	Semi-Lagrangian scheme
SOCOL	modeling tool for studies of SOlar Climate Ozone Links
SST/SI	See Surface Temperature and See Ice
SSU/MSU4	Stratospheric Sounding Unit and Microwave Sounding Unit
SPARC	Stratospheric Processes And their Role in Climate
SUSIM	Solar Ultraviolet Spectral Irradiance Monitor
QBO	Quasi-Biannual Oscillation
TOC	Total Ozone Column
TOVS	TIROS Operational Vertical Sounder
TSI	Total Solar Irradiance
UARS	Upper Atmosphere Research Satellite
UIUC	University of Illinois at Urbana-Champing
UKMO	United Kingdom Meteorological Office, UK
URAP	UARS Reference Atmosphere Project
UV	Ultraviolet radiation

Acknowledgements

I would like to thank all people whose help allowed the realization of this PhD work, even if some may not be mentioned below.

In particular I would like to thank:

Prof. Thomas Peter as my supervisor for accepting me as his PhD student and helpful discussions.

Prof. Atsumu Ohmura as my co-examiner and for helpful comments on the thesis.

Prof. Joanna Haigh as my external co-examiner for her critical review and helpful comments on the thesis.

Prof. Werner Schmutz for providing me a framework to prepare this thesis, respect and mutual understanding.

Dr. Eugene Rozanov for the continuous support and scientific advice, for the shared up and downs during research.

Poly Project participants for helpful discussions during Poly Project meetings.

Lon Hood, Kuni Kodera, Karin Labitzke, Simon Crooks for providing their data of solar signal analysis deduced from observations.

Elisa Manzini for providing MA-ECHAM4 code and fruitful collaboration during manuscripts preparation.

Petra Forney and **Sonja Degli Esposti** for the help with paper-work .

staff of PMOD/WRC for providing a friendly environment during my education.

my family for their support during my education.

This research was supported by the Poly Project of ETHZ and PMOD/WRC.

Publications

Egorova, T., E. Rozanov, E. Manzini, M. Haberreiter, W. Schmutz, V. Zubov, and T. Peter (2004). Chemical and dynamical response to the 11-year variability of the solar irradiance simulated with a chemistry-climate model, *Geophys. Res. Lett.*, **31**, L06119, doi:10.1029/2003GL019294.

Egorova, T.A., E.V.Rozanov, V.A.Zubov, and I.L. Karol (2003). Model for investigating ozone trends (MEZON). *Izvestiya, Atmospheric and Oceanic Physics*, **39**, 277-292.

Egorova, T., E. Rozanov, V. Zubov, E. Manzini, W. Schmutz, and T. Peter (2004). A new Chemistry-Climate Model SOCOL: description and validation, *Atmos. Chem. Phys. Discuss.*, **5**, 509-555, 2005 SRef-ID: 1680-7375/acpd/2005-5-509.

Egorova, T., E. Rozanov, V. Zubov, W. Schmutz, and T. Peter (2005). Influence of solar 11-year variability on chemical composition of the stratosphere and mesosphere simulated with a chemistry-climate model, *Adv. Space Res.*, in press.

Rozanov, E.V., M. E. Schlesinger , T. A. Egorova, B. Li, N. Andronova, and V.A. Zubov (2004). Atmospheric response to the observed increase of solar UV radiation from solar minimum to solar maximum simulated by the UIUC climate-chemistry model, *J. Geoph. Res.*, **109**, D01110, doi:10.1029/2003JD003796.

Zubov, V., E. Rozanov, A. Shirochkov, L. Makarova, T. Egorova, A. Kiselev, Y. Ozolin, I. Karol and W. Schmutz (2005). Modeling of the solar wind influence on the circulation and ozone concentration in the middle atmosphere, *J. Atmos. Solar-Terrestr. Phys.*, **67** (1-2), 155-162.

Curriculum Vitae

Name:	Tatiana Egorova
Date of birth:	9 March 1968
Place of birth:	St.-Petersburg, Russia

1975-1985: Primary, secondary and high school in St.-Petersburg, Russia

1987-1993: Studies of meteorology at the Russian State Hydrometeorological Institute, Department of Meteorology, St.-Petersburg, Russia.
Diploma in meteorology (theoretical group of numerical weather forecast) and diploma MS Thesis: "Development of 1-D transient radiative-convective model"

1993-2001: Scientist in Main Geophysical Observatory (MGO), St.-Petersburg Russia, research in field "Model development of the global atmosphere and its application for the estimation of the freons production limitations effects on atmospheric ozone"

2001-2002: Scientific collaborator at the MGO, St.-Petersburg, Russia

2002-2004: PhD student at the ETH Zurich, Switzerland, and at the PMOD/WRC in Davos, Switzerland. Ph.D. thesis" Modeling of the short and long-term solar fluxes variability effects on ozone and climate"